8-2001

EFFECT OF BONDING VARIABLES IN THERMAL BONDING OF POLYPROPYLENE NONWOVENS

Praveen Kumar Jangala
University of Tennessee - Knoxville

To the Graduate Council:

I am submitting herewith a thesis written by Praveen Kumar Jangala entitled "EFFECT OF BONDING VARIABLES IN THERMAL BONDING OF POLYPROPYLENE NONWOVENS." I have examined the final electronic copy of this thesis for form and content and recommend that it be accepted in partial fulfillment of the requirements for the degree of Master of Science, with a major in Consumer Services Management.

Gajanan S. Bhat, Major Professor

We have read this thesis and recommend its acceptance:

Joseph E. Spruiell, Kermit E. Duckett

Accepted for the Council:

Carolyn R. Hodges

Vice Provost and Dean of the Graduate School

(Original signatures are on file with official student records.)

To the Graduate Council:

I am submitting herewith a thesis written by PRAVEEN KUMAR JANGALA entitled "EFFECT OF BONDING VARIABLES IN THERMAL BONDING OF POLYPROPYLENE NONWOVENS." I have examined the final copy of this thesis for form and content and recommend that it be accepted in partial fulfillment of the requirements for the degree of Master of Science, with a major in Textiles, Retailing & Consumer Sciences.

Gajanan S. Bhat

Major Professor

I have read this thesis
and recommend its acceptance:

Joseph E. Spruiell

Committee Member

Kermit E. Duckett

Committee Member

Accepted for the Council:

Dr. Anne Mayhew

Interim Vice Provost and
Dean of the Graduate School

(Original signatures are on file in the Graduate Student Services Office)

EFFECT OF BONDING VARIABLES IN THERMAL BONDING OF POLYPROPYLENE NONWOVENS

A THESIS PRESENTED FOR THE
MASTER OF SCIENCE
DEGREE

THE UNIVERSITY OF TENNESSEE, KNOXVILLE

PRAVEEN KUMAR JANGALA
AUGUST 2001

DEDICATION

This thesis is dedicated to my parents

Mr. Rajasekhar Mrs. Saraswati

and my sister

Ms. Lavanya

ACKNOWLEDGMENTS

I would like to express sincere gratitude to my major professor Dr. Gajanan S. Bhat, who patiently guided and assisted me throughout this research. Many discussions with him have broadened my knowledge of nonwoven technology and fiber science. He has been both, a teacher and a friend! I would also like to thank Dr. Joseph E. Spruiell and Dr. Kermit E. Duckett for their suggestions and support.

Financial assistance from the Nonwovens Cooperative Research Center (NCRC), which made this research possible, is greatly appreciated. I would also like to thank Fiber Visions Inc. for calendaring the material and Kimberly-Clark Corp. for supplying the material, for this work.

Sincere thanks to Van Brentley, technician at the TANDEC, for his help in testing instruments. Appreciation is acknowledged to faculty, staff and colleagues of the textile science department.

Finally and most importantly, I would like to thank my dear family: Dad, Mom and Sister for their love, constant support and encouragement.

ABSTRACT

The aim of this research was to investigate the effect of some of the process variables on the structure and properties of the webs in a thermal point bonding process. The main objectives were to understand the changes taking place in the fiber structure due to applied heat and pressure, the effect of bond area and bond size on fiber morphology, and the physical properties of the web. Thermally bonded carded webs were produced and characterized in order to determine the role of bond area and bond size on strength and stiffness of the point bonded fabrics and fiber morphology. The webs were also characterized to see the changes taking place in fiber morphology on thermal bonding. It was observed that the bond strength increases with bond area and bond size. The effect of bond area and bond size on fiber morphology were negligible. Significant morphological differences were observed in the bonded and the unbonded regions of the thermally bonded webs. To see how the staple fiber studies relate to the behavior of continuous filaments, similar sets of samples were produced and characterized using the spunbond system. The observed trends for properties with respect to bonding conditions were similar for spunbond samples. However, actual values of tensile and other physical properties were much higher for spunbond webs.

TABLE OF CONTENTS

LIST OF TABLES

LIST OF FIGURES

LIST OF ABBREVIATIONS

1. PP = Polypropylene
2. SEM = Scanning Electron Microscope
3. WAXD = Wide Angle X-ray Diffraction
4. MD = Machine Direction
5. CD = Cross Direction

CHAPTER I

INTRODUCTION

Thermal bonding is the most popular method of bonding used in nonwovens. It offers high production rates because bonding is accomplished at high speed with heated calender rolls or ovens. Thermal bonding process has been used successfully with a number of thermoplastic fibers. It offers significant energy conservation with respect to latex bonding because of effective thermal contact, and because no water needs to be evaporated after bonding. It is environmentally friendly because there are no residual ingredients to be disposed of. A wide range of fibers are available for thermal bonding. These include homofil and bicomponent fibers, which in turn allow a wide range of fabric properties and aesthetics to be obtained. Among the various types of thermal bonding, point bonding is the most widely used technique [1].

Nonwoven fabric properties are determined by the characteristics of bond points, and in particular, by the stress-strain relationship of the bridging fibers. During point bonding, the bond points and the bridging fibers develop distinct properties. Among those properties are the bond area and bond size, which also affect the final fabric properties like the strength and stiffness. The properties such as strength and stiffness affect the final product of the thermal point bonding process. Limited research has been done to understand how the bond area and bond size variables affect the final properties of the thermal point bonded fabric. This has been mainly due to the fact that it is hard to

produce such samples, and moreover, it is a tedious and strenuous procedure to characterize the bond points and the fibers surrounding the bond.

Since thermal point bonding possesses so many advantages, it is important to determine how variables such as bond area and bond size along with bonding temperature affect the final properties of the web.

In this regard, the main objectives of this research were

1. To examine the changes taking place in the fibers in the bonded region, unbonded region and bond vicinity during thermal bonding.
2. To understand the failure behavior of thermally point-bonded fabrics, such as what factors limit extension, how failure begins and continues, the effect of fiber structure on bond strength, etc.
3. To be able to suggest optimum processing conditions for thermal bonding based on variables like bond area, bond size and bonding temperature, and
4. To understand how fiber properties translate into fabric properties in the thermal bonding processes.

A series of samples produced under various bonding conditions were thoroughly characterized. Studies were done with both staple fibers and spunbond fibers.

CHAPTER II

LITERATURE REVIEW

2.1 Nonwovens

Nonwoven fabrics are sheets made from natural or synthetic, organic or inorganic, fibers or filaments, which have not been converted to yarns, and are bonded to each other, not predominantly by hydrogen bonding but by any combination of the following means: adding an adhesive, thermally fusing the fibers or filaments to each other or to other meltable fibers or powders; fusing the fibers to be bonded by first dissolving and then re-solidifying their surfaces; creating physical tangles or tufts among the fibers; holding the fibers or filaments in place with sewing or knitting stitches with yarns made from the fibers of the sheet or from the fibers. The fibers may be natural or manufactured. They may be staple or continuous or be formed in situ [5]. The production of nonwovens amounts to approximately 20% of the total production of textiles, and their share continues to grow. Fibers, binders and a bonding process are needed to manufacture a nonwoven. The steps in the processing of manufacturing nonwovens are shown in Fig 2.1.

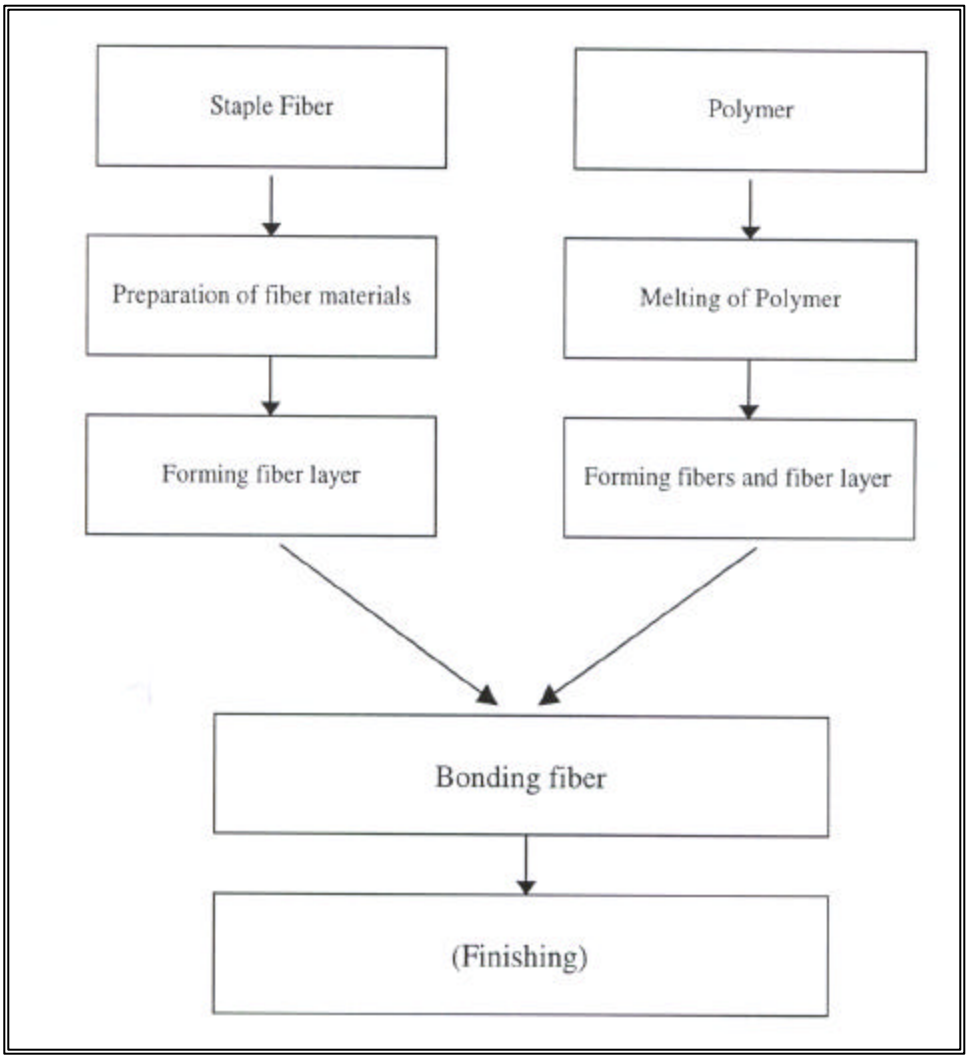

Fig 2.1 The Process of Manufacturing Nonwovens

Nonwoven fabrics demonstrate specific characteristics such as absorbency, liquid repellency, resilience, stretch, softness, strength, flame retardancy, washability, cushioning, filtering, bacterial barrier and sterility [4]. They are used in a wide variety of applications such as disposable diapers, sanitary items, hospital gowns, wiping cloths, computer diskette linings, base materials for coated fabrics, interlinings, and engineering fabrics.

All nonwoven fabrics are based on a fibrous web, they are:

1) Dry-Laid
2) Wet-Laid
3) Melt-Blown
4) Spunbond

2.2 Web Bonding Methods

Basically there are three types of bonding techniques used in nonwovens. They are:

Chemical Bonding

Mechanical Bonding

Thermal Bonding

(a) Chemical Bonding: Bonding a web by means of a chemical has been one of the most common methods. The chemical binder is applied to the web and is cured. The most commonly used binder is latex, because it is economical, easy to apply and very effective. Several methods are used to apply binder and these include saturation bonding, spray bonding, print bonding and foam bonding.

(b) Mechanical Bonding: This involves fiber entanglement. This can be achieved through needle punching or fluid jet action. In many applications, mechanical bonding is used as a first stage of bonding, followed by chemical or thermal bonding, which impart additional strength and other desirable characteristics not attainable through needling alone.

(c) Thermal Bonding: Thermal bonding is the process of using heat to bond or stabilize a web structure that contains of a thermoplastic binder. All or part of the fibers act as thermal binder, thus eliminating the use of latex or resin binders. Thermal bonding is the leading method used by the cover-stock industry for baby diapers. Polypropylene has been the most suitable fiber with its low melting point of approximately 165 °C. The thermal bonded polypropylene nonwovens are also soft to touch. The fiber web is passed between heated calender rollers, where the web is bonded. In most cases, point bonding using embossing rolls is the most desired method, adding softness and flexibility to the fabric. Use of smooth rolls bonds the entire fabric increasing the strength, but reducing drape and softness.

2.2.1 Characteristics of Thermal Bonding

The first thermally bonded nonwovens were produced in the early 1940s. The carrier fiber was rayon, and plasticized cellulose acetate or vinyl chloride was applied as the binder fiber [3]. However, the technology at that time was not developed very well and the cost of the available binder fibers was very high. With the increase in energy cost and the development of technology, manufacturers began to produce new binder fibers and

carrier fibers. These made it possible to produce more products incorporating thermal bonding.

There are three key components in thermal bonding [3]:

- Structure of carrier or base fiber.
- Heat activated binder fiber.
- The bonding process.

The carrier fiber is the skeleton structure of the nonwoven fabric. It gives the fabric strength, integrity and certain properties depending on the fiber composition.

The binder used in the thermal bonding process may be a fiber, binder sheaths in a sheath-core bicomponent fiber, powder, film, hot melt, netting or the outer surface of a homogeneous carrier fiber [3]. The physical properties of the thermal binder fibers, when they are used and deposited in and around the fibrous matrix, affect the ultimate product properties, as does the thermal bonding process itself.

All thermal bonding processes have two common features:

- The melting point of the binder fiber must be lower than that of the carrier fiber.
- Heat must be applied either alone, combined with pressure, followed by pressure as in the case of calenders, ovens and radiant heat sources- or simply generated as part of the process (e.g. ultrasonic bonding)

There are four methods of thermal bonding [6]. They are Hot Calendering, Oven Bonding, Ultrasonic Bonding, Radiant Heat Bonding.

I. Hot Calendering

There are three different types of hot calendering

(i) Area Bond Hot Calendering: This process involves the use of a calender with a hot metal roll opposed by a wool felt, cotton or special composition roll. The amorphous or co-polymeric binder fibers used in this process provide bonding at all cross-over points between the carrier and the binder fibers. The resultant product is smooth, thin and stiff.

(ii) Point Bond Hot Calendering: This method produces fabrics which range from thin, closed, inelastic, strong, and stiff to open, bulky, weak, flexible and elastic depending on the density, the size and the pattern of the bond points.

(iii) Embossing Hot Calendering: This method is a figured or sculptured area-bond hot calendaring. The area bonding is three dimensional. A "bulky but thin" product can be made in any pleasing or functional construction, depending on the face geometry of the embossing rolls.

II. Oven Bonding: Through air oven bonding involves the application of hot air to the surface of the nonwoven fabric. Products manufactured using through-air ovens tend to be bulky, open, soft, strong, extensible, breathable and absorbent.

III. Ultrasonic Bonding: This process involves the application of rapidly alternating compressive forces to localized areas of fibers in the web. The stress created by these compressive forces is converted to thermal energy, which softens the fibers as they are pressed against each other. Fabrics produced by this technique are soft, breathable, absorbent, and strong.

IV. Radiant Heat Bonding: Radiant heat bonding is achieved by exposing the web to a source of radiant energy in the infrared range, which increases the temperature of the web and soften the binder component. Radiant bonding is better used for powder bonded nonwovens to produce soft, open, and absorbent webs with low-to-medium strength.

Thermal bonding is an important technology. Compared to other bonding processes, thermal bonding offers a number of advantages [2]:

1. **Efficiency:** Chemical bonding methods use water or other solvents as a carrier for the bonding agent. This water has to be evaporated before the chemical bonding process can occur. Furthermore, additional energy is often required to cure the binder. As an example, the water evaporation heat load in a chemical spray application can easily be 10 to 12 times the heat used in thermally bonding process.
2. **Emissions:** No solvent vapors or other gases need to be released.
3. **Space and Capital Cost:** Smaller units can be used since less heat is transferred and speeds are higher.
4. **Cleanliness:** The spray station or pad of the wet systems in most plant environments require substantial clean-up efforts. Furthermore, downstream equipment, conveyors and rollers, require less cleaning as well in thermobonding systems.
5. **Quality:** Thermally bonded nonwoven webs usually are softer, especially as compared to spray bonding, wherein there is a tendency for the binder resin to concentrate at the surface of the batt. Thermal bonded products also have greater strength per unit weight and are more absorbent and porous due to smaller bonding points.
6. **Flexibility:** Since the binders are mixed into the web, thermal bonding processes are readily adaptable to the manufacture of design or composite structures. Cellulosic blends, acrylics or any other binder combination of the new material.

Emerging fiber production technology will further widen the applicability of thermal bonding techniques.

7. **Toxicology:** The product is usually made from a single polymer. Problems associated with food or chemical filtration and skin tolerability are reduced or eliminated entirely.

Among the thermal bonding methods, point bonding is the most widely used technique. PP fibers, by themselves or as binder fibers, are used most often for point bonding. Low melting copolymers of polyester are also used. Special sheath/core bicomponent fibers, where the core has a higher melting temperature, have also been developed for thermal bonding [1]

2.3 Point Bonding Process

In the point bonding process, the web is fed by an apron leading to a calender nip consisting of one engraved and one smooth roll. As the web enters the hot calender nip, fiber temperature is raised to the point at which tackiness and melting cause fiber segments caught between the tips of engraved points and smooth roll to adhere together. The heating time is of the order of milliseconds. The process is schematically shown in Fig.2.2 [1].

The fabric emerging from the nip may be cooled by contacting two water cooled rolls. Fiber shrinkage tendencies are accommodated by fabric relaxation; otherwise cooling

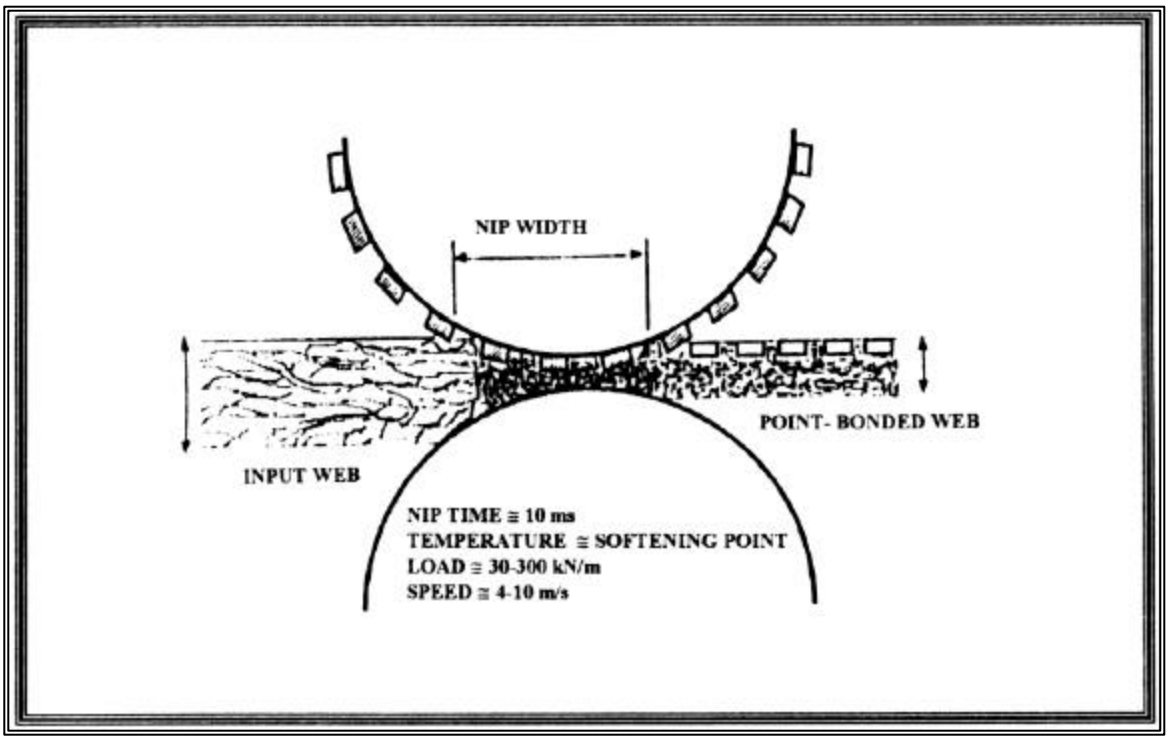

Fig 2.2 Schematic of the Thermal Point Bonding Process [1].

takes place under tension and a thin 'boardy' fabric results. Fabric is then wound up under controlled tension into a roll of appropriate hardness and integrity [7].

2.4 Process Variables

There are three main process variables, namely bonding temperature, bonding pressure, and time (or calendering speed). At a fixed bonding pressure, there is an optimal time and temperature, which gives maximum bond strength. Contact time is determined by production line speed, so temperature is the logical control variable [9]. Bonding temperature is the most influential parameter followed by pressure and speed [8].

2.4.1 Effect of Bonding Temperature

Shimalla and Whitwell [10] have studied the effect of bonding temperature on the strength of the fabrics and reported that higher bonding temperatures generally improves individual bond strength but can be detrimental to fiber strength. For pure polypropylene webs the temperature effect occurs less dramatically, but the maximum tenacity in the machine direction (MD) increases rapidly between 150°C and 155°C. At higher temperatures the resulting material resembles a film more than a textile. De Angelis [11] measured the dependence of the breaking strength of overall calendered polypropylene fiber nonwoven fabric on bonding temperature. Their results indicated that, for a given nip-line pressure and calendering speed, the breaking strength reaches a maximum at a critical bonding temperature. On keeping nip-line pressure constant, the critical temperature was found to be a function of the calendaring speed. The decrease in

breaking strength above the critical temperature level was attributed to the 'loss of fiber integrity and formation of film-like spots at high temperatures.' Bechter [13] also confirmed the existence of a critical bonding temperature (dependent on speed) for maximum tensile properties in point-bonded PP-fiber nonwoven fabrics. Malkan [14] studied the failure behavior of polypropylene spunbonded webs with respect to bonding temperature. Brittle failure was mainly associated with higher bonding temperatures and was initiated mainly by bond rupture. The temperature of maximum strength lies in close proximity to the surface melting temperature of the fibers [8].

2.4.2 Effect of Bonding Pressure

The nip line pressure is important since it influences the heat transfer to and through the web, as well as melting point, flow, and viscosity of the polymer. Bechter [13] observed that, in the case of point-bonded polypropylene webs, the bonding temperature at which the strength maximum occurred was unaffected by the nip line pressure. This influence depends upon melting behavior of the fibers. If the position of maxima occurs in the early-melting region, a low calendaring pressure is desirable so that the 'thin' melting zone is not disturbed. Muller [12] reported an optimum pressure for the bonding of heavy webs. The authors suggested that, at high nip pressures, flow from the fiber is disturbed and there is considerable fiber damage at the perimeter (as seen through SEM). Both of these effects lead to reduction in web strength.

2.4.3 Effect of Contact Time

The contact time of the web in the nip is primarily influenced by the production speed and roll diameters. Preheating the unbonded web, which may permit higher speeds, has been reported to cause bonded-web tensile properties to deteriorate [15]. This has been attributed to a slight crystallinity increase in the unbonded fibers, which requires a higher bonding temperature. Shimalla and Whitwell [10] studied the influence of time during bonding. Increasing the bonding time is expected to increase the extent of contact primarily due to the kinetics of wetting. Specific bond strength is also increased if diffusion is involved. Longer residence times can cause heat setting (stress relaxation under fixed length), which imparts a degree of dimensional stability against shrinkage that is dependent on the temperature of the heat-setting operation. Changes in fiber molecular orientation during exposure to elevated temperatures also influences bonded web properties [16]. DeAngelis [11] studied the influence of calendering speed on tensile properties. Increasing the calender speed while maintaining the roll temperature and pressure constant reduced the breaking strength. Muller [12] studied the thermal bonding of heavy webs with calendars. He showed that for heavy webs, the tensile strength in MD and CD was higher at the higher production speed. The influence of nip pressure is more intense at the lower speeds, which demonstrates the sufficiency of contact time to transfer the heat into the fibers also at high speeds. He observed three things when the speed increased:

(a) The calender temperature required for maximum strength increases to compensate for the reduced contact time.

(b) The influence of calendering pressure is greater at faster speeds. The author suggested that this was due to reduced heat transfer at higher production rates.

(c) The maximum strength achieved increases.

An increase in production rate, when compensated by an appropriate increase in temperature, reduced the bond point area and actually increased the fabric strength.

2.5 Point Bonded Fabric Strength Mechansims

Crane [17] has studied the fabric strength mechanism for polyester staple fiber thermally bonded nonwovens, and he came out with three observations, which are discussed below:

2.5.1 Bond Point Integrity Per Se

This reflects the effectiveness of providing anchor points to inter-connect all the fibers in the fabric. It is a measure of melt adhesion between fibers, realized under optimized temperature and pressure. Throughput speed, and hence nip residence time, affects the extent of heating and fiber softening necessary for effective melt adhesion. Fiber surface modification with finish could detract seriously from bond strength, depending on finish type and level.

If bond integrity is very poor, fabric fracture will occur by fiber slippage mode. In blends of binder fibers with matrix fibers, the melt adhesion bond between the two components will determine fabric strength. If bond point integrity is only moderate, partial fiber peel from the bond point surface will occur followed by fiber tip fracture at its anchorage to

the bonded area. Infrequently, as in fabrics which were overbonded at high temperature, the bond point itself was highly embrittled and it breaks by cracking into two parts, like a plastic chip.

2.5.2 Strength at Bond Point Perimeter

Crush damage at bond perimeter causes sharp reduction in the fiber's load bearing ability due to stress concentration at the crush mark. This physical discontinuity in fiber strength along its axis may also be viewed in terms of thermal discontinuity along fiber axis due to the difference in heat treatment, melting and re-crystallization between fiber segment under bond point, and free segment bridging bond points. Tenacity and crystallinity change along fiber axis from one bond point to the next, especially at the interface to the bonded area itself.

Fiber bending, at the root of its attachment to the bond area, does occur in fabric particularly in cross-directional tensile pull. Brittle fibers and those with low loop tenacity to straight tenacity ratios would be susceptible to fracture under severe bending [17].

2.5.3 Strength of Bridging Fibers

The fiber stress-strain curve is that of heat exposed fiber, as experienced in the bonding process, rather than that of the unbonded fiber. Upon fabric straining in MD pull, different fibers in the fabric will sustain varying magnitudes of strain levels. Some fibers will actually experience compressive buckling despite moderate fabric tensile pull. A fabric made of fibers of low breaking elongation will have its fibers break sequentially as

each reaches its own break strain level. On the other hand, a fabric of fibers of high break elongation will have its fibers continuously sharing in supporting the fabric tensile pull, followed by concurrent failure [17].

2.6 Influence of Calender Pattern

The calender pattern is important for achieving the desired combination of qualities in a bonded web. In the patent literature on calender patterns it is suggested that, to obtain a fabric with textile-like characteristics and adequate strength, there should be 15.5 x 104 to 77.5 x 104 bonds/m2 (100-500 bonds/ in2), covering 5- 25% of the web area [15, 18].

The height of lands on the roll is another calender-pattern variable. According to Brock [19], the height of lands should be less than the thickness of web entering the nip, so that surfaces of the web away from the bond points will also contact the rolls. This will produce light bonding of fibers between bond points. It can be pointed out that melting occurs only in the area of the engraving and that the fibers keep their characteristics in between [12]. Further, if the land height is substantially greater than the thickness of the web, the intermediate regions would experience no compression, and filaments in these regions would hardly be bonded. The result would be a low web strength [19]. The strength of the bonded web does not come from partial bonding of the intermediate regions. A recent trend is to use a land height greater than the web thickness so as to avoid intermediate bonding and achieve an optimum combination of strength and softness. The strength of a fabric can be manipulated to some extent by changing the frequency and placement of the fiber bonding points in the thermal bonding process [25]. The best combination of strength and softness is obtained when the raised lands are

vertical (i.e. the sides are perpendicular to the surface), with a little rounding at the edges to minimize damage to the fibers [19]. In practice, the sides of the lands are made at a small angle with respect to the normal to the roll surface owing to the difficulty of engraving vertical sides.

2.7 Morphology of Bond Points and Bridging Fibers During Thermal Bonding

Mi et al. [20] suggested that bond strength is important in determining the strength of point-bonded fabrics. Theoretical results of their model indicate that 'high-strength' bonds defined by fabric failure being caused by failure of the bridging fibers, led to the strongest fabrics.

As the fabric passes through the calender, it gets compressed to approximately one tenth of its original thickness at bond points [21]. From scanning electron micrograph pictures, bond areas appear void free, although density measurements have suggested void content up to 5%. Drelich et al. [26] studied thermal bonding with fusible fibers and reported that polymer in the bond region no longer has any fiber characteristics.

Fabric failure was determined by the character of bond points and, in particular, by the stress-strain relationship of the bridging fibers. During point bonding, the bond points and the bridging fibers develop distinct properties, different from those of the virgin fibers, depending on the process variables employed. This change in properties has been hinted at by several authors but has not been investigated.

Warner [21] suggested that fibers break at the bond periphery because of the local thermo-mechanical history of the polymer. The material at the perimeter is weak and

brittle and he attributed this brittleness to crystallization in an unoriented state, especially at the perimeter where polymer is a result of extrusion from under the pin. Thus he suggested that the strength of the point-bonded fabrics will be governed by the bond-periphery strength.

Crane et al. [17] suggested that 'physical discontinuity in fiber strength along its axis may be viewed in terms of thermal discontinuity due to differences in heat treatment, melting and re-crystallization between fiber segments under the bond points and free segments bridging bond points.' Wei et al. [22] observed that 'significant morphological changes occur in the bonding regions, and the physical properties of thermally bonded fabrics are a manifestation of the nature and quality of the bonding regions' (including the parts of the bridging fibers that have been affected by bonding).

The results of Akai and Aspin [23] in the manufacture of embossed PP tapes indicated that embossing increased crystallinity, improved crystal perfection, and caused some molecular orientation. A correct choice of embossing conditions increased the strength of these tapes by 15%. In point bonding, therefore, the molecular orientation of the fibers compressed by the land probably changes, but these changes have not been investigated. Pressure is expected to increase melting point and glass transition temperature and thus could exert a significant influence on the rate of crystallization. Pressure also influences the rates of crystal nucleation and growth, and could therefore lead to complicated interactive effects. Philips and Tseng [24] studied the influence of pressure on the crystallization in PET. Their results showed that the volume density of crystal nuclei increased, resulting in high crystallinity levels, when polymers were crystallized under pressure. Malkan [14] studied thermal bonding of polypropylene spunbonded webs and

reported that size and characteristics of bond are not very much affected by bonding temperature or bonding pressure. However, edges of bond sites become sharper at high temperatures and pressures. On the other hand Wei et al. [22] have reported that bond area increases with increase in bonding temperature. They also have reported shrinkage of fibers during thermal bonding, especially in the case of highly drawn fibers.

2.8 Theoretical Modeling

Attempts have been made to theoretically model the effects of bond area, bond pattern, fiber tensile properties, fiber orientation distribution and bonding intensity on fabric tensile properties. Grindsaff and Hansen [27] developed the first computer simulation of the stress-strain behavior of point-bonded nonwoven fabrics. The fiber stress-strain curve was truncated at the point of plastic deformation to simulate the weakening at the bond edge. The fiber-orientation distribution was adjusted on the basis of micrographs. There was good correlation between the model and the experimental curves.

Mi et al. [20, 25] developed a computational model incorporating the effects of bond pattern, bond area fraction, bond-site shape, fabric-failure mechanism, and fiber orientation distribution for predicting the load-deformation behavior of point bonded webs. Mi used some assumptions to accommodate the actual stress-strain behavior of the fiber in the digitized form. The fabric load-deformation was calculated by stepping through increments of fabric strain. The change in fiber orientation distribution function was calculated at each step. The theoretical results indicate that the shape of bond sites, pattern, layout and percentage of bond area do have a significant influence on the

strength of the fabric. The model also predicts that higher fiber elongation leads to stronger fabrics, as was reported by Kwok [7].

Although the model does not predict exact web properties, it is useful for conceptually experimenting with the effects of the bond pattern, percentage bond area, fiber tensile properties, fiber-orientation distribution, and bonding intensity on fabric tensile properties.

2.9 Spunbonding

2.9.1 Process Description

Spunbonding is a one step process, which involves fiber extrusion, fiber attenuation, web formation and bonding of the web to impart strength, cohesiveness and integrity to it. The filament spinning, drawing and deposition are the most critical steps in the spunbonding process. Hartman [40] proposed some of the various basic possible variations of the process, which are shown in Fig 2.3.

The first process (A) uses longitudinal spinnerets, with air slots on both sides of the spinneret for the expulsion of drawing air$^{(1)}$. The room air$^{(2)}$ is carried along and, after lay-down of the filaments, is removed by suction$^{(3)}$. This process is very well suited for tacky polymers, such as polyurethane. Bonding takes place due to tackiness of the filaments.

The second process (B) allows a higher draw-ratio, with subsequently increased orientation of the filaments. Filaments are drawn with several air or gas streams$^{(1),(2)\ \&\ (3)}$ using drawing conduits. The air is removed by suction$^{(4)}$ after web formation. This

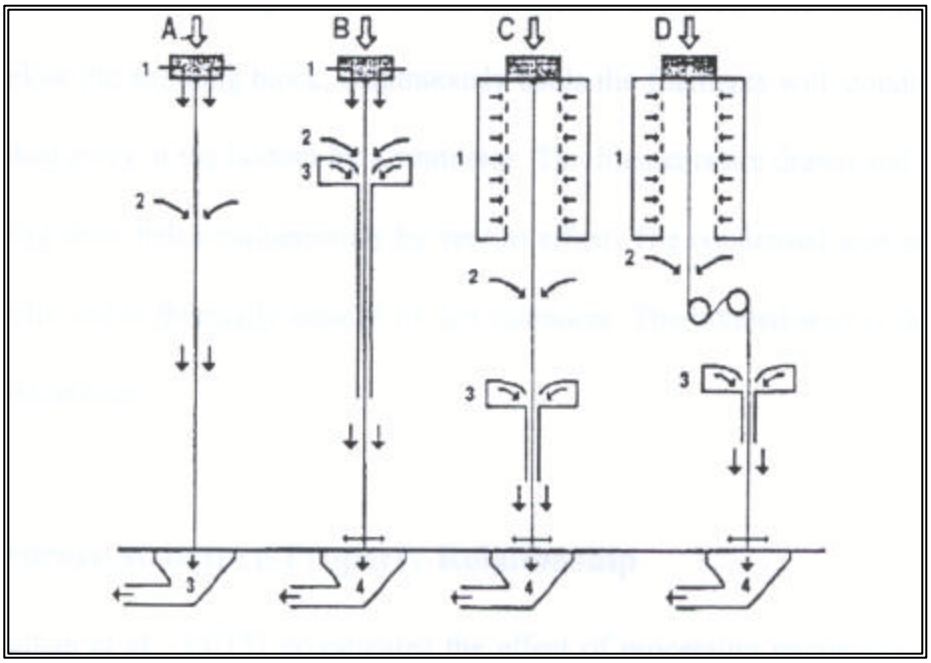

Fig 2.3 Four Basic Variations of the Spunbond Process

process has special advantage in preparing fine spunbonded webs with a textile-like appearance and handle of the web.

The third process C operates with regular cooling ducts(1) and drawing jets(3). The drawing and cooling arrangements can be operated to give very high spinning speeds. The temperature and humidity of room air(2) can be controlled. The air is removed by suction(4) after web formation.

The fourth process (D) has a mechanical drawing step between spinneret and lay-down zone. A very high level of molecular orientation can be achieved with this method. The remainder of the process is similar to process C.

A number of spunbonding processes can be classified into one of the above basic four types of the process. The method of bonding may be chemical, mechanical or thermal. Thermal bonding is the most widely used technique for spunbonding.

The Reicofil® system shown in Fig 2.4 has been developed by the Reifenhauser GmbH of Germany. The polymer pellets are fed into the extruder hopper. Polymer is melted and mixed as it moves along the extruder. The molten polymer is delivered to a metering pump, which in turn feeds the polymer to the spinning block at a constant rate through a feed distribution system. The feed distribution, which is very critical, balances the flow, the temperature and the residence time of the polymer across the width of the die. The spinneret, which is rectangular in shape, has several thousand holes. The cooling air-duct, located below the spinning block, continuously cools the filaments with conditioned air.

Air is sucked away at the bottom by a ventilator. The filaments are drawn and laid down on a moving sieve belt simultaneously by a venturi effect. The condensed web passes

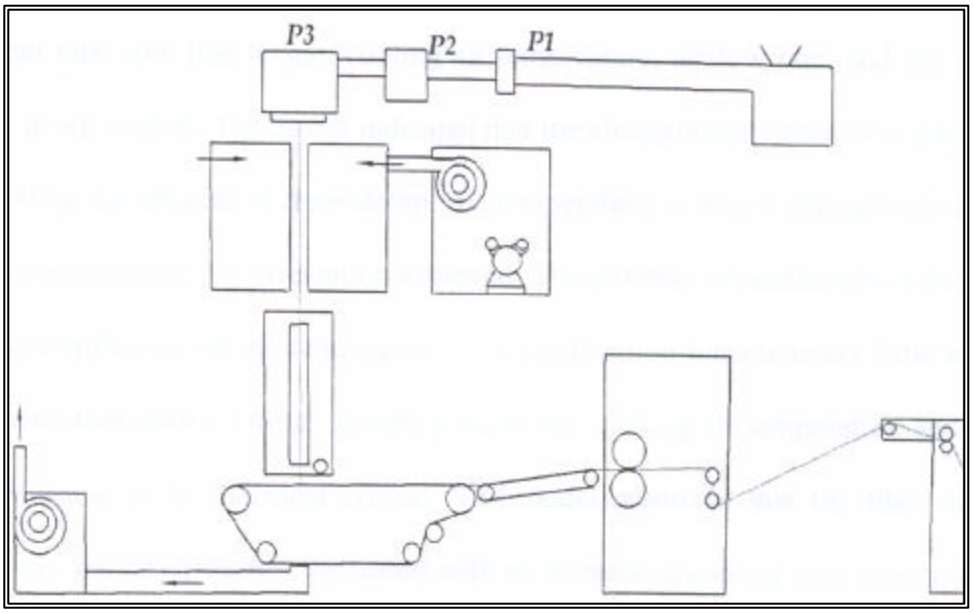

Fig 2.4 Schematic of Reicofil-II Spunbond Line

over moving belts and is thermally bonded by hot calenders. The bonded web is then wound under slight tension.

2.10 Fiber Morphology in Thermal Bonding

A good understanding of the role of fiber morphology in thermal bonding is very important to understanding the changes taking place during the process. Wei [22] studied the effect of bonding temperature on the aesthetic and textile properties of the thermally bonded polypropylene nonwoven fabrics. He observed that the mechanical properties (tensile strength and stiffness) of the fabrics were found to be greatly affected by the bonding temperature. The tensile strength and stiffness of the fabrics made from lower birefringence (less oriented) fibers showed higher values than those made from highly oriented structure. He also observed that this could be attributed to partial melting of ordered regions in the amorphous region; however, at higher temperature, shrinkage that coincides with the melting of small and imperfect crystals occurs abruptly and very steep for both fibers. It was observed that low orientation fibers yield fabrics that are generally stronger, and exhibit lower shrinkage.

Zhang [28], and many authors [29-34] have studied the evolution of structure and properties in the spunbonding process. The studies showed that fiber morphology plays an important role in bond formation. The nature of bond points depends on fiber morphology.

Chand [35] showed that fiber morphology plays a very important role in determining optimum bonding conditions of the webs. The studies showed that fibers with relatively less developed morphology yielded stronger and tougher webs as compared to fibers with

more developed morphology. The fiber with high molecular orientation and crystallinity tended to form a weak and brittle bond due to the lack of polymer flow and to the fibrillation of the fibers in the bonded regions.

CHAPTER III

EXPERIMENTAL DETAILS

3.1 Processing

3.1.1 Staple Fiber Webs

Polypropylene staple fibers produced at FiberVisions, Inc., were carded and then calendered at their laboratories. Bonding was carried out using different sets of pattern rolls, to obtain a range of bond areas and bond sizes (Table 3.1) so that a comparison could be made. The effective bond areas used varied from about 10% to 23.2%. The bonding temperature, was varied from 144°C to 172°C in increments of 4°C for different fabrics. The nip pressure of 45 psi (pounds per square inch) was kept constant for all the samples, and production speed of the samples was 250 ft/min.

Table 3.1 Details of Staple Fiber Samples Produced

Sample Series	Bond Area, %	Bond Size (inches X inches)
I	10.8	0.020 X 0.0385
II	23.2	0.022 X 0.040
III	15.2	0.020 X 0.039
IV	18.8	0.025 X 0.053
V	19.9	0.030 X 0.057

2.1.2 Spunbond Webs

Spunbond studies were carried out using a 35 MFR Exxon PP. The Spunbond fiber webs were prepared at Kimberly Clark, Roswell, GA and calendered at Fiber Visions, Covington, GA. A total of 6 series of samples were produced at temperatures varying from 120 to 160°C in increments of 10°C. Bonding was carried out using different sets of pattern rolls, to obtain a range of bond areas and bond sizes so that a comparison could be made. The effective bond areas used varied from about 10.8% to 23.5%. The pressure was kept constant at 45 psi and production speed was 250 feet/min for all the samples. The sample description is given in Table 3.2.

3.2 Characterization of the webs

3.2.1 Basis Weight

The basis weight was measured using the IST 130.1-92 Standard Test Method for the Mass per Unit Area of Nonwoven Fabrics. Two 10" x 1" samples were cut from each web and weighed. The average values of weight measures were calculated and divided by the area to get the fabric basis weight (g/m^2).

3.2.2 Tensile Properties

Tensile properties of the fabrics were measured using a United Tensile Tester with test conditions described in the ASTM D1117-80 for nonwoven fabrics [36]. A gauge length of 5" (12.7 cm), width of 1" (2.54 cm) and extension rate of 5"/min (12.7 cm/min) were

Table 3.2 Details of Spunbond Samples Produced

Sample No	Bonding Temperature	Bond Area (%)	Bond Size (in X in)
1-130	130	23.5	0.022 X 0.041
1-140	140		
1-150	150		
1-160	160		
2-120	120	10.8	0.020 X 0.040
2-130	130		
2-140	140		
2-150	150		
2-160	160		
3-130	130	15.2	0.020 X 0.039
3-140	140		
3-150	150		
3-160	160		
4-130	130	18.6	0.025 X 0.053
4-140	140		
4-150	150		
4-160	160		
5-140	140	12.0	
5-150	150		
5-160	160		
6-140	140	14.3	0.020 X 0.040
6-150	150		
6-160	160		

used in both machine direction and cross direction for the webs.

3.2.3 Single Bond Strip Tensile Test

This test was done in order to estimate bond strength and the degree of load sharing between fibers during the tensile deformation of the web. A schematic of this test is shown in Figure3.1. A strip of size 80 mm x 5 mm was cut from the web. The strip was cut across the width direction from two sides to leave only one bond uncut in the middle of the strip, as shown. The strip was then subjected to a conventional tensile test.

The test was conducted on the United Tensile Tester with a gauge length of 1" (2.54 cm) and extension rate of 0.5"/min (1.27 cm/min). A total of twenty tests were done for each sample.

3.2.4 Fabric Flexibility (Cantilever Method)

According to ASTM D1388-64 Standard Test Method for Stiffness of fabrics, four 1"x 6" specimens were cut and tested using the F.R.L. Cantilever Bending Tester with an inclination angle of 41.5°. The bending length I is exactly half-length of the fabric that overhangs the edge and bends under its own weight. Each test specimen was measured with four readings on each end of both sides. Flexural Rigidity (G), a measure of the interaction between weight and stiffness, was calculated using the equation:

$G = W \times c^3$

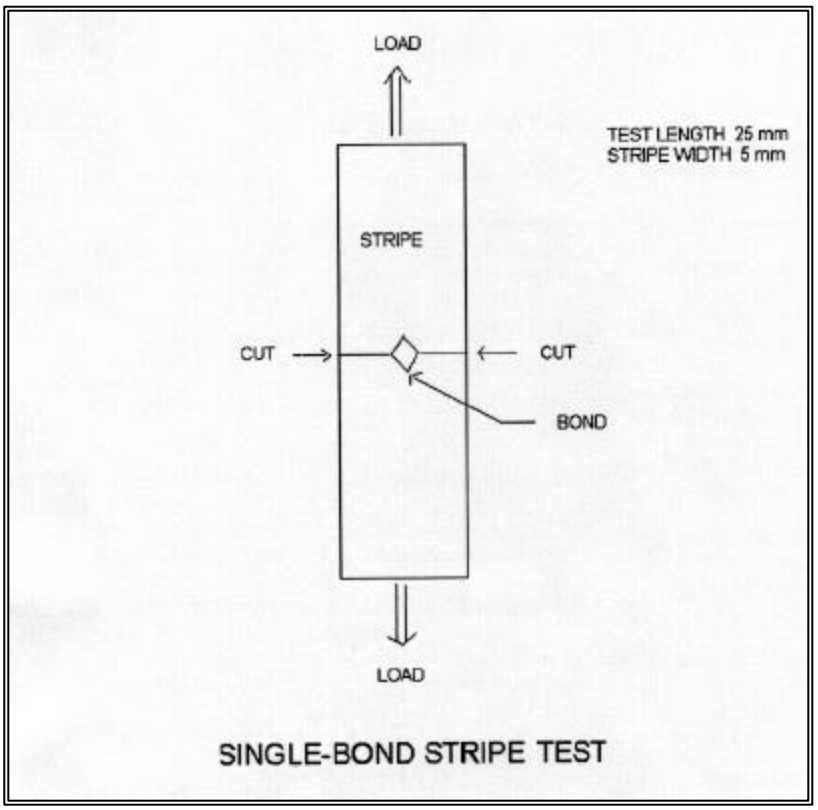

Fig 3.1 Schematic of Single Bond Strip Tensile Test

3.2.5 Tear Strength

The tear strength was determined using the Elemendorf tear tester. INDA standard test 100.1 (ASTM D5734) was the method used to measure the tear strength. Measurements were taken along the machine and cross directions. A total of five measurements were taken for each web sample.

3.2.6 Diameter and Birefringence

Fiber diameter and birefringence were measured using an optical microscope. The retardation technique was used for measurement of birefringence. For unbonded regions of the web, fibers in that region were cut and separated from the web using a sharp pair of scissors. Thirty measurements were taken in all cases.

3.2.7 Wide Angle X-ray Diffraction (WAXD)

Crystallite size was measured using the Rigaku WAXD system in reflection mode. Crystallite size was calculated automatically by the computer from full-width at half maximum intensity of reflection peaks in equatorial scans [38]. Equatorial scans were obtained from $2\theta = 10°$ to $30°$ in steps of $0.01°$ and a dwell time of 4 seconds. "Duco Cement" was used as a glue for sample preparation for equatorial scans. Use of Duco Cement was helpful in sample preparation from only bonds and very short fibers from unbonded regions of the web. Duco Cement is totally amorphous and does not interfere with crystalline peaks of polypropylene. The Rigaku WAXD system was operated at 35

kV and 30 mA. Bonded and unbonded regions were carefully separated from the web using a pair of sharp scissors.

3.2.8 Scanning Electron Microscopy

SEM images of the fabrics and the samples from tensile tests were taken using a Hitachi S- 3500N electron microscope. Back-scattered images, under 30 Pa gas pressure, were taken in order to minimize the problems due to static charge generation. Images were obtained at magnification ranges of 90 to 1000x. Samples of staple and spunbond webs were examined for single bond strength and tensile strip test under conventional tensile tester. The samples were tested at intermediate stages (65% to 80% of strength of webs tested for failure stage) to see at what stage of loading the web failure began at the bond point, in addition to observing at the fractured stage (failure stage).

3.2.9 Statistical Analysis

Statistical analysis was done using the 'Analysis of Variances' method, the GLM procedure in SAS. Statistical analysis was done for both staple fiber and spunbond studies. Fifteen null hypotheses were tested:

1. No significant effect of bonding temperature on peak load (MD and CD have significant difference), tear strength (MD and CD have no significance difference) and bending length (MD and CD are significantly different) for staple fiber webs.
2. Significant effect of bond area on peak load (Significant differences were also observed among the sample series), tear strength (III is significantly different from I and II). But, bond area does not have a significant effect on bending length

(II is significantly different from I and III across all temperature levels) for staple fiber webs.

3. Significant effect of bond size on peak load (Significant differences were also observed among the samples across all the temperature levels). No significant effect of bond size on tear strength and bending length for staple fiber webs.
4. Significant effect of bond area on peak load (Significant differences among the samples across the temperature levels), tear strength (sample 3 is different from samples 1 and 2) and significant effect of bond area on bending length (sample 2 is significantly different from samples 1 and 3) of spunbond webs.
5. Significant effect of bond size on peak load (significant effect within the sets of the samples), tear strength (significant difference among the sets of the samples, sample 4 is significantly different from samples 3 and 6), and no significant effect of bond size on bending length of spunbond webs.

CHAPTER IV

RESULTS AND DISCUSSION

4.1 Staple Fiber Studies

4.1.1 Web Properties

A single bond strip tensile test was done in order to estimate the bond strength and the degree of load sharing between the fibers during tensile deformation. This single bond strip test was chosen for the investigation since, during this test, stress is forced to concentrate on a single bond. As a result, it is possible to obtain a good estimate of the strength of a bond. Obviously the fabric strength should relate in some way to bond strength. The single bond tensile strength values of the webs bonded over a wide range of bonding temperatures are shown in Fig 4.1. From the figure, it is observed that with increase in bonding temperature, the web strength increases up to a maximum and then decreases with further increase in temperature. Chand [35] and Dharmadhikary [39], observed similar trends. Web elongation and initial modulus are shown in Figures 4.2 and 4.3, respectively. Web elongation exhibited a similar trend to that of tensile strength. However, initial modulus did not show any optimum and continued to increase with increase in bonding temperature. Higher strength, breaking elongation and initial modulus may be partly attributed to higher breaking elongation of the fibers. Higher breaking elongation of the fibers leads to greater degree of load sharing between the fibers during web deformation. Tear strength values are shown in Fig 4.4. It

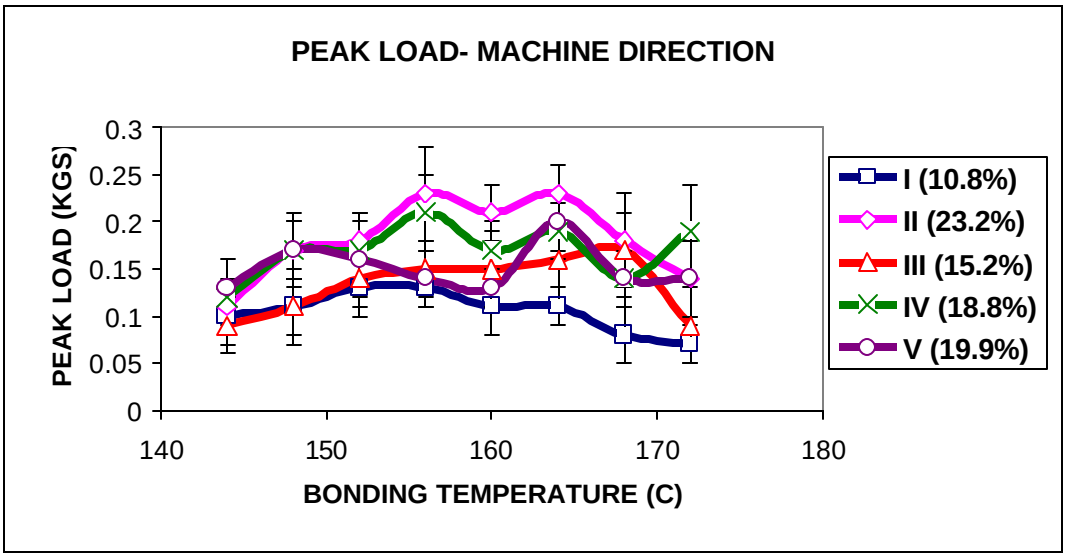

Fig 4.1. Peak Load From Single Bond Strip Test (MD) vs Bonding Temperature for Staple Fiber Webs

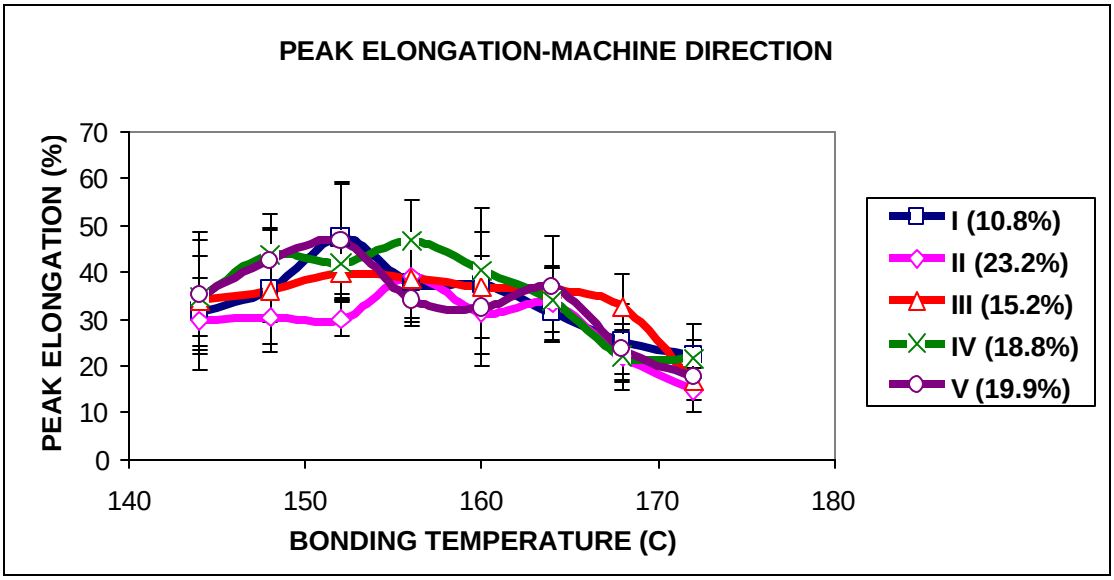

Fig 4.2. Peak Elongation From Single Bond Strip Test (MD) vs Bonding Temperature for Staple Fiber Webs

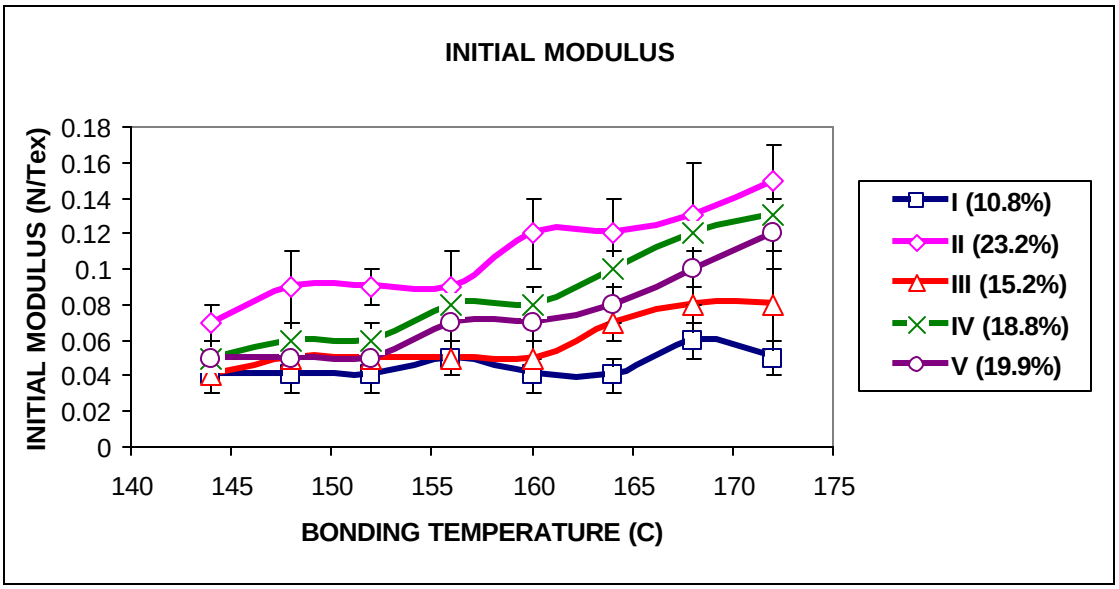

Fig 4.3 Initial Modulus From Single Bond Strip Test (MD) vs Bonding Temperature for Staple Fiber Webs

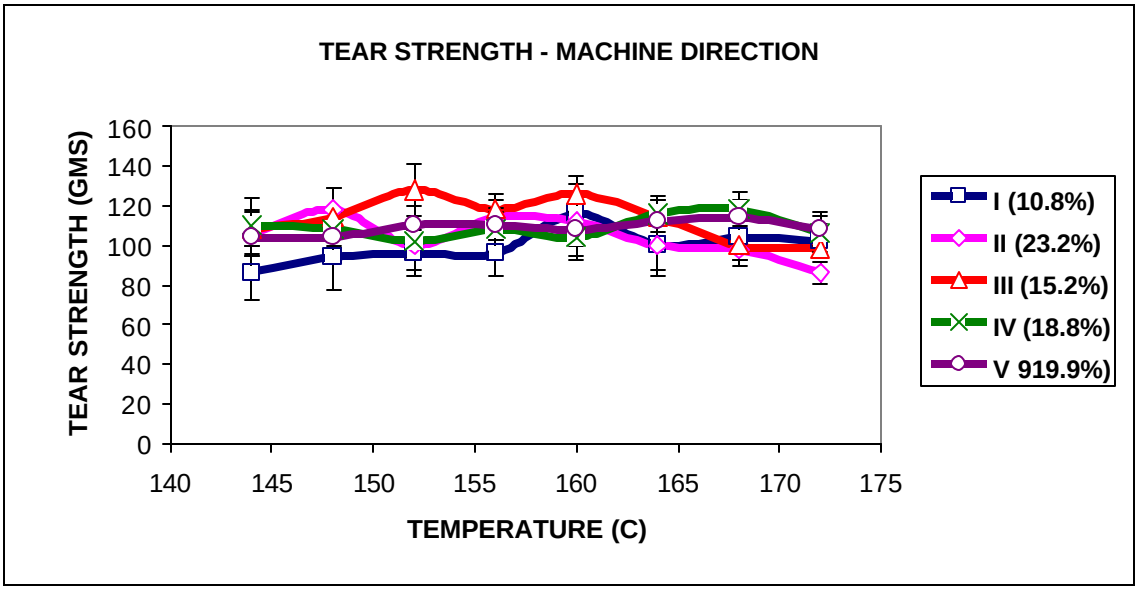

Fig 4.4. Tear Strength (MD) vs Bonding Temperature for Staple Fiber Webs

is observed that the changes in tear strength values along the range of bonding temperature are minimal for all the set of staple fiber samples. The bending length values of the staple fiber webs is given in Fig 4.5, and there is a slight increase in bending length with increase in bonding temperature for all the set of samples. The fracture mechanism of the single bond tensile test samples is analyzed and discussed in the next section.

Effects of bond area, bond size and bonding temperatures, and their combined effects are discussed below with respect to staple (thermal bond) and spunbond samples

4.1.2 Effect of Bonding Temperature

To determine the effect of bonding temperature on the fiber morphology and strength of the web, Set I series of samples were chosen which have 10.8% of bond area and (0.020 X 0.0385) of bond size, respectively. From Fig 4.6, it was observed that there is a large difference between the values of peak loads (from single bond strip tensile test) in the two directions. The difference in peak load between the two directions is larger at lower temperatures. With increase in bonding temperature, the difference decreases, largely due to drop in the strength values in the MD. This change in values with bonding temperature is attributable to change in failure mechanism. Fig 4.7 shows the tear strength values for the control series in both MD and CD. Here, we can observe that the values in the CD are higher than the MD along the range of bonding temperature. Fig 4.8, bending length values are shown where it is observed that the values in both the

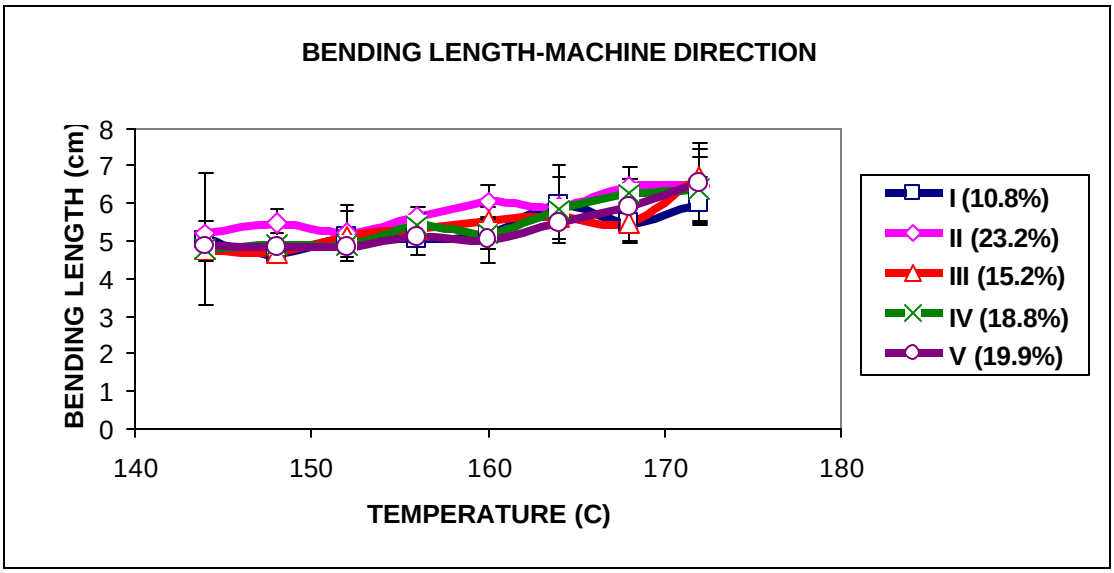

Fig 4.5. Bending Length (MD) vs Bonding Temperature for Staple Fiber Webs

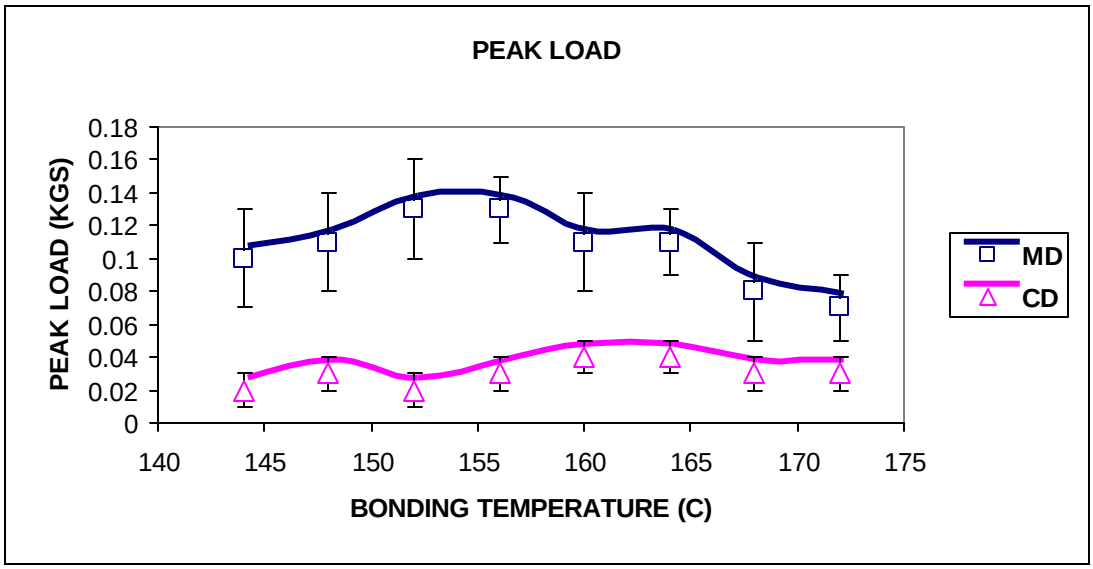

Figure 4.6. Peak Load (Single Bond Test) vs Bonding Temperature for Set –I Sample of Staple Fiber Webs

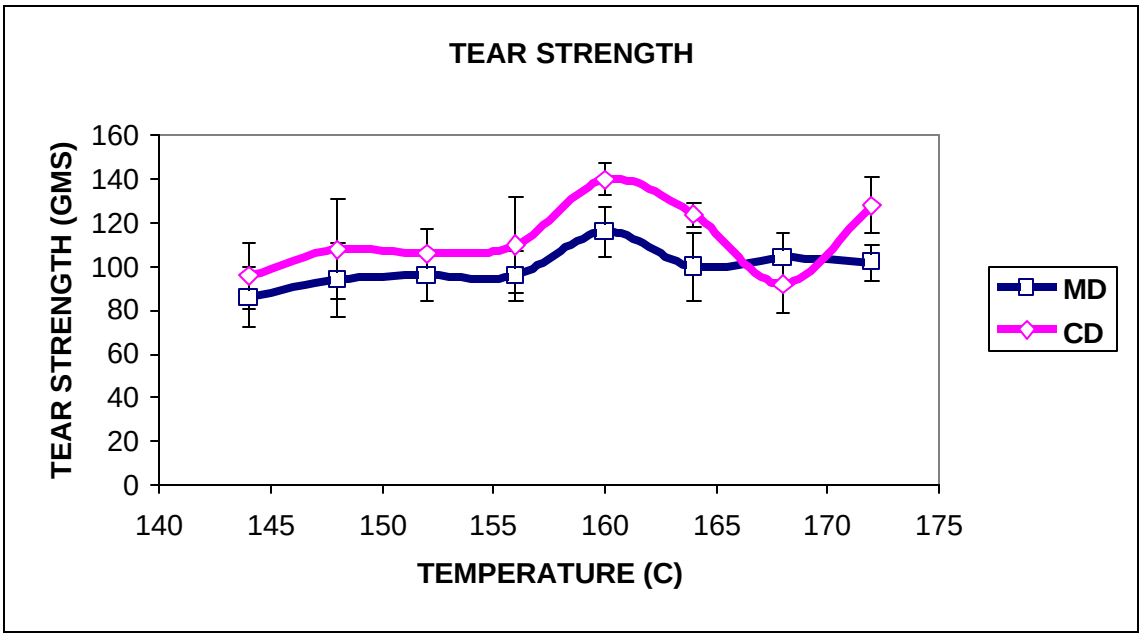

Fig 4.7. Tear Strength Values for Set – I Sample vs Bonding Temperature for Staple Fiber Webs

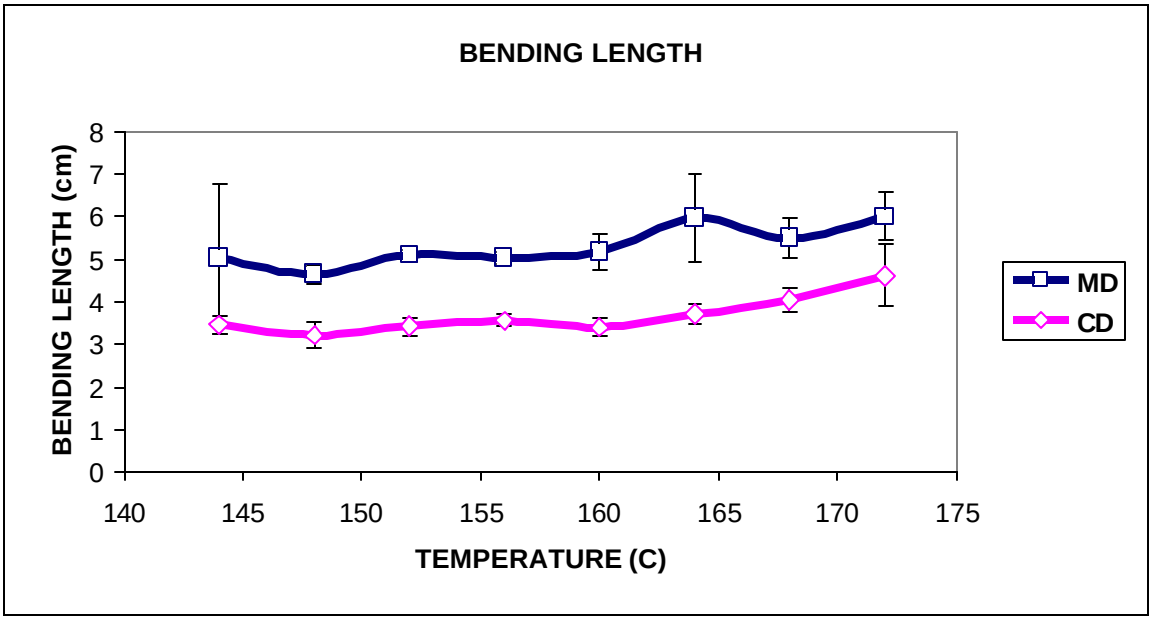

Fig. 4.8. Bending Length Values of Set – I Sample vs Bonding Temperature for Staple Fiber Webs

directions, machine and cross directions follow the same pattern along the range of bonding temperature, but, the values of MD are higher than the values in CD. This shows that the web becomes stiffer with increase in bonding temperature

4.1.3 Effect of Bond Area

The effect of Bond Area was studied using three sets of samples which vary in bond area, but have bond size in the same range (Set-I (0.020 X 0.0385), Set-III (0.020 X 0.039), Set-II (0.022 X 0.040)). For this, Set- I (10.8%), Set- III (15.2%) and Set-II (23.2%) were chosen, so that we can clearly see the differences of the effect of bond area on morphology and strength of the web.

Fig 4.9, shows results of the comparison of bond area with peak load values from single bond strip test in MD for the three sets of samples. It is observed that the sample Set- II (23.2%) shows higher strength along the range of the bonding temperature investigated, when compared with the other two sets of samples, which had lower bond areas compared to Set- II. This shows that the higher strength values with increased in bond area are observed. There is a simultaneous decrease in elongation and an increase in modulus as well. These differences may also be attributable to differences in the failure mechanism. As a result of more efficient bonding with increase in bond temperature, the web becomes stiffer. Fig 4.11, shows the observed bending length values, which clearly show the trend with temperature for all the samples. But, the bending length differences taking place in all the samples across the range of the bonding temperatures are very small. Fig 4.10 shows the tear strength values of the three sets of samples to compare the

effect of bond area. It is observed that the webs with higher bond areas Set- II and Set- III show higher tear strength values along the range of the bonding temperature when compared to web of Set- I (10.8%). The differences in the tear strength values for all the three sets of samples are minimum.

4.1.4 Effect of Bond Size

For comparing the effect of bond size on strength of the web and the morphology, three sample series were selected and they are Set- III (0.020 in X 0.039 in), Set- IV (0.025 in X 0.053 in) and Set- V (0.030 in X 0.057 in) (Bond Areas are, Set-III- 15.2%, Set-IV- 18.8%, Set-V-19.9%) (Table 3.1, p-27) respectively. These samples are selected in such a way that the bond areas are in the same range, so that these bond area differences do not interfere with the bond size differences.

Fig 4.12 shows the values of the peak load of the three samples along the range of bonding temperature from the single bond strip test. It is observed that the webs having higher bond sizes show higher load values compared to samples with lower bond sizes. That is, samples from Set- IV and Set- V show higher peak load values compared to Set- III. This difference can be due to differences in the failure mechanism. Also, there is a slight increase in the peak load values with an increase in the bonding temperature for all three sets of samples. The differences observed for tear strength values for the three set of samples are very minimal. From Fig 4.13, it is clear that a mixed pattern was observed for all the set of samples. Its also observed for a range of bonding temperature that, the sample Set- III, with least bond size compared to the other two, showed higher tear

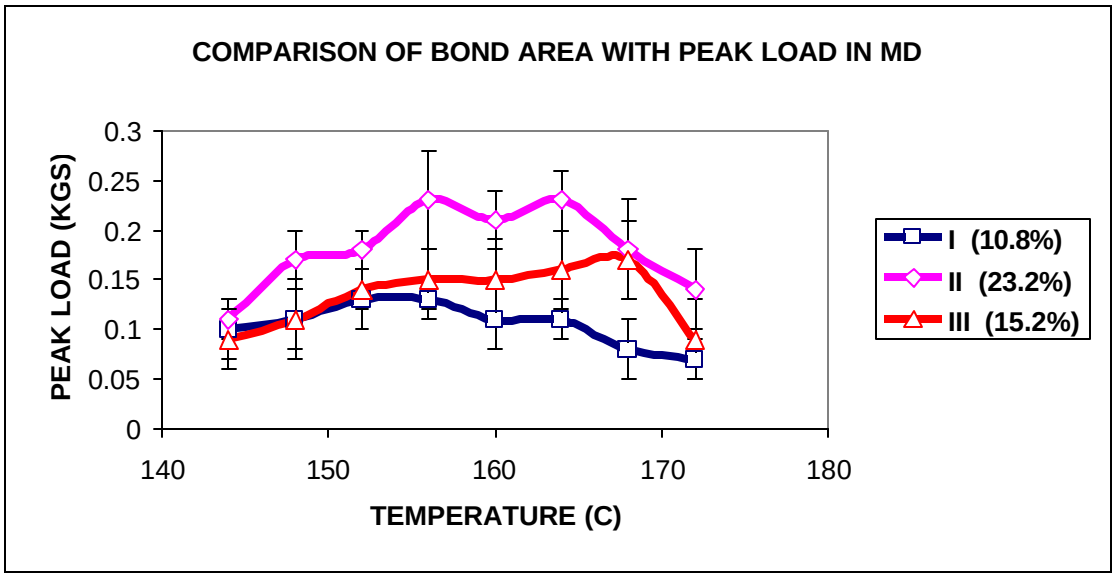

Fig 4.9. Comparison of Bond Area with Peak Load From Single Bond Strip Test (MD) vs Bonding Temperature for Staple Fiber Webs

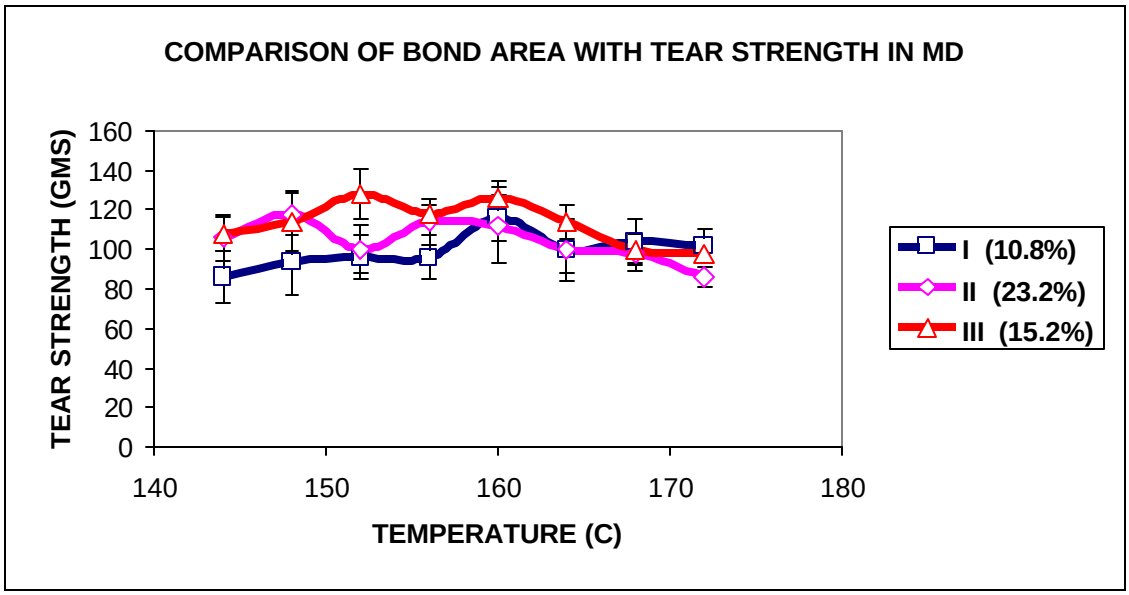

Fig 4.10. Comparison of Bond Area (MD) with Tear Strength vs Bonding Temperature for Staple Fiber Webs

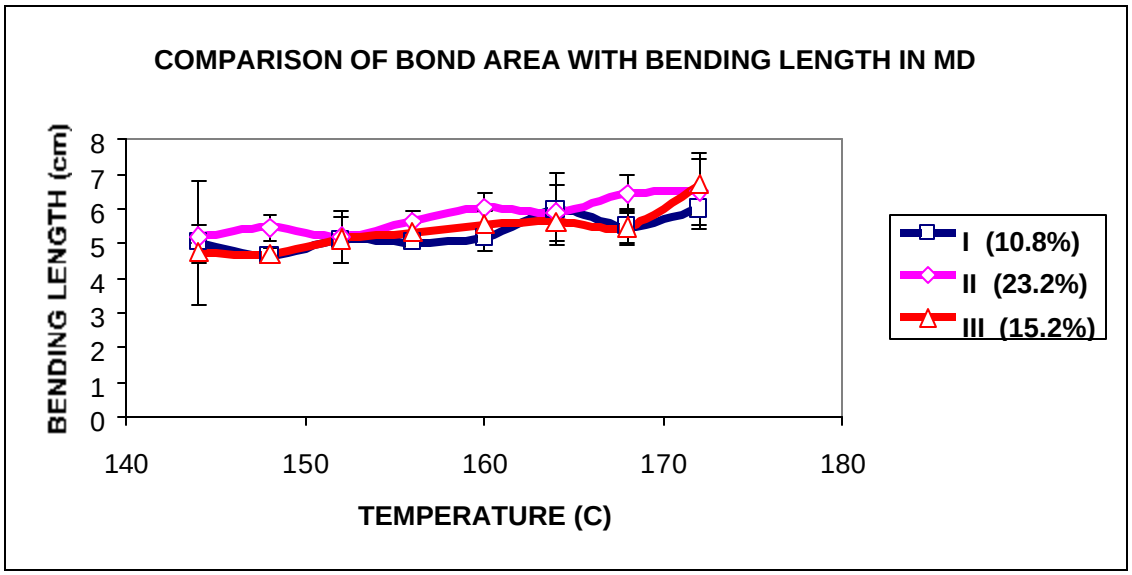

Fig 4.11. Comparison of Bond Area (MD) with Bending Length vs Bonding Temperature for Staple Fiber Webs.

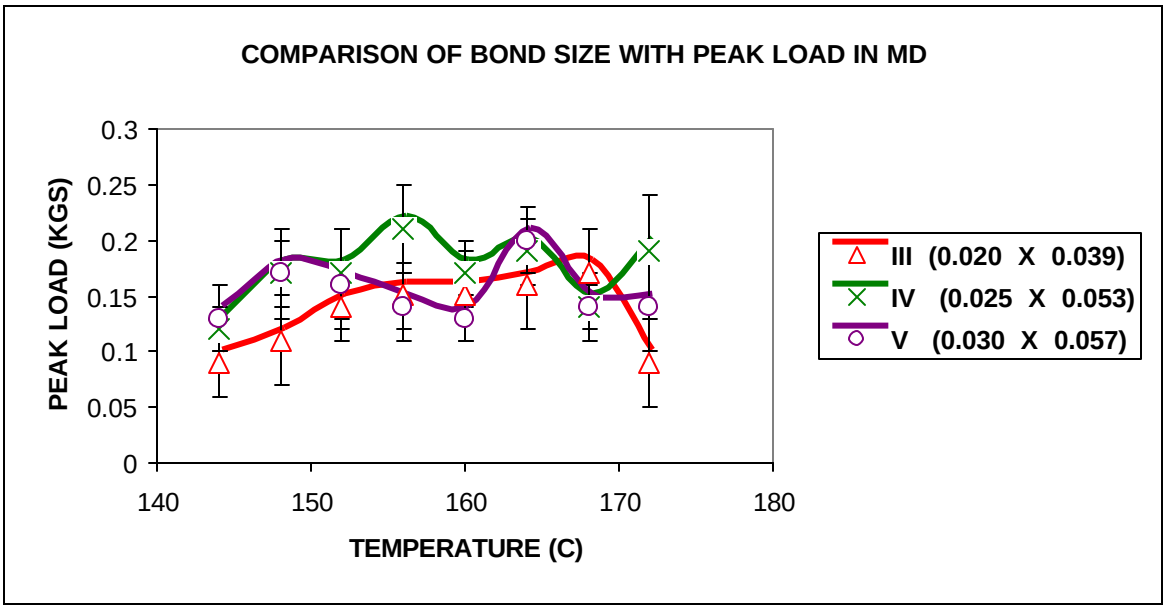

Fig 4.12. Comparison of Bond Size with Peak Load From Single Bond Strip Test (MD) vs Bonding Temperature for Staple Fiber Webs

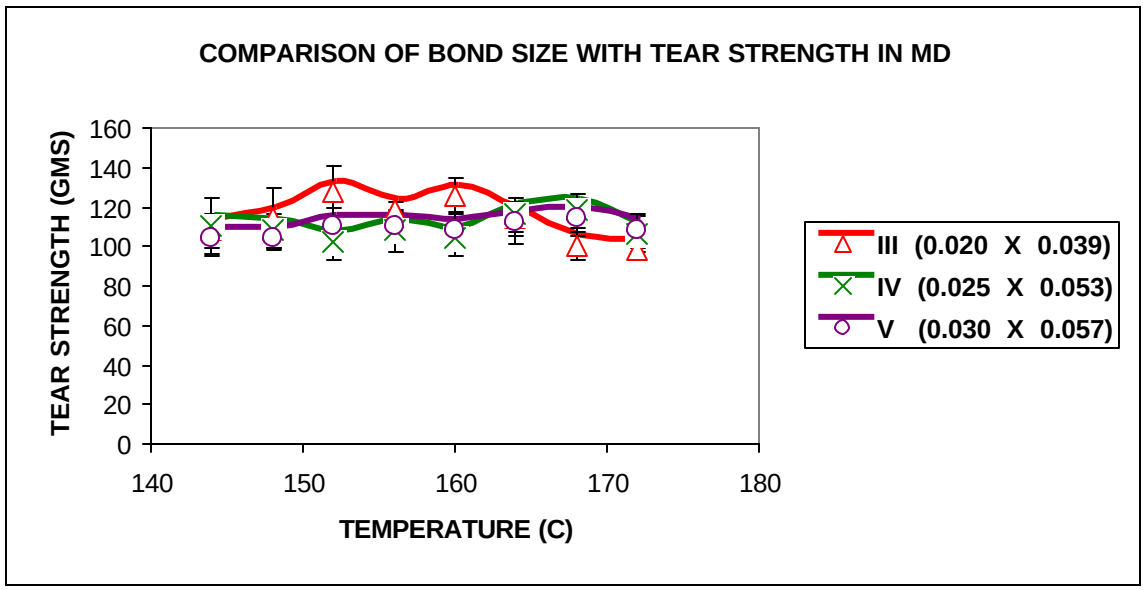

Fig 4.13. Comparison of Bond Size with Tear Strength (MD) vs Bonding Temperature for Staple Fiber Webs

strength. These minimal differences, which were observed in peak load and tear strength values are also seen in bending length values from Fig 4.14. Despite minimal differences in bending length values, all the three set of samples show increase in stiffness values along the range of bonding temperature. This is true as the webs become stiffer with the increase in the calender temperature.

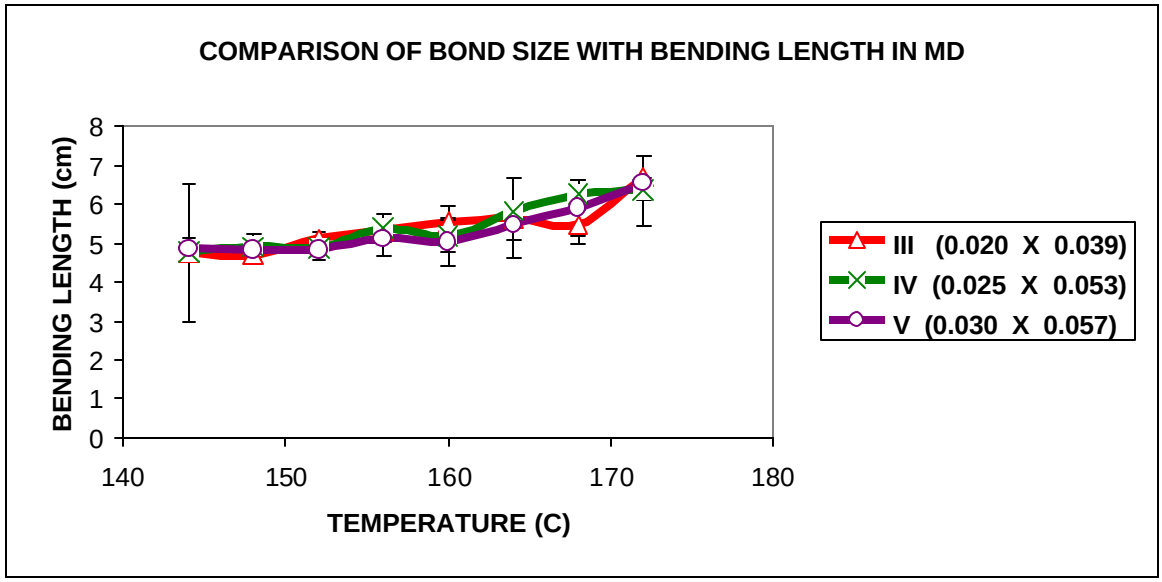

Fig 4.14. Comparison of Bond Size with Bending Length (MD) vs Bonding Temperature for Staple Fiber Webs

4.1.5 Analysis and Discussion

Fracture mechanisms of the webs were studied using the scanning electron microscope (SEM) photographs. All the samples were analyzed after the tensile test. The pictures were taken for samples produced at lower, medium (optimum) and higher bonding temperature at intermediate (65% to 80% of the breaking load) and failure stages, respectively.

4.1.6 Effect of Bonding Temperature

Samples, stretched to intermediate stages were examined to see how the bond deforms during single bond tensile testing. (Fig 4.15) At lower bonding temperature of 148°C, we can see that the bond starts disintegrating i.e., fibers start pulling out one by one from the bond point. The first picture shows the neighboring bond point, where the bond stays intact. From Fig 4.16, it is obvious that at the neighboring bond point (either above or below the bond at the notch), where the fibers start pulling out from the bond and the bond disintegrates. This is the main reason why the bond strength is less at lower bonding temperatures.

As observed from the Fig 4.17, webs bonded at medium bonding temperature (160°C), at the intermediate stage the fibers stretch out from the bond point and at the neighboring bond, re-orientation of fibers takes place making the bond point weak. In the failure stage

Neighboring Bond **Strained Bond**

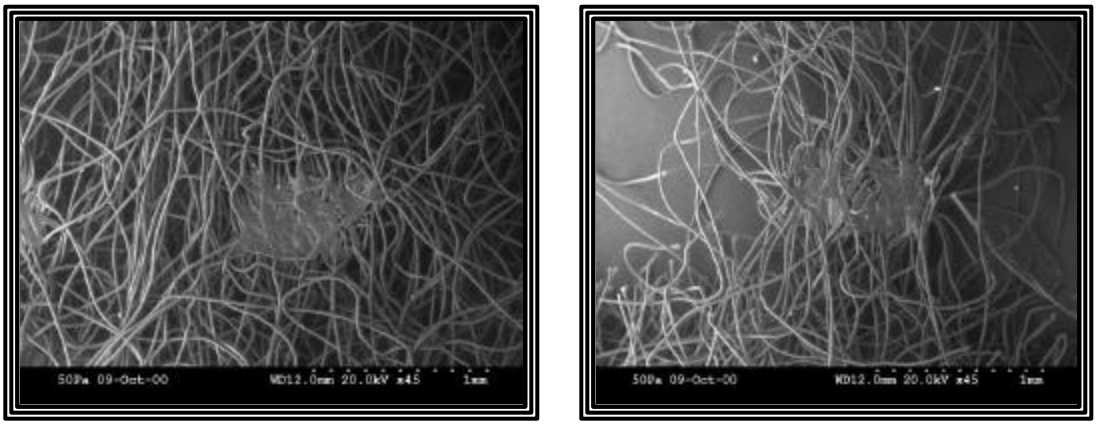

Fig 4.15 SEM Image Showing Disintegration of Bond at 148° C (Intermediate Stage)

Neighboring Bond **Strained Bond**

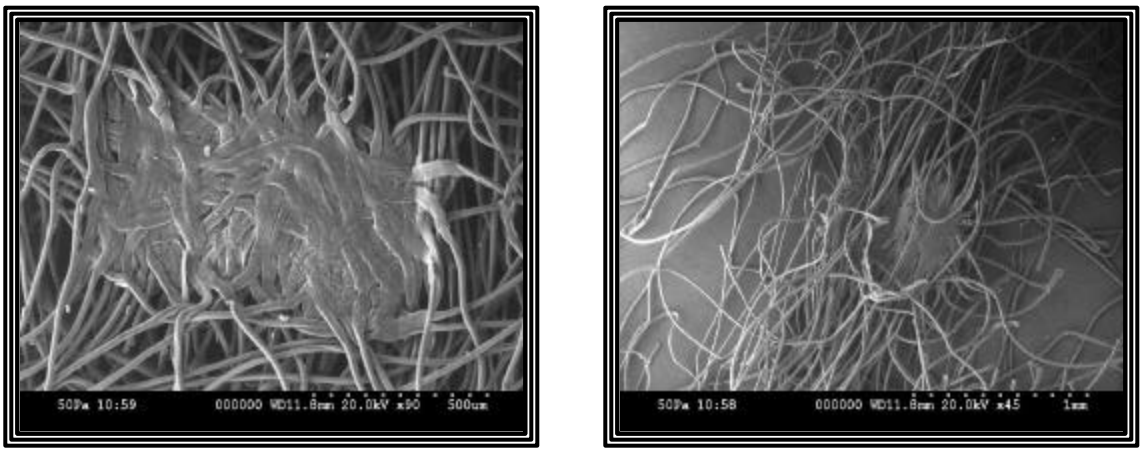

Fig 4.16 SEM Image Showing Disintegration of Bond at 148° C (Failure Stage)

Neighboring Bond **Strained Bond**

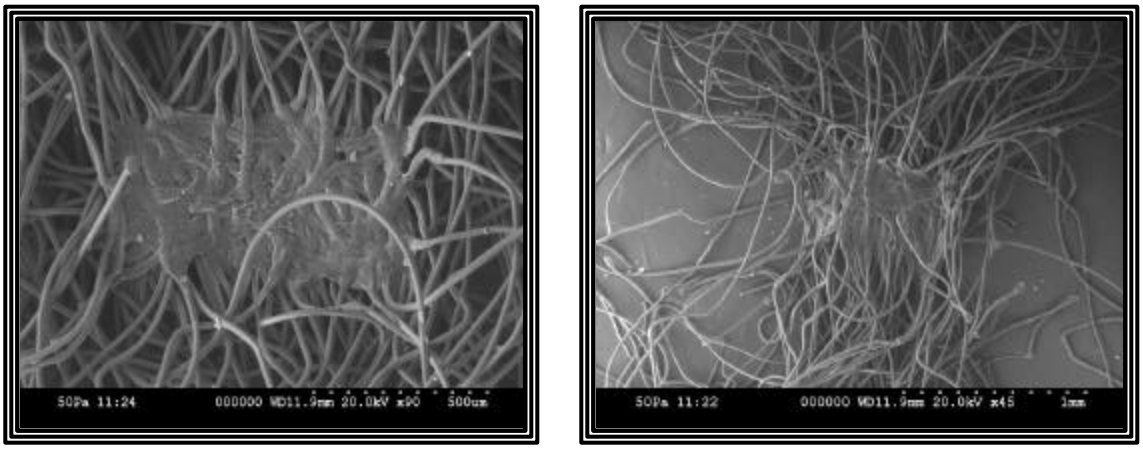

Fig 4.17 SEM Image Showing Re-Orientation of Fibers and Disintegration of Bond at 160° C (Intermediate Stage)

Neighboring Bond **Strained Bond**

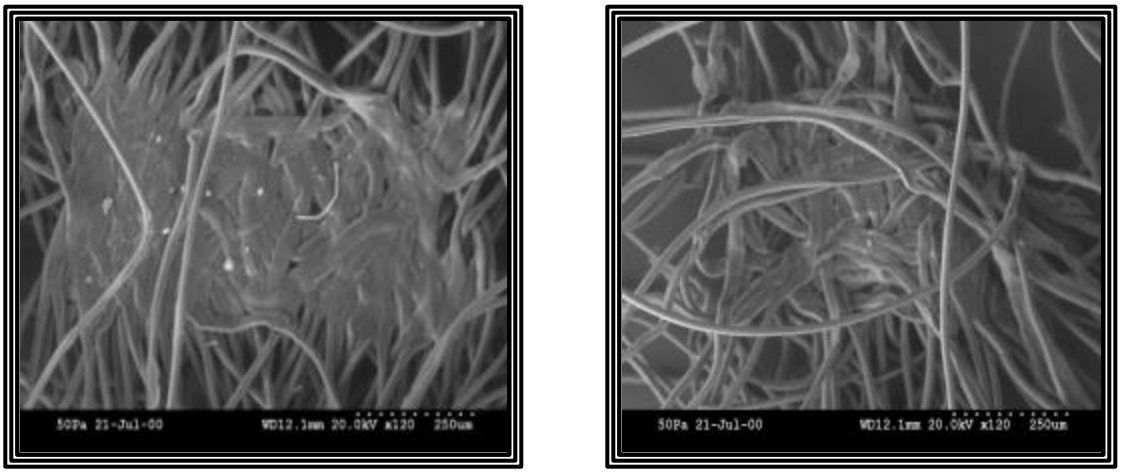

Fig 4.18 SEM Image Showing Re-Orientation of Fibers and Disintegration of Bond at 160° C (Failure Stage)

(Fig 4.18), fiber re-orientation takes place and slight disintegration of the bond can be seen. That is why at bonding temperatures around 160°C, the web strength was higher.

At higher bonding temperature (172°C), (Fig 4.19, Fig 4.20), it was observed both at intermediate and failure stages, the filaments break at the bond perimeter and the bond is still intact. Fiber morphology tests were done by birefringence and X-ray diffraction. (Table 4.1) The values of fiber birefringence are the same for all the samples indicating that the changes that might be taking place during bonding in the unbonded regions in these cases are minimal. This is due to the fact that the starting fibers have a fairly high level of orientation and, also due to higher processing speeds, since the dwell times in the calender are very low. However, the crystal sizes show differences in the bonded and unbonded regions, with the values being higher in the bonded areas. In the unbonded areas, crystal sizes are in the same range for all the process conditions investigated.

4.1.7 Effect of Bond Area

From the SEM photographs of the webs, which were taken from samples tested after the single bond tensile test and the fiber morphology parameters, we can see the effect of bond area on the strength and morphology of the web can be seen.

At lower bonding temperature (148°C), the fibers pull out from the bond point at the intermediate stage and during the failure stage, total disintegration of the web takes place (Figures 4.21 and 4.22), i.e., fibers pull out one by one from the bond point making the bond weak. Chand [35] also showed a similar trend of disintegration of the bond point at

Neighboring Bond **Strained Bond**

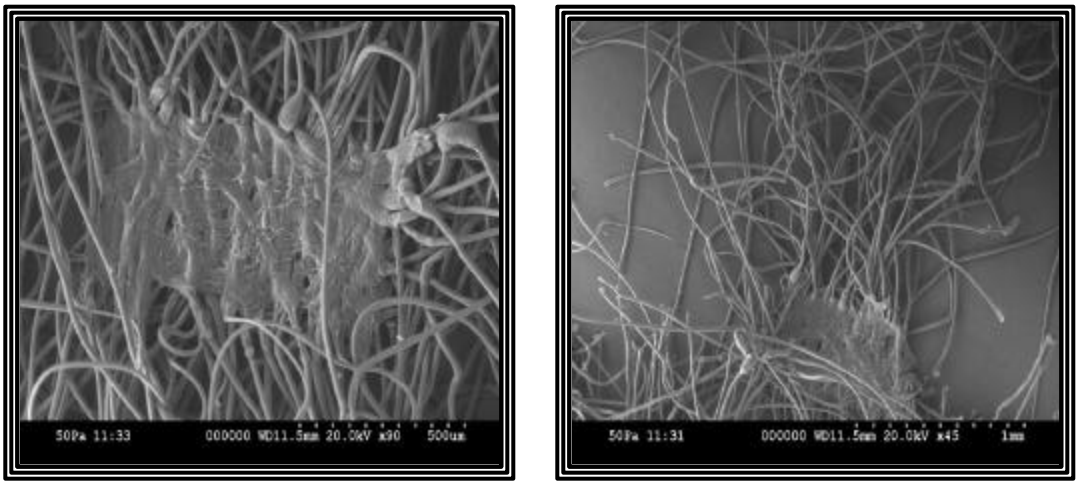

Fig 4.19 SEM Image Showing Filaments Breaking Near The Bond Boundary at 172° C (Intermediate Stage)

Neighboring Bond **Strained Bond**

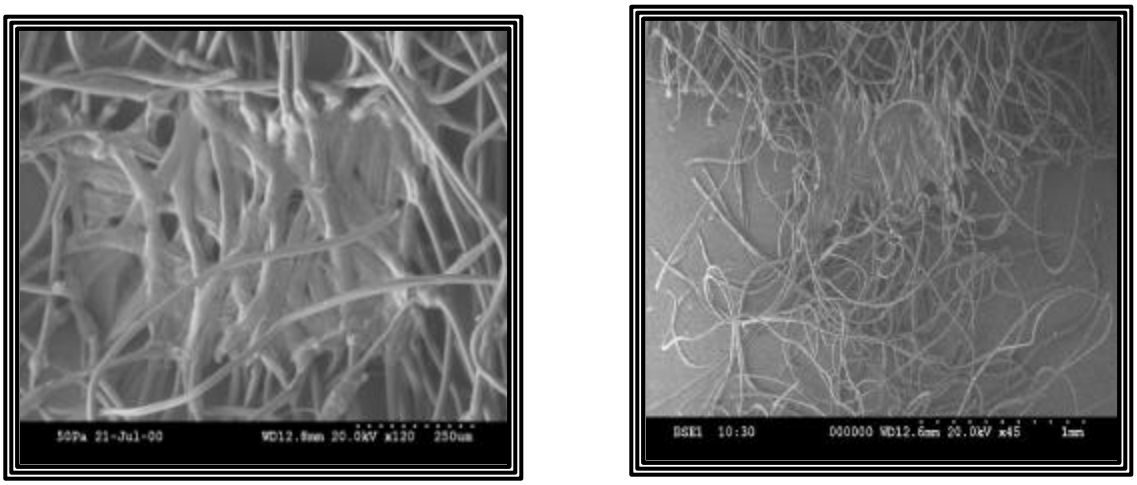

Fig 4.20 SEM Image Showing Filaments Breaking Near The Bond Boundary at 172° C (Failure Stage)

Table 4.1 Staple Fibers Morphological Parameters-Effect of Bonding Temperature

Temperature (°C)	Fiber Diameter (mm)	Birefringence	Crystal Size (A°) Unbonded	Crystal Size (A°) Bonded
SET – I				
144	18.1	0.024	106	156
148	18.4	0.023	107	171
156	18.3	0.023	106	170
160	17.8	0.024	102	171
168	19.4	0.020	110	163
172	18.1	0.024	108	179

Neighboring Bond **Strained Bond**

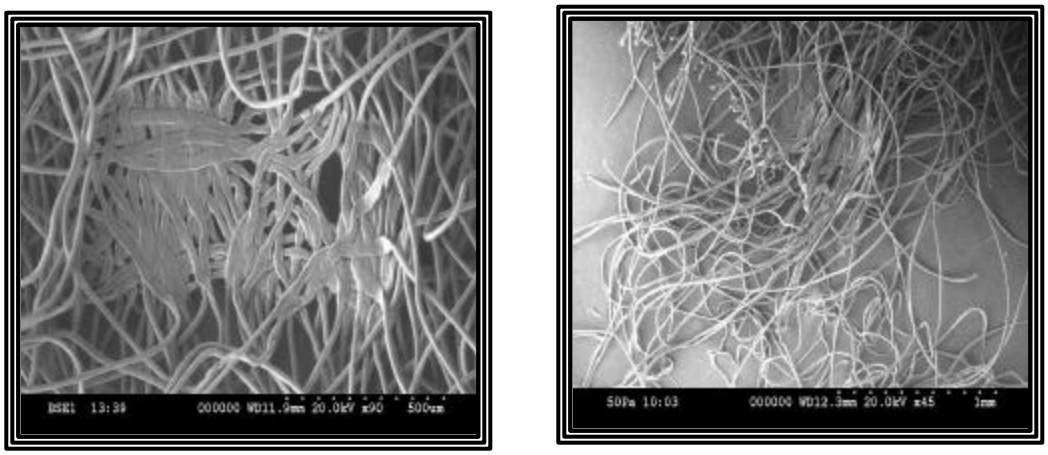

Fig 4.21 SEM Image Showing Disintegration of Bond at 148° C (Intermediate Stage)

Neighboring Bond **Strained Bond**

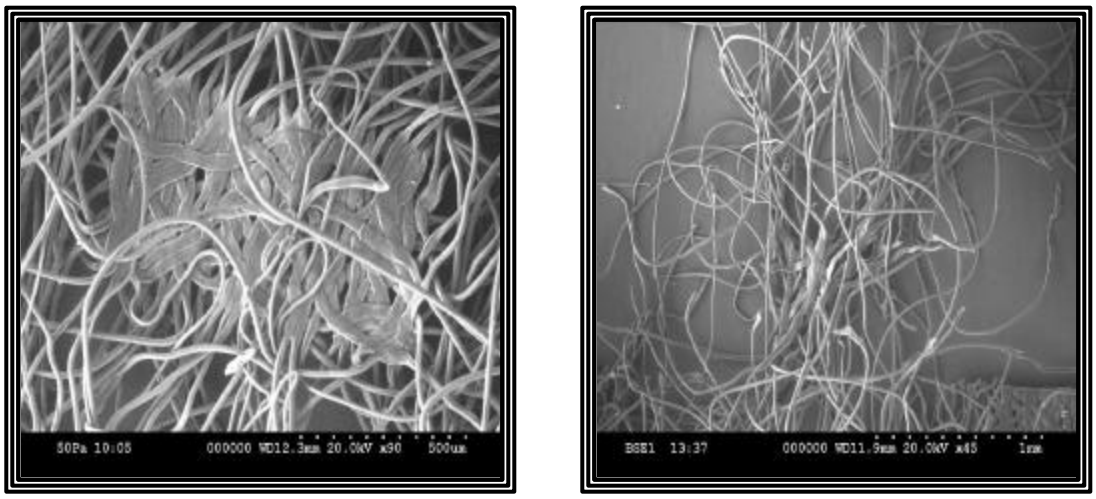

Fig 4.22 SEM Image Showing Disintegration of Bond at 148° C (Failure Stage)

Neighboring Bond **Strained Bond**

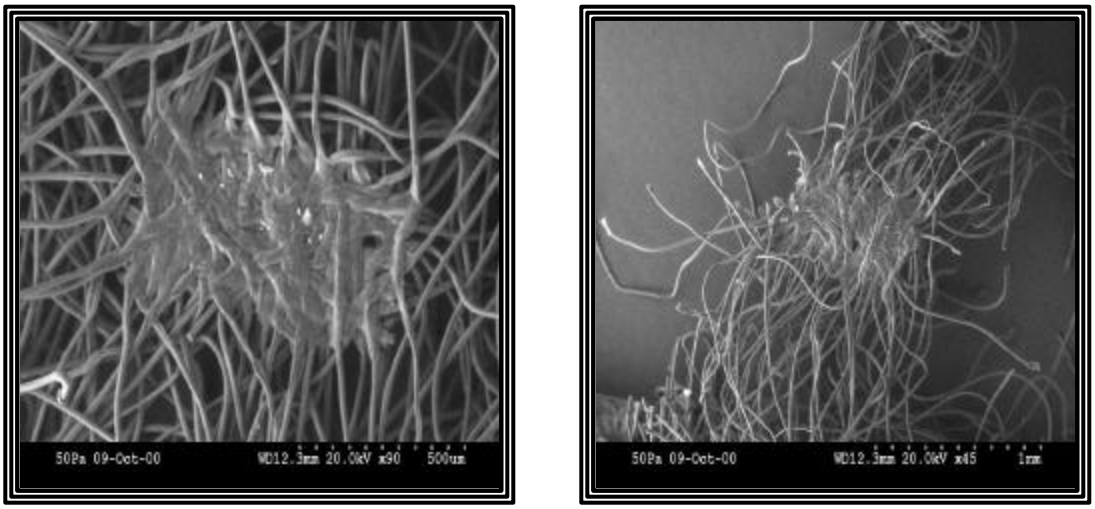

Fig 4.23 SEM Image Showing Re-Orientation of Fibers and Disintegration of Bond at 160° C (Intermediate Stage)

low bonding temperature. It is also seen that, there is a slight disintegration of fibers in the neighboring bond points at intermediate and failure stages. At a medium temperature of 160°C, from, re-orientation of fibers takes place in the neighboring bond points in both the intermediate and the failure stages (Fig 4.23 and Fig 4.24). The fibers stretch at the vicinity of the bond point, but the bond still remains intact at both the stages. At higher bonding temperature of 172°C, (Fig 4.25 and Fig 4.26), it is observed that the filaments break at the perimeter of the bond point. At this stage, the neighboring bond point is still intact because of higher bonding temperature. This phenomena is clearly seen both in the intermediate and failure stages. From Table 4.2, it is seen that the fiber diameter and fiber birefringence in the unbonded regions remain the same for all the samples indicating that the changes taking place during bonding in these cases are minimal. However, the crystal size values in the unbonded regions remain the same for all the samples and the crystal size values of bonded regions are higher than that of the unbonded regions. Within the bonded areas, the crystal sizes are slightly affected by bonding temperatures.

4.1.8 Effect of Bond Size

From Figures 4.27 and 4.28, it is obvious that at a lower bonding temperature of 148°C, at intermediate and failure stages the fibers pull out one by one from the bond point, i.e., the bond disintegrates and the bond becomes weak. Even the neighboring bond points exhibit the same trend, even though, not to that extreme. At medium bonding temperatures of 160°C, it can be seen that from Figures 4.29 and 4.30, re-orientation of

Neighboring Bond **Strained Bond**

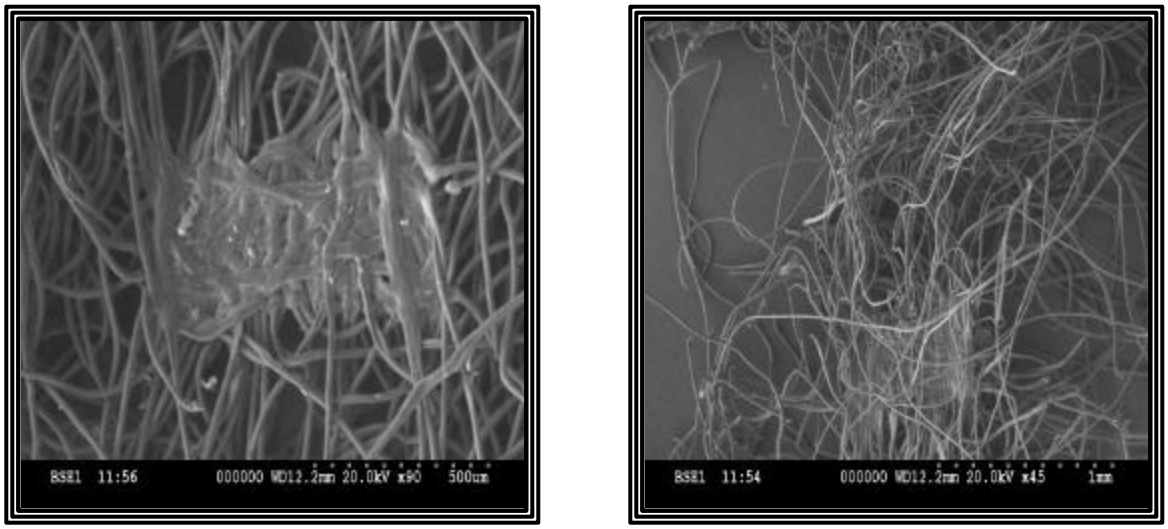

Fig 4.24 SEM Image Showing Re-Orientation of Fibers and Disintegration of Bond at 160° C (Failure Stage)

Neighboring Bond **Strained Bond**

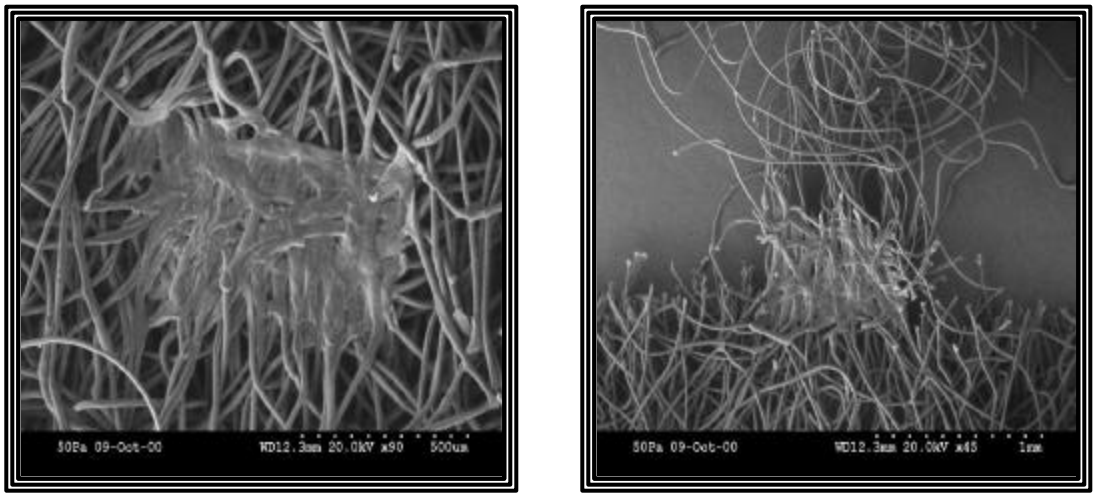

Fig 4.25 SEM Image Showing Filaments Breaking Near The Bond Boundary at 172° C (Intermediate Stage)

Neighboring Bond **Strained Bond**

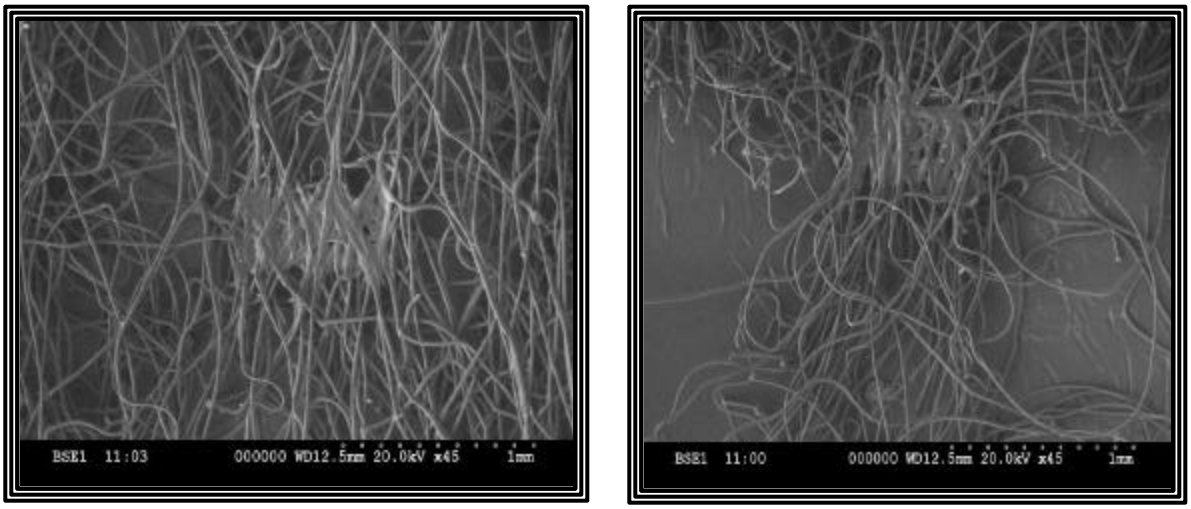

Fig 4.26 SEM Image Showing Filaments Breaking Near The Bond Boundary at 172° C (Failure Stage)

Table 4.2. Staple Fibers Morphological Parameters, Effect of Bond Area

Sample - (Temp) (° C)	Fiber Diameter (mm)	Birefringence	Crystal Size (A°) Unbonded	Crystal Size (A°) Bonded
SET- I (160)	17.8	0.024	102	171
SET- II (160)	18.3	0.024	109	163
SET- III 160)	18.8	0.023	104	153

Neighboring Bond **Strained Bond**

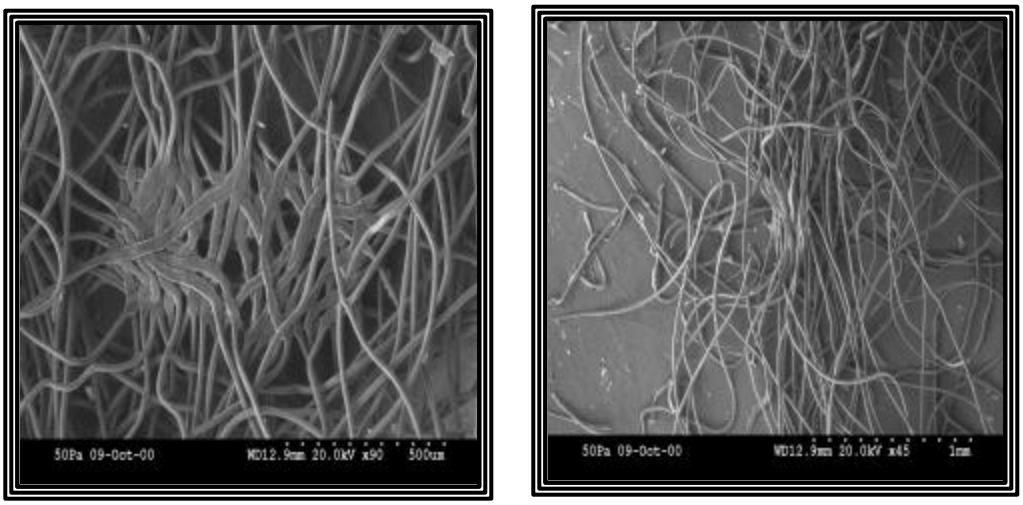

Fig 4.27 SEM Image Showing Disintegration of Bond at 148° C (Intermediate Stage)

Neighboring Bond **Strained Bond**

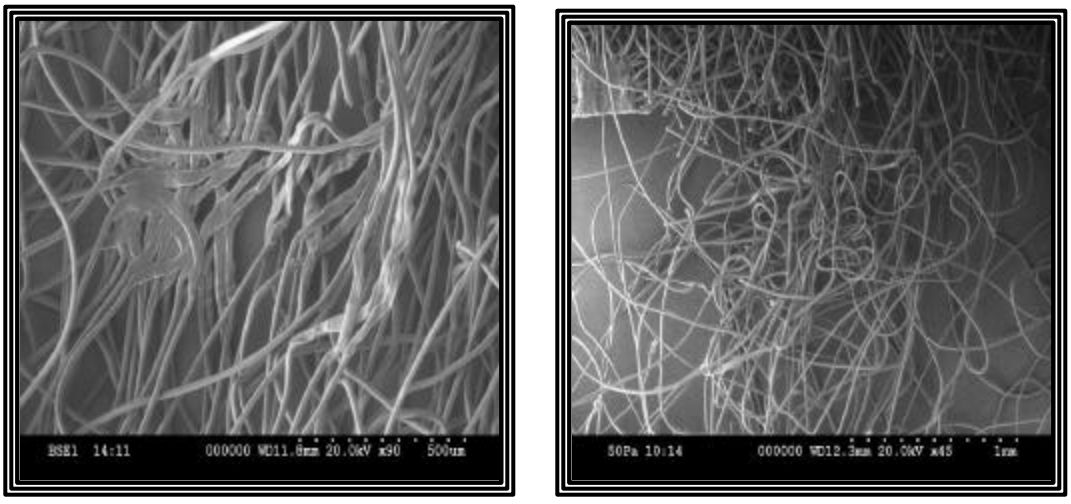

Fig 4.28 SEM Image Showing Disintegration of Bond at 148° C (Failure Stage)

Neighboring Bond **Strained Bond**

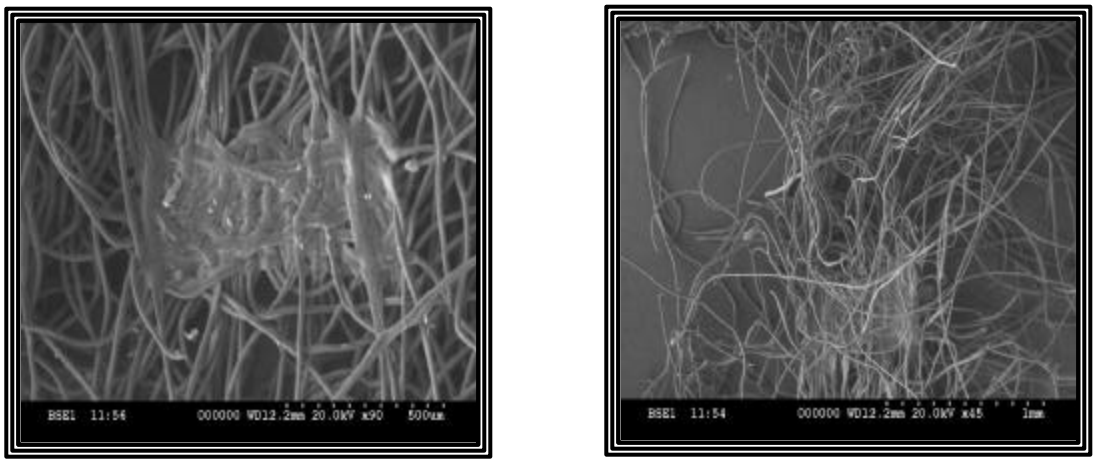

Fig 4.29 SEM Image Showing Re-Orientation of Fibers and Disintegration of Bond at 160° C (Intermediate Stage)

Neighboring Bond **Strained Bond**

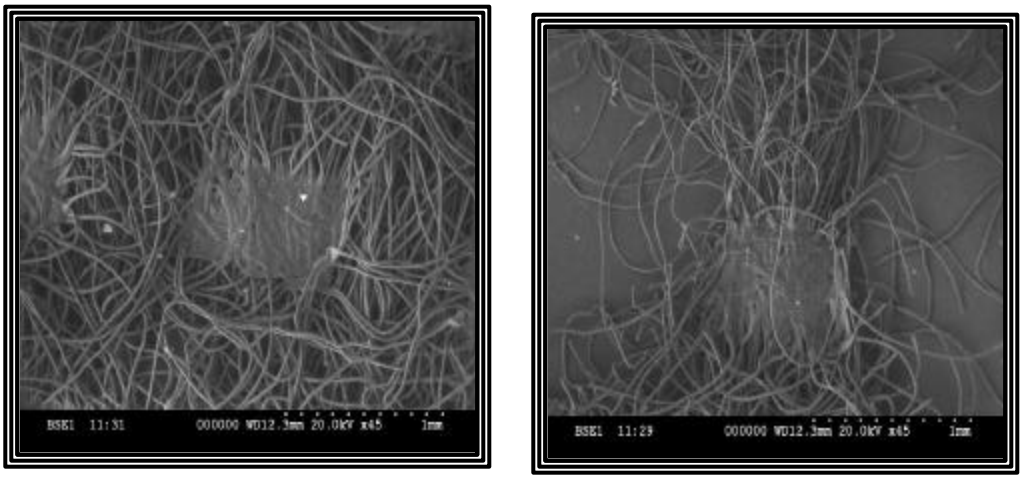

Fig 4.30 SEM Image Showing Re-Orientation of Fibers and Disintegration of Bond at 160° C (Failure Stage)

fibers take place in the bond point at both intermediate and failure stages. Fibers stretch from the main web making the bond point region stretch. But, the bond point stays intact in both the stages. At higher bonding temperature of 172°C, from Fig 4.31 and Fig 4.32, it is observed that the bond points stays intact, but, the filaments break at the periphery of the bond point making the bond weak. The bond point stays intact in both the stages. The neighboring bond point stays intact with the web in both the stages. This trend is also observed with the webs of other bond areas.

From the data in Table 4.3, it is seen that the fiber diameter and fiber birefringence values remain the same for all the samples. From these values it can be said that the changes taking place in the unbonded region during calendaring are minimal. Also the crystal size values for the unbonded regions remain in the same range. The crystal size values in the bonded regions are higher than those in the unbonded regions and the values in bonded regions vary because higher temperature and bonding conditions making these morphological changes taking place due to bond size variations insignificant.

4.2 Spunbond Studies

4.2.1 Web Properties

In this section, results from spunbond samples are discussed. A total of 6 series of samples were produced at bonding temperatures varying from 120 to 160°C. Bonding was carried out using different sets of pattern rolls, to obtain a range of bond areas and

Neighboring Bond **Strained Bond**

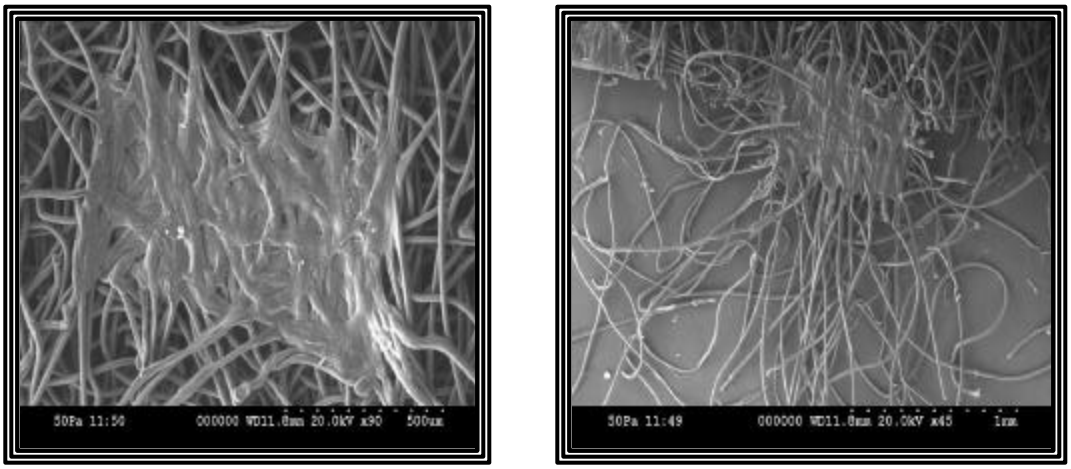

Fig 4.31 SEM Image Showing Filaments Breaking Near The Bond Boundary at 172° C (Intermediate Stage)

Neighboring Bond **Strained Bond**

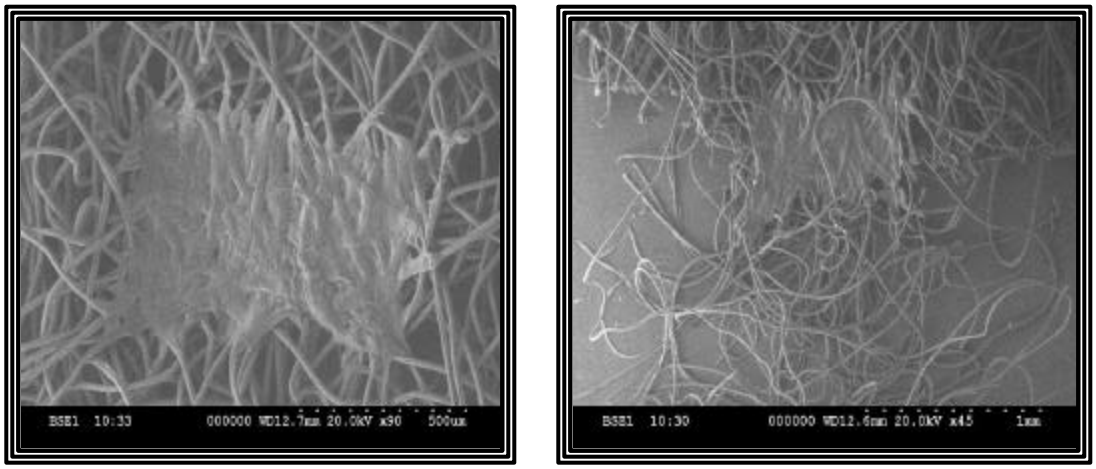

Fig 4.32 SEM Image Showing Filaments Breaking Near The Bond Boundary at 172° C (Failure Stage)

Table 4.3 Staple Fibers Morphological Parameters, Effect of Bond Size

Sample - Temp (°C)	Fiber Diameter (mm)	Birefringence	Crystal Size (A°) Unbonded	Crystal Size (A°) Bonded
SET- III (160)	18.8	0.023	104	153
SET – IV (160)	18.4	0.023	106	142
SET- V (160)	18.6	0.023	99	140

bond sizes so that a comparison can be made. The effective bond areas and bond sizes used varied from about 10.8% to 23.5% and (0.020 X 0.039) to (0.025 X 0.053). The pressure was kept constant at 45 psi for all the samples and the samples were produced at a rate of 250 feet/min.

Like staple fibers, a single bond strip test was chosen for this investigation. For spunbond samples, a strip tensile test was also carried out, as the stress-strain response is determined, to a significant extent, by the changes taking place in the unbonded region, as well as by the load transfer between the bonds.

Peak load values (from single bond strip test) of all the sample series are shown in Fig 4.33. The strength values show the expected trend with the increase in bond temperature for all the series. In the case of the strip tensile test, it is observed that the web strengths follow similar trends with single bond tensile test strength, except that the values of the fabric strip test are much higher than the single bond test values as shown in Fig 4.34. The web tensile strength increases up to an optimum bonding temperature and then decreases with the increase in bond temperature. Similar trends in comparable conditions were also observed by Chand [35] and Dharmadhikary [39]. The peak-elongation values (Fig 4.35) show a smaller increase with increase in bond temperature, and initial modulus values (Fig 4.36) show minimal changes for all the set of spunbond samples. As a result of more efficient bonding with increase in bond temperature, the web becomes stiffer and all the samples show a slight increase (Fig 4.37) in bending length values with increase in bond temperature.

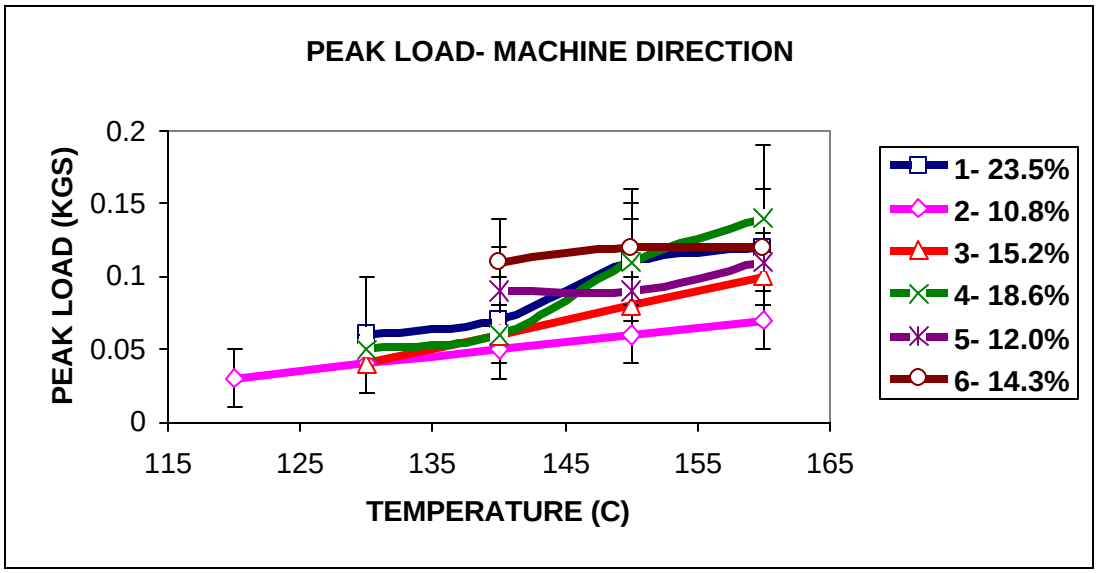

Fig 4.33. Peak Load (Single Bond Strip Test)(Machine Direction) vs Bonding Temperature for all the sets of Spunbond samples.

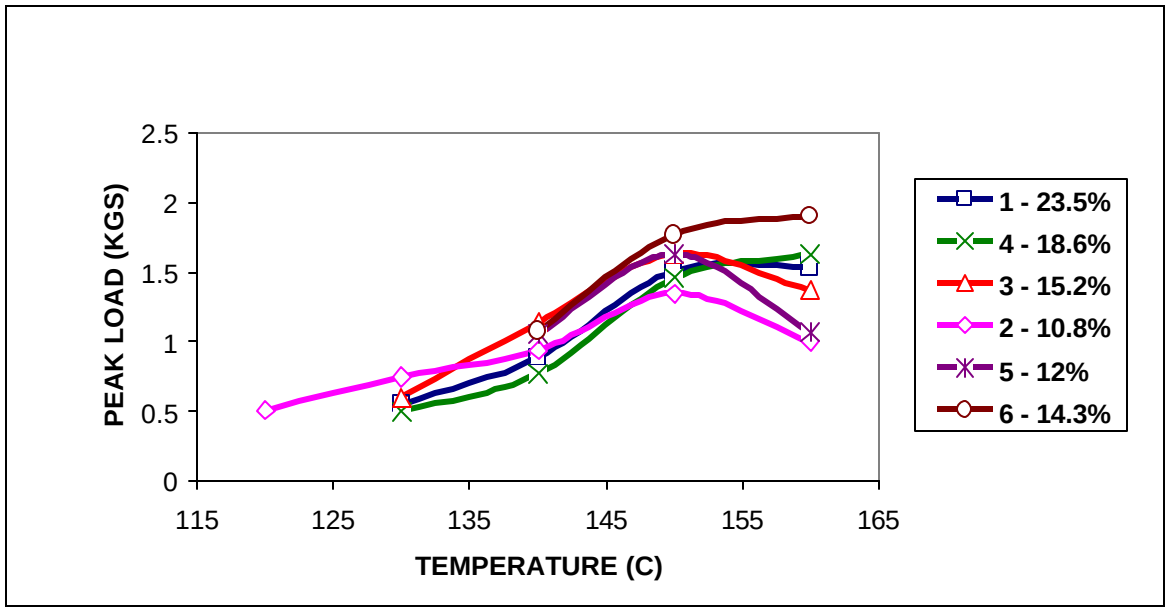

Fig 4.34. Peak Load From Tensile Strip Results in MD vs Bonding Temperature for all Spunbond Samples

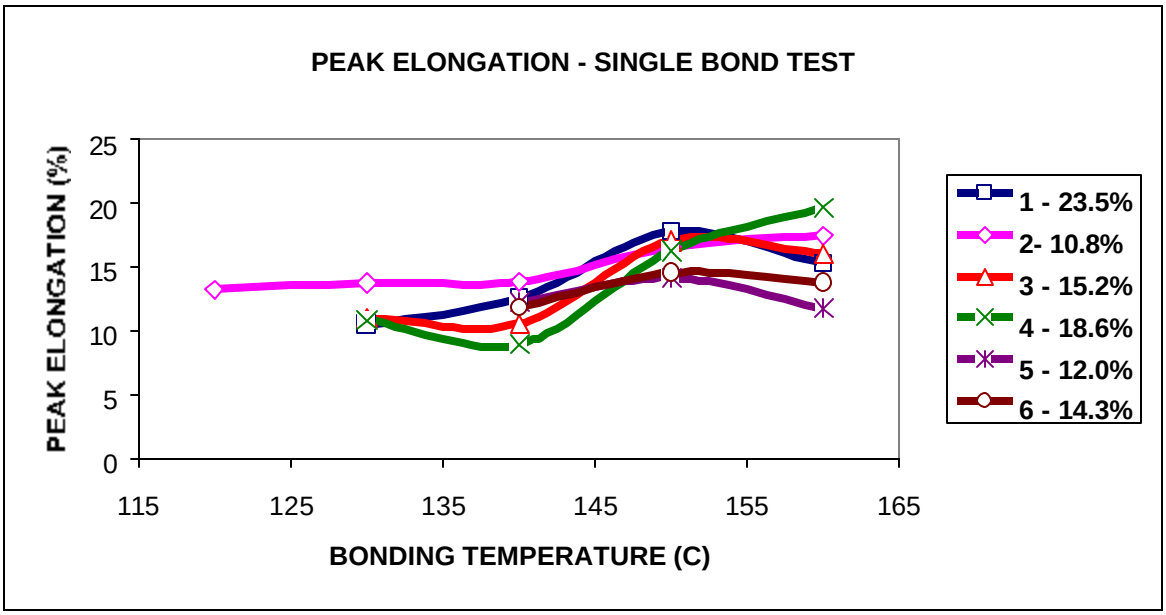

Fig 4.35. Peak Elongation (From Single Bond Strip Test) (MD) vs Bonding Temperature for Spunbond Samples

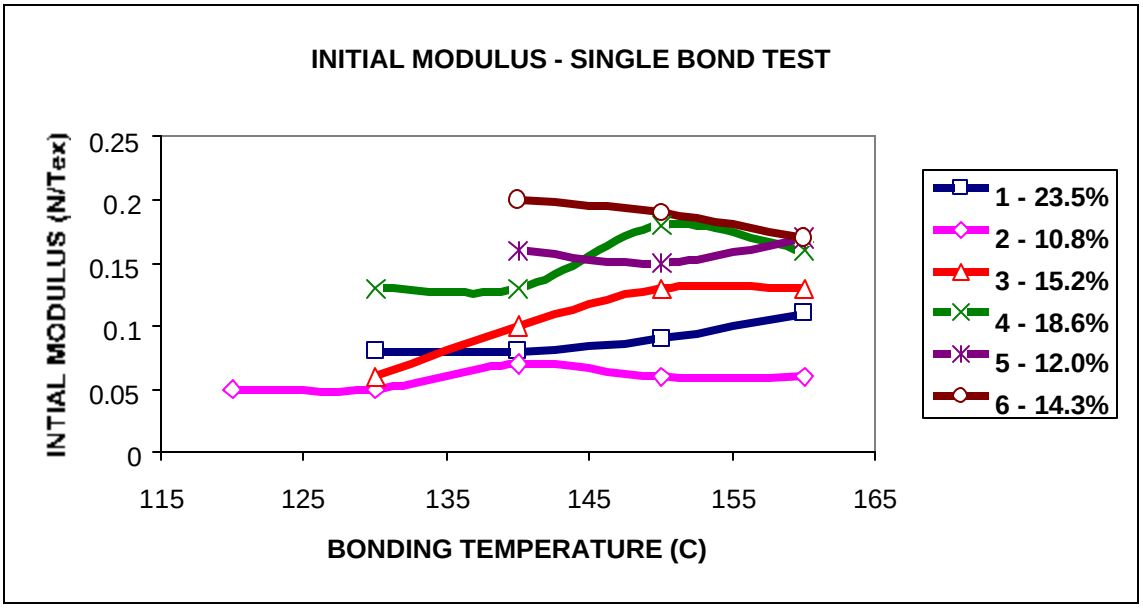

Fig.4.36 Initial Modulus (MD) vs Bonding Temperature for Spunbond Samples.

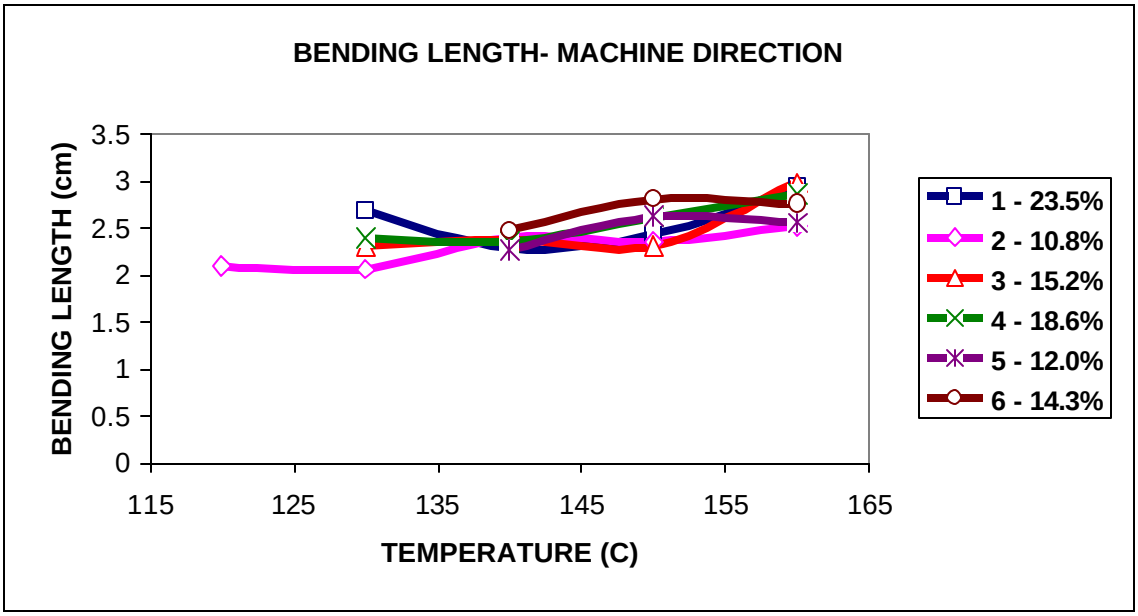

Fig.4.37 Bending Length (MD) vs Bonding Temperature for Spunbond Samples.

4.2.2 Effect of Bonding Temperature

To see the effect of bonding temperature on strength, stiffness and fiber morphology of the web, a sample having a bond area of 23.5% and bond size of (0.022 X 0.041), respectively, was chosen. The peak load values (from the single bond strip tensile test) in the two directions MD and CD for the sample having bond area of 23.5% increases. And is shown in Fig 4.38. There is a large difference between the values in the two directions. The difference between the loads is small at lower temperatures. With increase in bonding temperature, the difference increases, largely due to the increase in the strength values in the MD. The same trend is also observed when the same sample undergoes the tensile strip test (Fig 4.41); the only difference is that the load values in strip test are much higher than that of the single bond tensile test. The same trend is also observed with samples having different bond areas, as seen from Fig 4.39. This change in values with bonding temperature is attributable to change in the failure mechanism. The optimum temperature for these samples was observed to be about 150°C (Fig 4.40), which are the break elongation values from the tensile strip test results. These results are close enough for the peak load values (Fig 4.39) from the tensile strip test. The tear strength values for this sample in both MD and CD are shown in Fig 4.42. The tear strength values in the MD are higher than in the CD at lower bonding temperatures. But this difference between MD and CD reduces with increasing in bonding temperature and tear strength values reduce in both directions with increase in bonding temperature. The change in bending length values (Fig 4.43) are minimal in both directions with increase

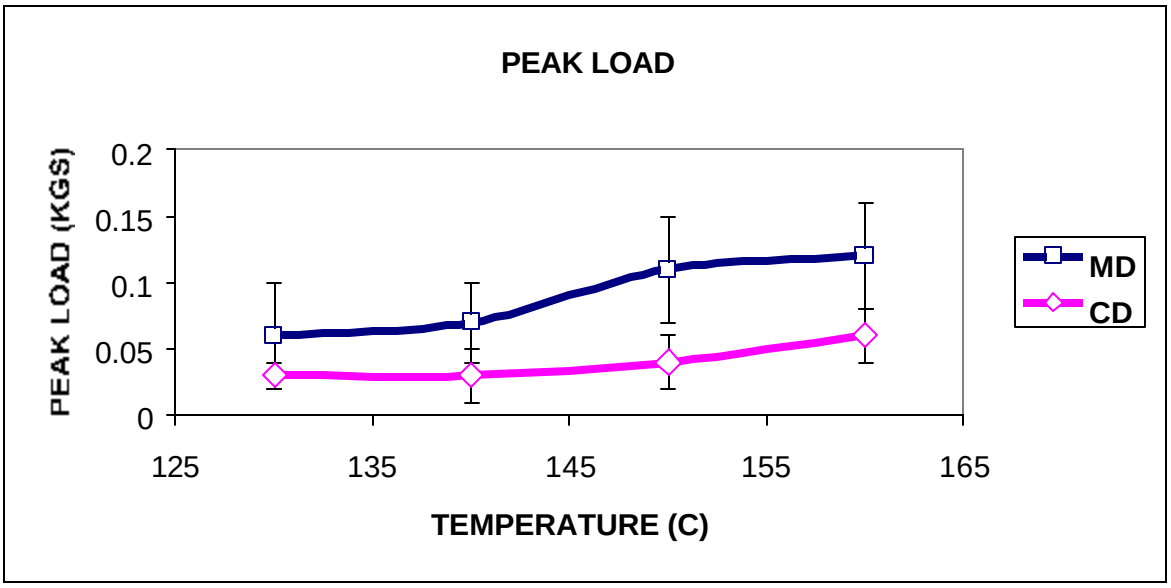

Fig 4.38 Peak Load (Single Bond) Values of Sample Having 23.5% of Bond Area vs Bonding Temperature

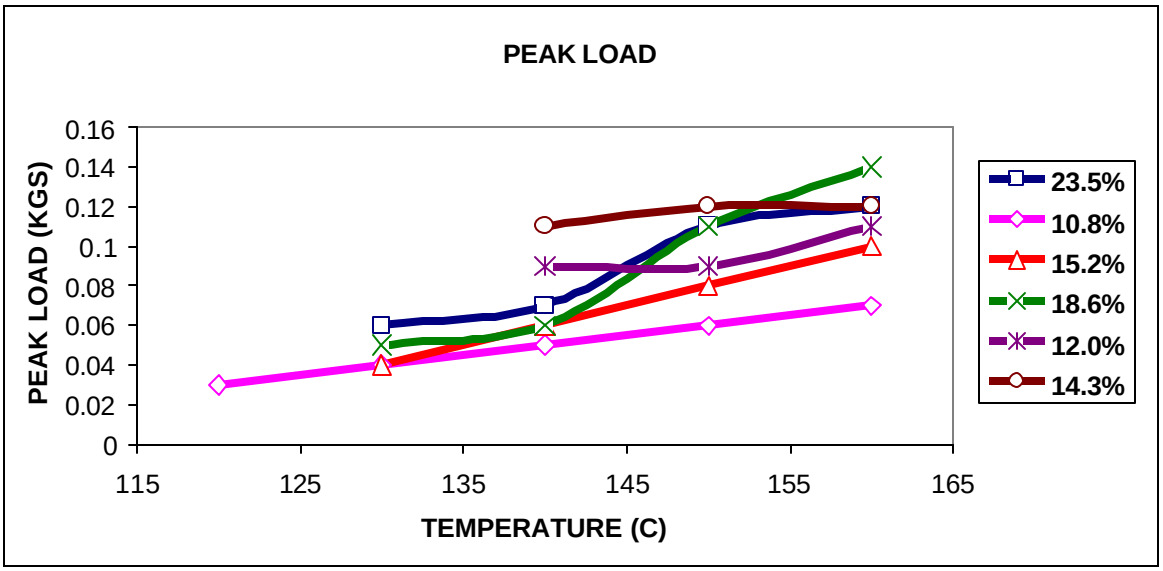

Fig 4.39 Peak Load Values (MD) From Single Bond Strip Test vs Bonding Temperature for Spunbond Samples

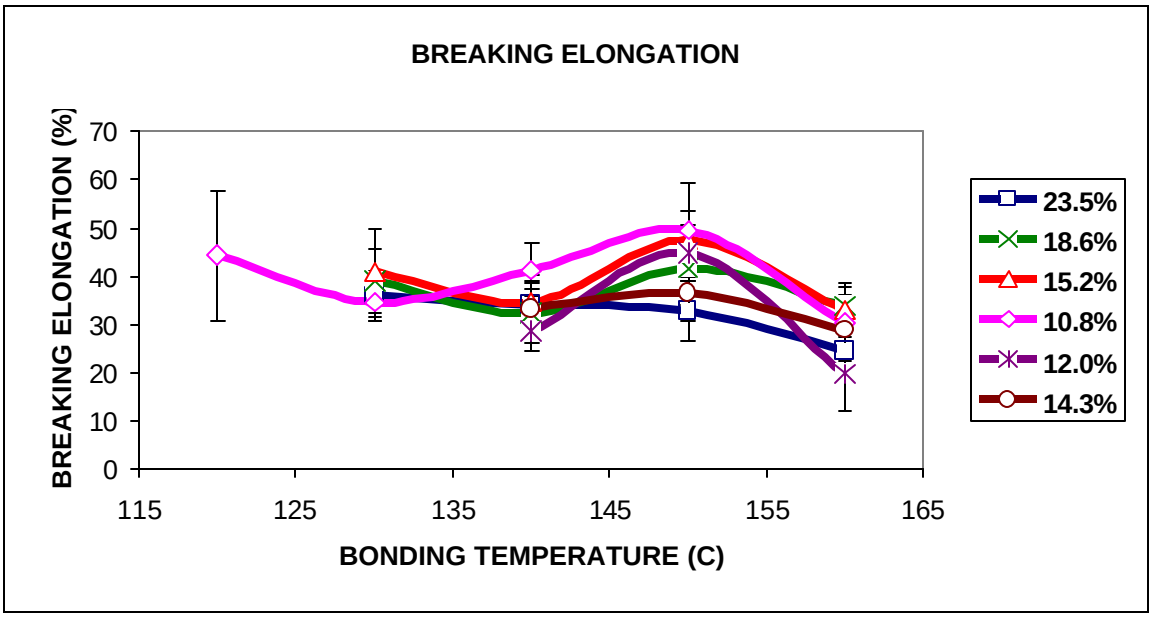

Fig 4.40 Breaking Elongation Values (MD) From Tensile Strip Test vs Bonding Temperature of Spunbond Samples

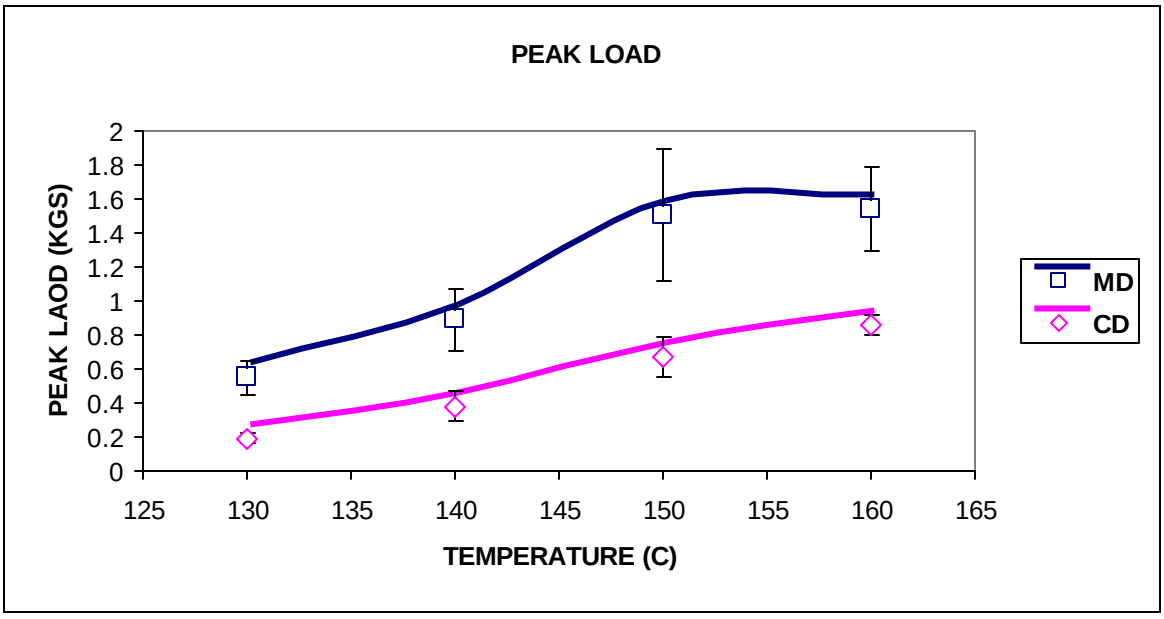

Fig 4.41 Peak Load Values From Tensile Strip Test of Sample With Bond Area of 23.5% vs Bonding Temperature

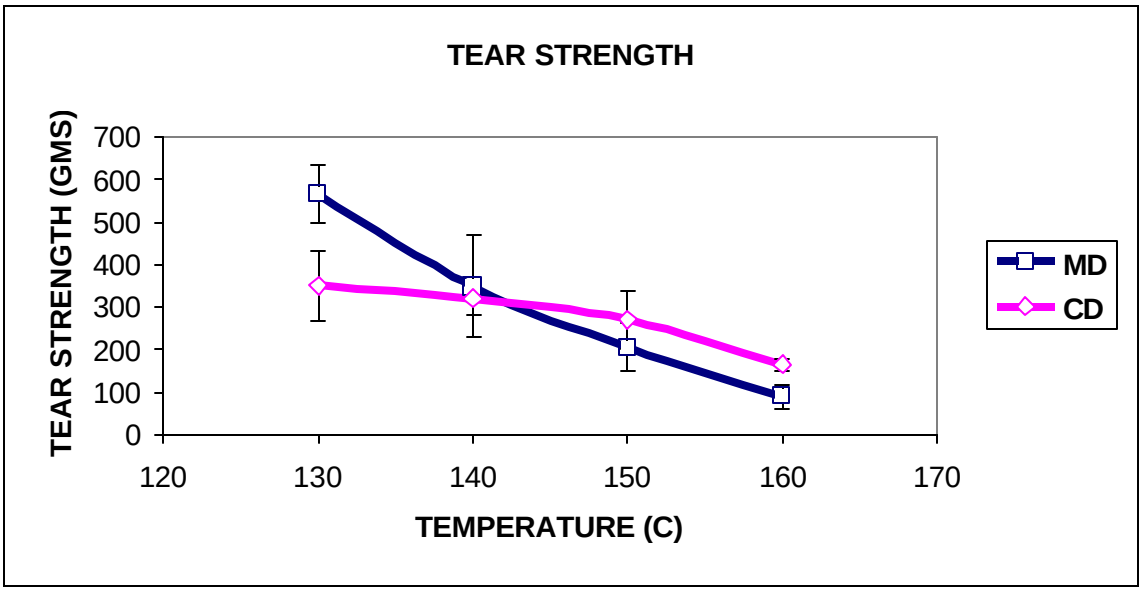

Fig 4.42 Tear Strength Values of Sample With Bond Area of 23.5% vs Bonding Temperature

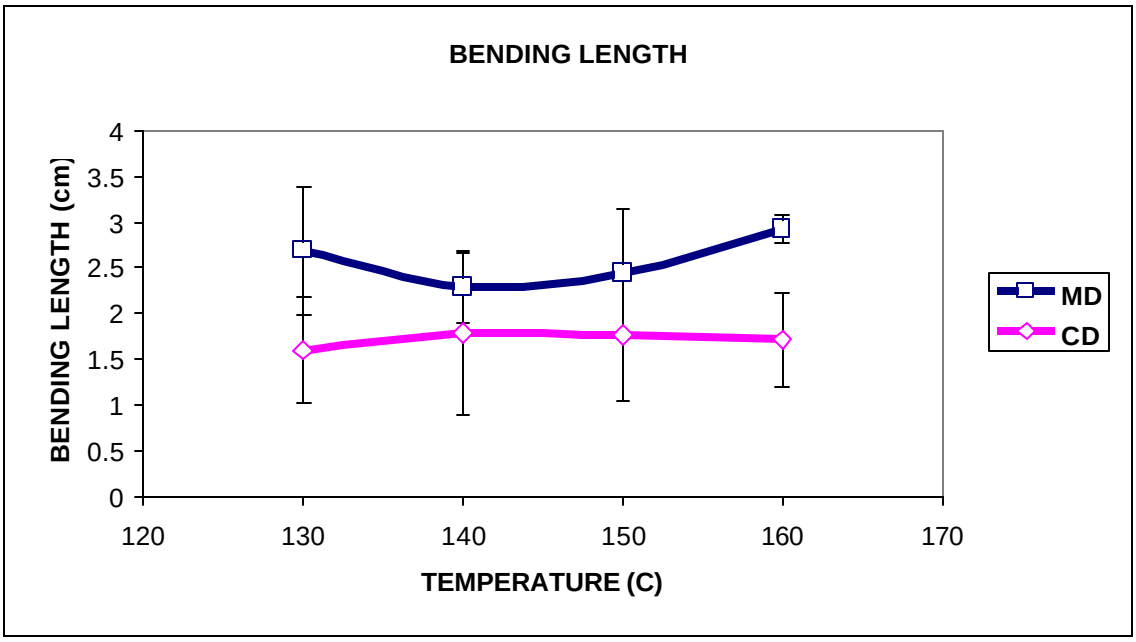

Fig 4.43 Bending Length Values of Sample With Bond Area of 23.5% vs Bonding Temperature

in bonding temperature.

4.2.3 Effect of Bond Area

The effect of Bond Area was studied using three sets of samples, with different in bond area, but bond a size in the same range (p-29), so that the differences occurring due to bond size were minimum and the effect of bond area on fiber morphology and strength of the fabric could be analyzed. For this analysis, the three samples compared have bond areas 10.8%, 15.2% and 23.5%, respectively. Figure 4.44 shows the comparison of bond area with peak load values in MD for the three sets of samples. During the single bond strip test, it was observed that the sample having high bond area 23.5% had higher strength across the range of the bonding temperature when compared to the other two sets of samples. At low temperatures, all three webs showed low strength and with increase in temperature, the peak load values increased for all the three bond areas, making the webs much stiffer. For the strip tensile test values (Fig 4.45), it is observed that the peak load values for the samples with higher bond areas reach a maximum and then fall off, and these values are higher than those samples having lower bond area with increase in bonding temperature. The differences observed in Fig 4.44 and Fig 4.45 may be attributable to the differences in the failure mechanism. The tear strength results correlate with the strip tensile results, i.e., it is tougher to tear the webs bonded at low bonding temperatures compared to those bonded at higher temperatures. It can be clearly seen from Fig 4.46, that webs having higher bond areas show higher tear strength values at low bonding temperatures and then decrease as the bonding temperature increases. This

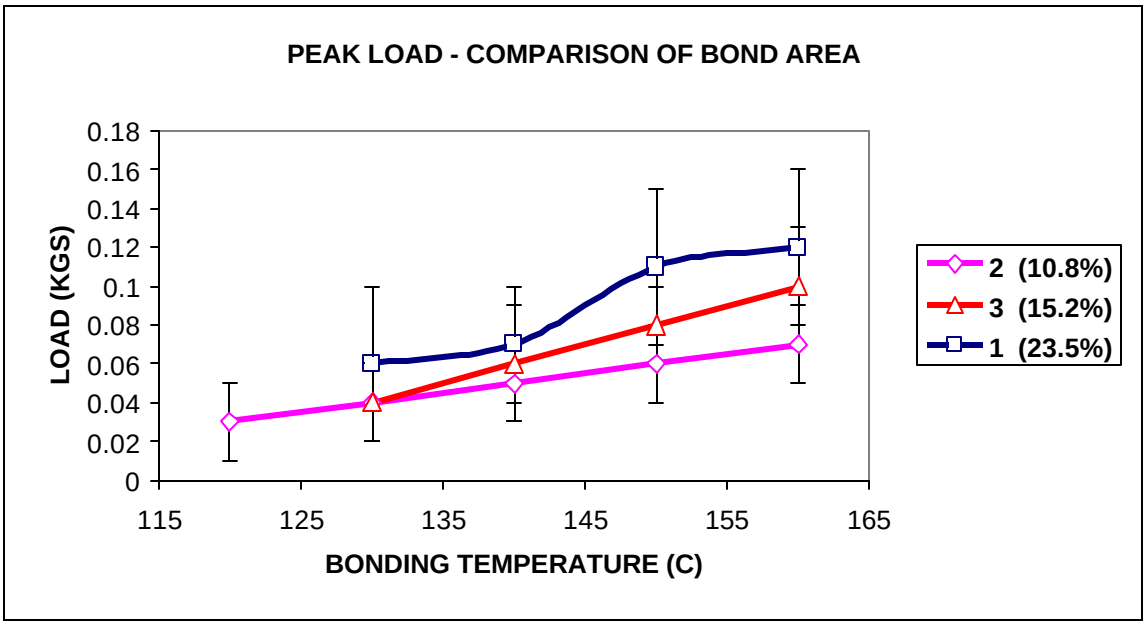

Fig 4.44 Single Bond Strip Results of Peak Load Values (MD) vs Bonding Temperature for Bond Area Comparison

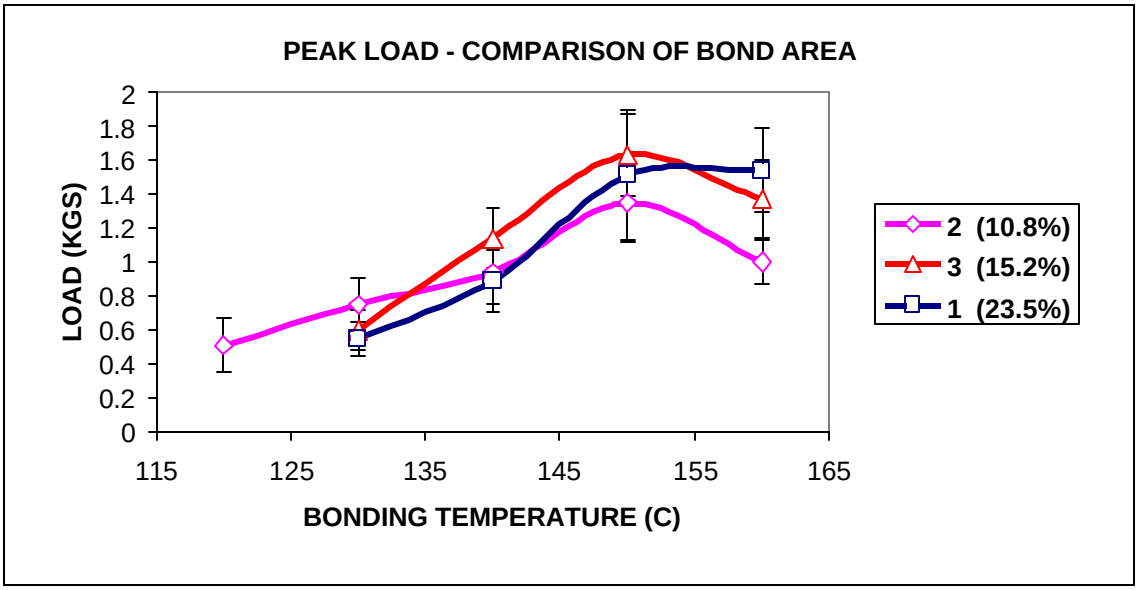

Fig 4.45 Tensile Strip Results of Peak Load Values in MD vs Bonding Temperature for Bond Area Comparison

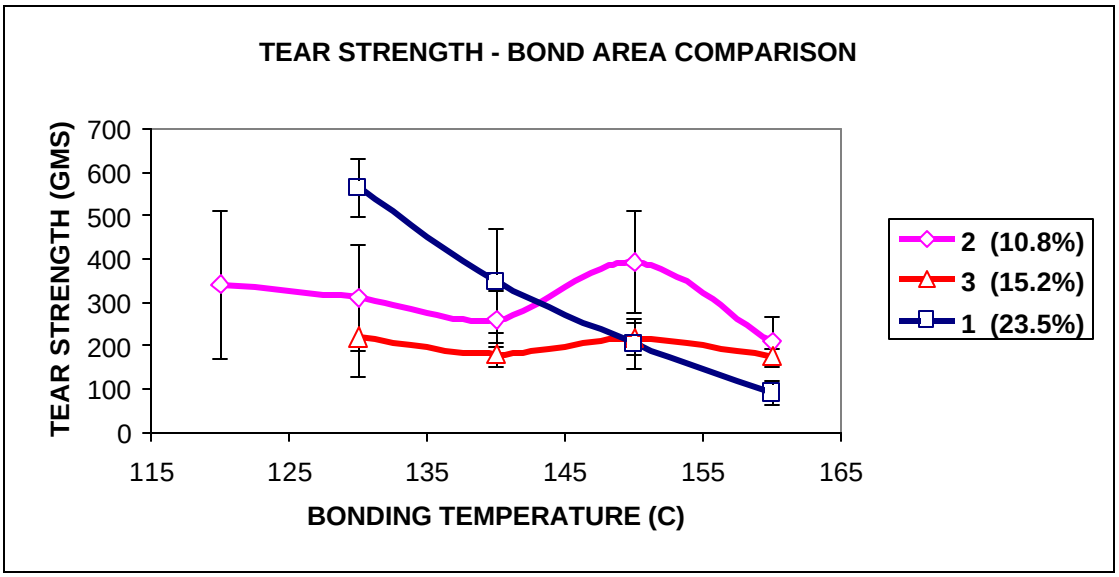

Fig 4.46 Tear Strength Results in MD vs Bonding Temperature for Bond Area Comparison

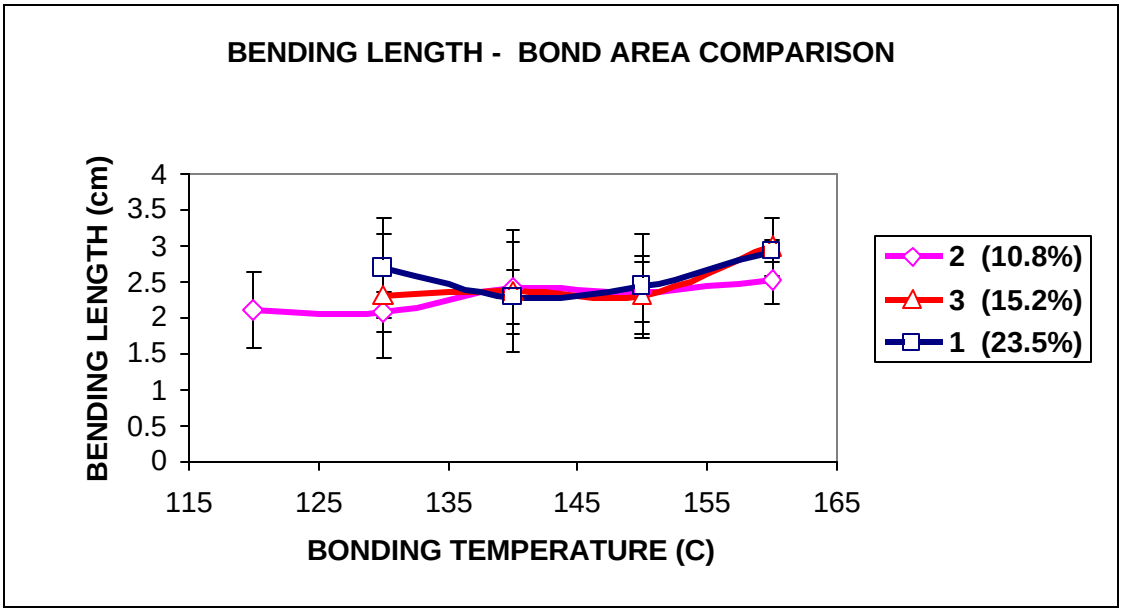

Fig 4.47 Bending Length Results in MD vs Bonding Temperature for Bond Area Comparison

is true for the remaining webs as well. It is also observed that the differences in values of bending length (Fig 4.47) are not as large as seen for strength values. But the sample with higher bond area (23.5%) shows higher bending length compared to the sample having bond area of 10.8% with increase in bond temperature. These differences reflect bond area differences.

4.2.4 Effect of Bond Size

For comparing the effect of bond size with different physical properties, three sets of samples having bond sizes (0.020 X 0.039), (0.020 X 0.040) and (0.025 X 0.053) were selected, whose bond areas (15.2%, 14.3%, 18.6%) are in the same range. From Fig 4.48, it is observed that the webs having higher bond sizes show higher peak load values, as obtained from the single bond strip test. At lower bonding temperatures, webs with different bond sizes show lower strengths, and as the temperature increases the strength also increases with webs having higher bond sizes showing higher strength values compared to the webs of smaller bond size. These differences can be attributed to the differences in the failure mechanism, which are explained in the next section. From the tensile strip test results (Fig 4.49), it is observed that the webs with different bond sizes increase in strength with increase in the bonding temperature, just as observed from the single bond test results. From Fig 4.50, it is observed that the webs having larger bond size have higher tear strength at lower bonding temperature and then the tear strength decreases as the temperature increases. This is true for the remaining set of samples, i.e., as the bonding temperature increases, the tear strength values decrease. The bending length values (Fig 4.51), show almost the same pattern for all the samples. At higher

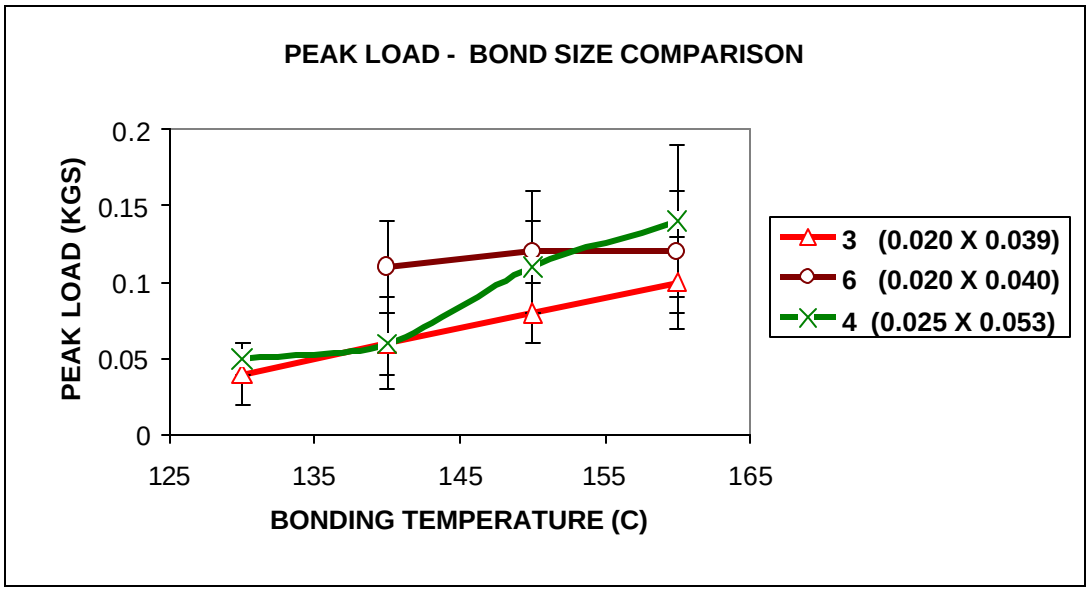

Fig 4.48 Single Bond Strip Results of Peak load Values in MD vs Bonding Temperature for Bond Size Comparison

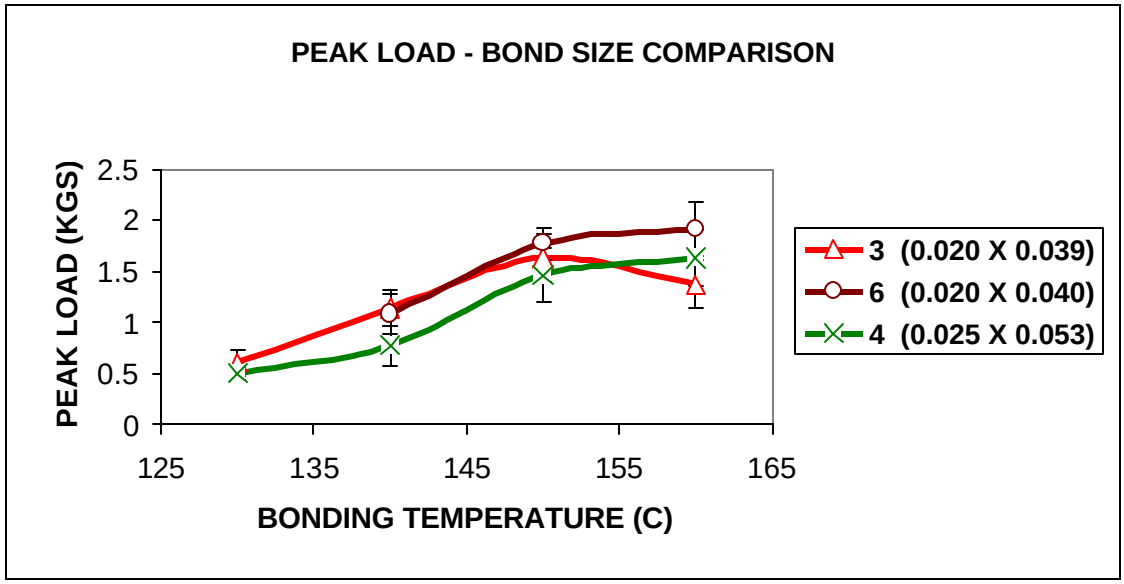

Fig 4.49 Tensile Strip Results of Peak Load Values in MD vs Bonding Temperature for Bond Size Comparison

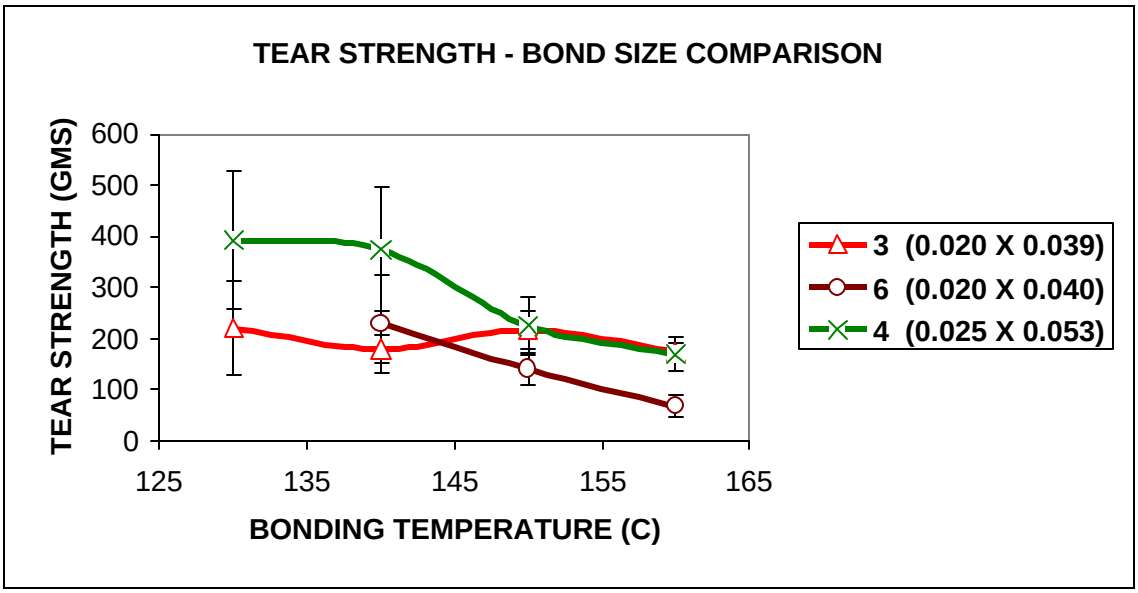

Fig 4.50 Tear Strength Results in MD vs Bonding Temperature for Bond Size Comparison

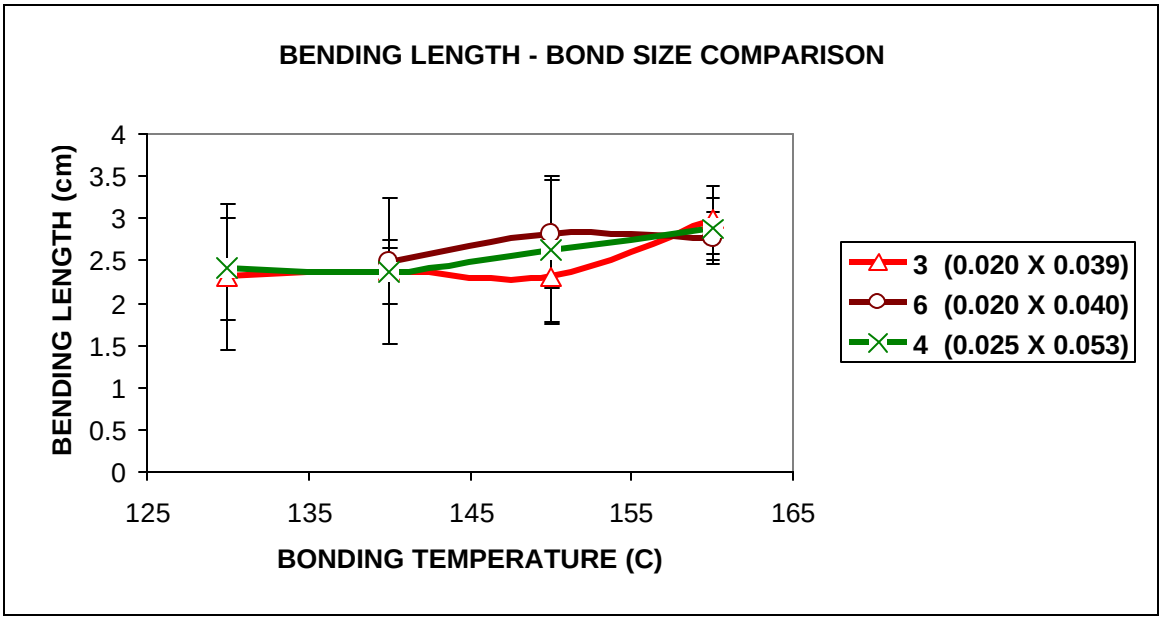

Fig 4.51 Bending Length Results in MD vs Bonding Temperature for Bond Size Comparison

temperature (160°C), the values are almost the same for all the three sets of samples. It appears that the effect of bond size on the stiffness values is minimal, which is consistent with the observations in the staple fiber studies as well.

4.2.5 Analysis and Discussion

4.2.6 Effect of Bonding Temperature

Single bond tensile tested webs examined under scanning electron microscope and images were taken from the failure mechanism of the webs. It was done to see how the bond deforms during the tensile testing. At lower bonding temperature of 130^0C, we can see that the bond disintegrating, i.e., fibers pull out one by one from the bond point (Fig 4.52). The first image shows the neighboring bond point, where a little trend of disintegration was observed. This shows that the effect of failure mechanism during tensile testing, is also seen in the neighboring bond points along with the bond point which undergoes tensile testing.

At a medium bonding temperature of 140^0C, a similar trend of disintegration was observed (Fig 4.53), as seen at low bonding temperatures at the failure stage of the single bond tensile testing of the webs.

At higher bonding temperatures of 160^0C (Fig 4.54), it was observed from the SEM image that filaments break at the vicinity of the bond point, but the bond stays intact. At this point, the neighboring bond point is still intact because of higher bonding temperature. The breaking of filaments at the vicinity of the bond makes it a weak bond point. This phenomenon was also observed in staple fiber studies.

Neighboring Bond **Strained Bond**

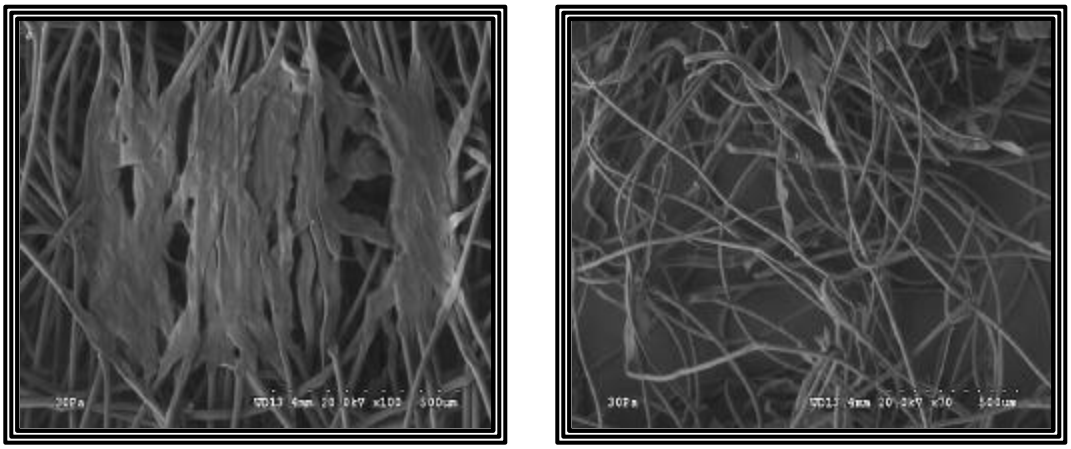

Fig 4.52 SEM Image Showing Disintegration of Bond at 130° C (Failure Stage)

Neighboring Bond **Strained Bond**

Fig 4.53 SEM Image Showing Bond Disintegration and Re-orientation of Fibers at 140° C (Failure Stage)

Neighboring Bond **Strained Bond**

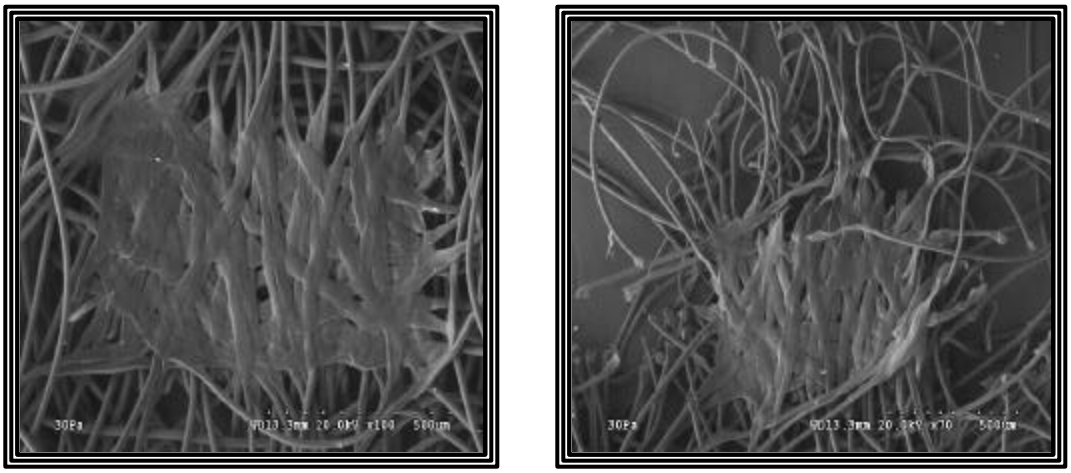

Fig 4.54 SEM Image Showing Filaments Breaking Near The Bond Boundary at 160° C (Failure Stage)

Table 4.4 Spunbond Fibers Morphological Parameters, Effect of Bond Temperature

Sample – Bond Area - Temp (° C)	Fiber Dia (㎜)	Birefringence	Crystal Size (A°) Unbonded	Crystal Size (A°) Bonded
1 – 23.5% (130)	19.9	0.021	123	168
1 – 23.5% (160)	19.9	0.019	118	162

From Table 4.4, we can see that the values of fiber birefringence and fiber diameter in the unbonded regions is in the same range for the sample at low and high bonding temperatures indicating that the changes taking place during calendering, with short intervals of calendering, are very low. However, the crystal size values in the unbonded regions remain in the same range and the crystal size values of bonded regions are higher than that of the unbonded regions.

4.2.7 Effect of Bond Area

From the SEM images of the webs, which were taken from samples tested after single bond tensile tests and obtaining the fiber morphology parameters, we can see the effect of bond area on the strength, stiffness and morphology of the web can be seen.

From Figure 4.55, it is observed that at lower bonding temperature (130°C), the fibers pull out from the bond point. During the failure stage, total disintegration of the bond takes place, i.e., fibers pull out one by one from the bond point making the bond weak. Chand [35] also showed a similar trend of disintegration of bond point at low bonding temperature. It is also seen that there is a slight disintegration of the fibers in the neighboring bond points during the failure stage and this shows that the effect of disintegration not only occurs on the bond which undergoes tensile testing but, also in the neighboring bonds. For fabrics bonded at medium temperature (140°C), as shown in Fig 4.56, the bond starts to stretch from the filaments of the web and re-orientation of fibers takes place in the neighboring bonds. At higher bonding temperature of 160°C, (Fig 4 .57), the filaments break at the vicinity of the bond point. At this stage, the neighboring

Neighboring Bond **Strained Bond**

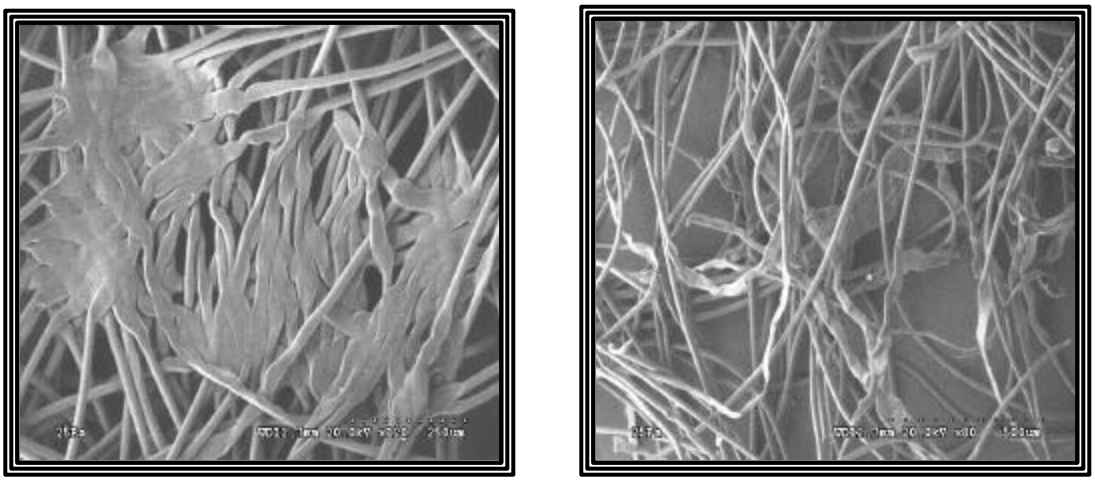

Fig 4.55 SEM Image Showing Disintegration of Bond at 130° C (Failure Stage)

Neighboring Bond **Strained Bond**

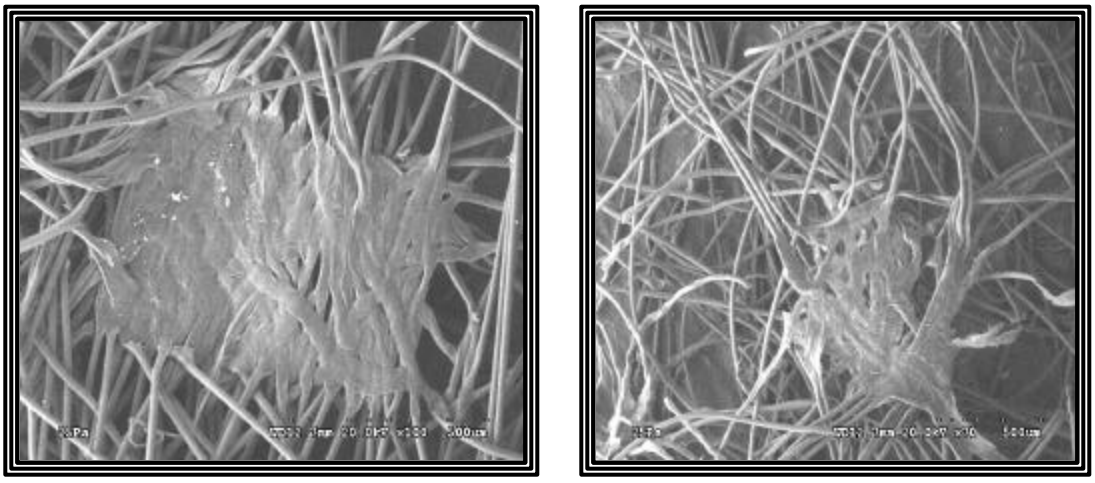

Fig 4.56 SEM Image Showing Bond Stretching at 140° C (Failure Stage)

bond point is still intact because of higher bonding temperature. From Table 4.5, it is seen that the fiber diameter and fiber birefringence values in the unbonded regions remain the same for all the samples indicating that the changes taking place during the processing speeds, with short dwell times in the calender, are very low. But, the crystal size varies from unbonded regions to bonded regions. However, the crystal size values in the unbonded regions remain the same for all the samples and the crystal size values of bonded regions are higher than that of the unbonded regions.

4.2.8 Effect of Bond Size

From Fig 4.58, it is obvious that at a lower bonding temperature of 130°C, at failure stage, the fibers pull out one by one from the bond point, i.e., the bond disintegrates and the bond becomes weak. Even the neighboring bond points also exhibit the same trend, eventhough, not of that extreme. At medium temperatures of 140°C, (as observed from Fig 4.59) disintegration of the bond takes place and fibers pull out one by one from the bond point and fiber re-orientation takes place at the neighboring bond making it a weak bond. At a higher bonding temperature of 160°C, (Fig 4.60), it is observed that the bond point stays intact but, the filaments break at the periphery of the bond point making the bond weak. The neighboring bond point stays intact during the failure stage. This trend is also observed with the webs of other bond sizes. From Table 4.6, it is seen that the fiber diameter and fiber birefringence values remain the same for all the samples indicating that the changes that might be taking place during these processing speeds, with short

Neighboring Bond **Strained Bond**

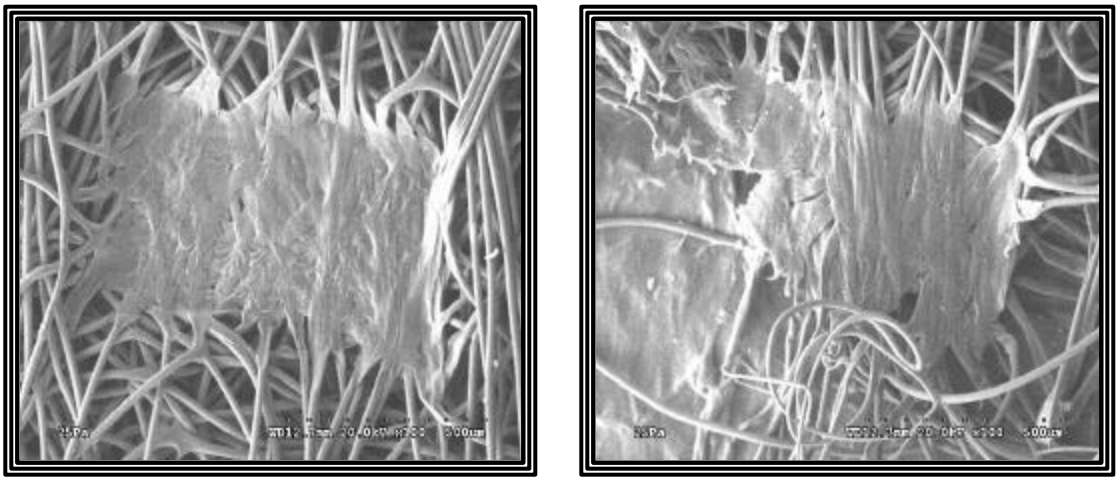

Fig 4.57 SEM Image Showing Filaments Breaking Near The Bond Boundary at 160° C (Failure Stage)

Table 4.5 Spunbond Fibers Morphological Parameters, Effect of Bond Area

Sample - Bond Area -Temp (° C)	**Fiber Dia (mm)**	**Birefringence**	**Crystal Size (A°) Unbonded**	**Crystal Size (A°) Bonded**
2 – (10.8%)	20.2	0.021	107	162
3 - (15.2%)	20.1	0.020	112	162
1 - (23.5%)	19.9	0.019	118	162

Neighboring Bond **Strained Bond**

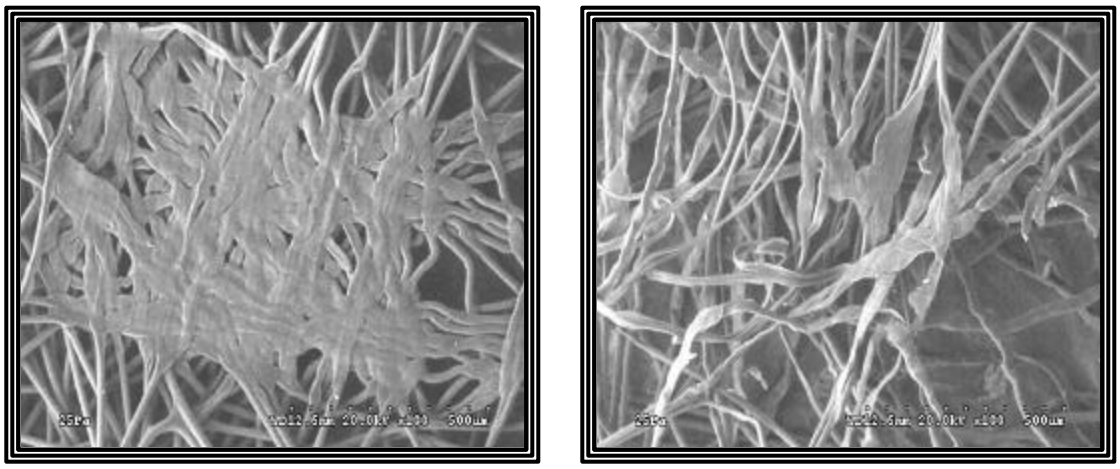

Fig 4.58 SEM Image Showing Disintegration of Bond at 130° C (Failure Stage)

Neighboring Bond **Strained Bond**

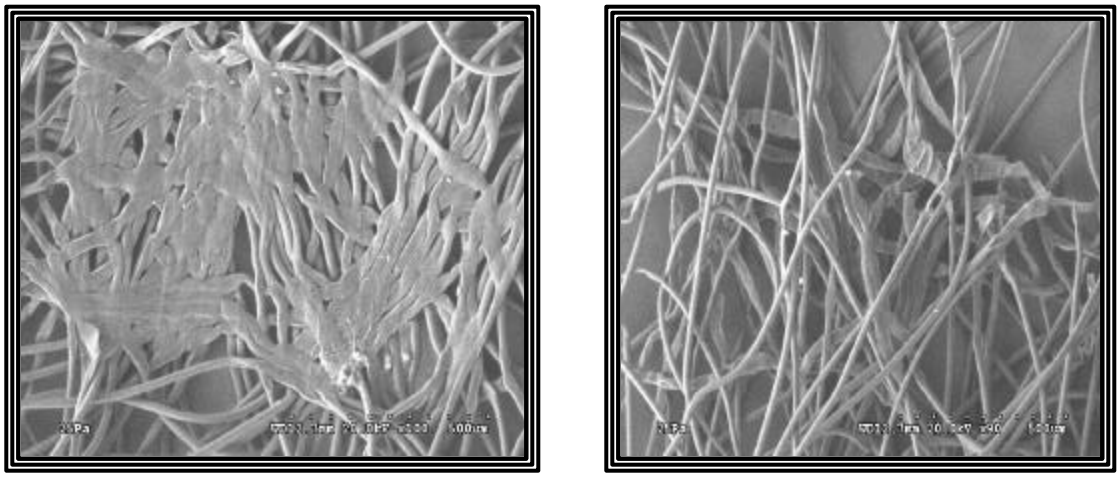

Fig 4.59 SEM Image Showing Bond Disintegration at 140° C (Failure Stage)

Neighboring Bond **Strained Bond**

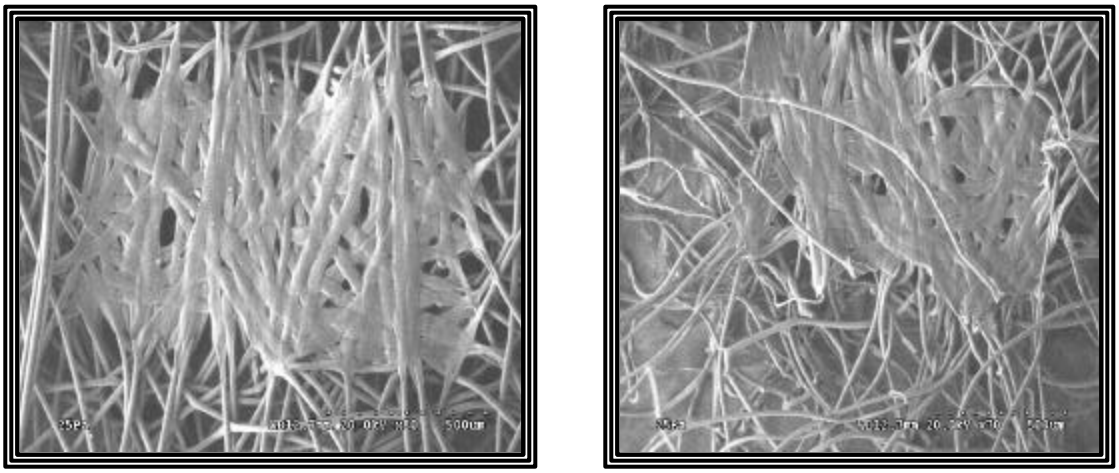

Fig 4.60 SEM Image Showing Filaments Breaking Near The Bond Boundary at 160° C (Failure Stage)

Table4.6 Spunbond Fibers Morphological Parameters, Effect of Bond Size

Sample – Bond Size - Temp (° C)	Fiber Diameter (mm)	Birefringence	Crystal Size (A°) Unbonded	Crystal Size (A°) Bonded
3 – (0.020 X 0.039)	20.1	0.020	112	162
6 – (0.020 X 0.040)	19.8	0.019	116	170
4 – (0.025 X 0.053)	19.7	0.022	109	160

dwell times in the calender, are very low. Also, the crystal size values for the unbonded regions remain in the same range. The crystal size values of bonded regions are higher than those of unbonded regions and the values in bonded regions vary because of higher temperature and bonding conditions making the morphological changes taking place due to bond size variations insignificant.

CHAPTER V

CONCLUSIONS

The series of samples produced under various bonding conditions, using both staple fibers and spunbond fibers, were thoroughly characterized. Based on this study, the following conclusions can be drawn as far as the effect of bond temperature, bond area and bond size are concerned

1. Effect of Bonding Temperature

a) Bond strength increases up to a maximum and then decreases with increase in bonding temperature for both staple fiber and spunbond studies.

b) Tear strength changes are small with for range of samples investigated, but the values in CD show a higher tear strength than MD over the range of the bonding temperature for staple fiber webs. However, tear strength values are higher with spunbond samples and show a decreasing trend with increase in bonding temperature.

c) Bending length values show a slight increase with bonding temperature for staple fiber webs. For spunbond webs, the bending length value differences are small with the bonding temperature for the range of study.

d) Effect of bonding temperature on fiber morphology in the unbonded regions is negligible for both staple and spunbond studies.

e) 150°C was found to be the optimum bonding temperature for spunbond studies.

2. Effect of Bond Area

a) Bond strength increases with increae in bond area for both staple and spunbond samples.

b) Slightly higher tear strength values for samples having higher bond areas than samples having lower bond areas along the range of bonding temperature are observed for staple fiber webs. For spunbond samples, tear strength decreases with increase in bonding bond area.

c) Bending length values are slightly higher for samples having higher bond areas for staple fiber webs. For spunbond webs, the bending length differences are small with respect to bond area for the range of samples investigated.

d) Effect of bond area on fiber morphology in the unbonded region is negligible for both staple and spunbond studies.

3. Effect of Bond Size

a) Bond strength increases with increase in bond size for staple and spunbond webs.

b) Tear strength differences are small for staple fiber webs and for spunbond webs, tear strength decreases with increase in bonding temperature for larger bond size.

c) Bending length value differences are minimal for both staple and spunbond webs with respect to the bond size for the range of samples investigated.

d) Effect of bond size on fiber morphology in the unbonded region is negligible for both staple and spunbond webs.

In all the cases, crystal sizes were different in the unbonded and bonded regions, values being higher in the bonded regions. This is due to the effect of heat in the bonded region. However, in the unbonded regions, the effect is negligible at these processing conditions, for fibers investigated, which may be due to fairly well developed structure of the fibers.

REFERENCES

1. R.K.Dharmadhikary, T.F.Gilmore, H.A.Davis, and S.K.Batra, " Thermal Bonding of Nonwoven Fabrics,", Textile Progress, 26 (2)

2. Joseph O' Leary, " Thermal Bonding: Principles and Applications", June, 1996, p. 1-11.

3. A.G.Hoyle, "Thermal Bonding of Nonwoven Fabrics," July 1990, Tappi Journal, p. 85-88.

4. Batra S.K., Fred L.Cook., "The Nonwoven Fabrics Handbook," 1992.

5. Tom H. "What are Nonwovens – Again?," Nonwoven Industry, March 1989.

6. http://trcs.he.utk.edu/textile/nonwovens, 1999.

7 Kwok W.K., Crane J.P., Gorrafa A., and Iyengar Y. "Polyester Staple fibers for Thermally Bonded Nonwovens," Nonwovens Industry, June 1988, p.30-33.

8. Bechter D., Roth A., Schaut G., Ceballos R., Kleinmann K., and Schafer K. " Thermal Bonding of Nonwovens", Melliand Textilberichte, 1997, No.3, p. E39-40.

9. Gibson P.E., and McGill R.L. "Thermally bondable polyester fiber: The effect of calender temperature", Tappi Journal, December, 1987, p. 82-86.

10. Charles J.Shimalla and John C. Whitwell, "Thermomechanical Behavior of Nonwovens, Part I: Responses to Changes in Processing and Post-Bonding .

11. De Angelis V., Digiaoacchino T., and Olivieri P. " Hot Calenderd Polypropylene Nonwoven fabrics", Proceedings of 2nd International Conference on Polypropylene Fibers and Textiles, Plastics and Rubber Institute, Univeristy of York, England, 1979, p. 52.1-52.13.

12. Muller D. " Thermal Bonding of Heavy Webs With Calenders",EDANA'S 1998 Nordic Nonwovens Symposium.

13. Bechter D., Kurz G., Maag E., and Schutz J. " Thermobonding of Nonwovens", Textil-Praxis., 1991, 46,p. 1236-1240.

14. Malkan S.R., Wadsworth L.C., and Devis C. "Parametric Studies of the Reicofil Spunbonding Process", Third TANDEC Conference, 1993.

15. Schwartz R.J. U.S. Patent 3,912,567, assigned to Kimberly-Clark Corp., 1975.

16. Ericson C.W. " Bonding in Spunbonded Nonwovens," Seminar presented at

Textile Research Institute, Princeton, N.J., February 21, 1974.

17. Crane J.P., Wo Kong Kwok., Gorrafa A-M.A., Iyengar Y. " Polyester Staple For Thermally Bonded Nonwovens", Nonwovens Industry, June,1988, p.30-33.

18. Schwartz R.J. U.S. Patent 4,100,319, assigned to Kimberly-Clark Corp., 1978.

19. Brock R.J. U.S. Patent 3,855,045, assigned to Kimberly-Clark Corp., 1974.

20. Mi Z.X., Batra S.K., and Gilmore T.F. " Computational Model for Mechanical Behavior of Point-Bonded Webs," First Annual Report, NCRC, 1992.

21. Warner S.B. " Thermal Bonding of Polypropylene Fibers," Textile Research Journal., 1989, 59, p. 151-159.

22. Wei K.Y., Vigo T.L. and Goswami B.C. " Structure-Property Relationships of Thermally Bonded Polypropylene Nonwovens," Journal of Applied Polymer Science., 1985, 30, p. 1523-1534.

23. Akai M. and Aspin A.F. "Properties, Structure and Applications of Embossed Polypropylene Tapes," Plast. & Rubber Process. & Appl. 1981, 1, p. 327-329.

24. Philips P.J. and Tseng H.T. " Influence of Pressure on Crystallization in PET," Macromolecules, 1989, 22, p. 1649-1655.

25. Gillmore, T.F., Mi Z.X., and Batra S.K. "The Effect of Point Design and Bond Strength on the Load Deformation of Point Bonded Nonwoven," TAPPI Proc. 1987-1993. p. 87-92.

26. Drelich A. "Thermal Bonding with Fusible Fibers," Nonwovens Industry, September 1985, p. 12-26.

27. Grindsaff T.H., and Hansen S.M. "Computational Model for Predicting Point-Bonded Nonwoven Fabric Strength.Part I," Textile Research Journal, 56 (1986), p. 383-388.

28. Zhang D. "Fundamental Investigation of the Spunbonding Process," Ph.D. Thesis, The University of Tennessee, Knoxville, 1995

29. Zhang D., Bhat G., Malkan S., Wadsworth L., "Structure And Properties Of Polypropylene Filaments In A Spunbonding Process," Journal of Thermal Analysis, Vol 49, (1997), p. 161-167.

30. Gajanan S. Bhat, Rammohan Nanjundappa, "Structure And Properties Of Spunbonded Nonwovens Produced From Polypropylene Polymers," World

Congress, University of Huddersfield, July 2000, p.175-184.

31. Gajanan S. Bhat, Subhash Chand, Joseph E. Spruiell and Sanjiv Malkan, "Implication Of Fiber Morphology On The Structure And Properties Of Thermally Bonded Polypropylene Nonwovens," Book of Papers, INTC, Dallas, September 2000.

32. Rammohan Nanjundappa, Gajanan S. Bhat, and Sanjiv R. Malkan, "Process And Property Optimization In A Spunbonding Process," Procedings of the Ninth TANDEC Conference, November 1999, p. 5.6-1 - 5.6-12.

33. Zhang D , Gajanan Bhat, Malkan S, And Wadsworth L., "Evolution of Structure And Properties In A Spunbonding Process," Textile Research Journal, 68 (1), 1998, p. 27-35.

34. Gajanan Bhat, "Performance Of Polyolefin Polymers In Spunbond Applications," Paper presented at Polypropylene Technology, Clemson, August 1995.

35. Subhash Chand "Role of Fiber Morphology in Thermal Bonding," M.S. Thesis, The University of Tennessee, Knoxville, 1999.

36. Storer R.A., ASTM, Easton, MD, USA, 1986.

37. Instructions Manual, Mettler Thermal Analysis System, p. 91.

38. Cullity B.D., "Elements of X-Ray Diffraction," Addison-Wesley Publishing Company Inc., Massachusetts, 1978, p. 284.

39. Dharmadhikary R.K., Hawthorne Davis, Thomas F. Gilmore, and Subhash K. Batra, "Influence of Fiber Structure on Properties of Thermally Point Bonded Polypropylene Nonwovens," Textile Research Journal, 69(10), 1999, p. 725-734.

40. Hartman L., TM, 101 (1974), No. 9,p.26-30.

APPENDICES

APPENDIX I

SAS Output for ' Analysis of Variances' using GLM method to see the Effect of Bond Temperature on Peak Load of Set – I sample of Staple Fiber Web.

The GLM Procedure

Dependent Variable: pload

Source	DF	Sum of Squares	Mean Square	F Value	Pr > F
Model	13	7348.4026	565.2617	0.47	0.9357
Error	130	155026.8514	1192.5142		
Corrected Total	143	162375.2539			

R-Square	Coeff Var	Root MSE	pload Mean
0.045256	451.4501	34.53280	7.649306

Source	DF	Type I SS	Mean Square	F Value	Pr > F
Direction	1	7322.673556	7322.673556	6.14	0.0145
Temp	6	13.059028	2.176505	0.00	1.0000
Direction*Temp	6	12.669970	2.111662	0.00	1.0000

Source	DF	Type III SS	Mean Square	F Value	Pr > F
Direction	1	7310.444660	7310.444660	6.13	0.0146
Temp	6	11.815399	1.969233	0.00	1.0000
Direction*Temp	6	12.669970	2.111662	0.00	1.0000

APPENDIX II

SAS Output for ' Analysis of Variances' using GLM method to see the Effect of Bond Temperature on Tear Strength of Set – I sample of Staple Fiber Web.

The GLM Procedure

Dependent Variable: tstrength

Source	DF	Sum of Squares	Mean Square	F Value	Pr > F
Model	15	5355.0000	357.00000	2.20	0.0155
Error	64	10400.0000	162.50000		
Corrected Total	79	15755.0000			

R-Square	Coeff Var	Root MSE	tstrength Mean
0.339892	12.84388	12.74755	99.25000

Source	DF	Type I SS	Mean Square	F Value	Pr > F
Direction	1	0.000000	0.00000	0.00	1.0000
Temp	7	5355.00000	765.00000	4.71	0.0003
Direction*Temp	7	0.00000	0.00000	0.00	1.0000

Source	DF	Type III SS	Mean Square	F Value	Pr > F
Direction	1	0.00000	0.00000	0.00	1.0000
Temp	7	5355.00000	765.00000	4.71	0.0003
Direction*Temp	7	0.00000	0.000000	0.00	1.0000

APPENDIX III

SAS Output for 'Analysis of Variances' using GLM method to see the Effect of Bond Temperature on Bending Length of Set – I sample of Staple Fiber Web.

The GLM Procedure

Dependent Variable: bendlgth

Source	DF	Sum of Squares	Mean Square	F Value	Pr > F
Model	15	108.5799219	7.2386615	19.73	<0.001
Error	112	41.0862500	0.3668415		
Corrected Total	127	149.6661719			

R-Square	Coeff Var	Root MSE	bendlgth Mean
0.725481	13.47581	0.605674	4.494531

Source	DF	Type I SS	Mean Square	F Value	Pr > F
Direction	1	84.33757813	84.33757813	229.90	<.0001
Temp	7	21.88304688	3.12614955	8.52	<.0001
Direction*Temp	7	2.35929687	0.33704241	0.92	0.4948

Source	DF	Type III SS	Mean Square	F Value	Pr > F
Direction	1	84.33757813	84.33757813	229.90	<.0001
Temp	7	21.88304688	3.12614955	8.52	<.0001
Direction*Temp	7	2.35929687	0.33704241	0.92	0.4948

APPENDIX IV

SAS Output for 'Analysis of Variances' using GLM method to see the Effect of Bond Area on Peak Load of Sets – I, II, III samples of Staple Fiber Webs.

The GLM Procedure

Dependent Variable: pload

Source	DF	Sum of Squares	Mean Square	F Value	Pr > F
Model	23	0.46240475	0.02010455	18.89	<0.0001
Error	213	0.22666444	0.00106415		
Corrected Total	236	0.68906920			

R-Square	Coeff Var	Root MSE	pload Mean
0.671057	23.10598	0.032621	0.141181

Source	DF	Type I SS	Mean Square	F Value	Pr > F
Group	2	0.23890983	0.11945492	112.25	<.0001
Temp	7	0.15249972	0.02178567	20.47	<.0001
Group*Temp	14	0.07099520	0.00507109	4.77	<.0001

Source	DF	Type III SS	Mean Square	F Value	Pr > F
Group	2	0.23890983	0.11945492	112.25	<.0001
Temp	7	0.15249972	0.02178567	20.47	<.0001
Group*Temp	14	0.07099520	0.00507109	4.77	<.0001

APPENDIX V

SAS Output for 'Analysis of Variances' using GLM method to see the Effect of Bond Area on Tear Strength of Sets – I, II, III samples of Staple Fiber Webs.

The GLM Procedure

Dependent Variable: tstrength

Source	DF	Sum of Squares	Mean Square	F Value	Pr > F
Model	23	14679.16667	638.22464	4.83	<0.0001
Error	96	12680.00000	132.08333		
Corrected Total	119	27359.16667			

R-Square	Coeff Var	Root MSE	tstrength Mean
0.536536	10.88501	11.49275	105.5833

Source	DF	Type I SS	Mean Square	F Value	Pr > F
Group	2	4026.666667	2013.333333	15.24	<.0001
Temp	7	5172.500000	738.928571	5.59	<.0001
Group*Temp	14	5480.000000	391.428571	2.96	0.0009

Source	DF	Type III SS	Mean Square	F Value	Pr > F
Group	2	4026.666667	2013.333333	15.24	<.0001
Temp	7	5172.500000	738.928571	5.59	<.0001
Group*Temp	14	5480.000000	391.428571	2.96	0.0009

APPENDIX VI

SAS Output for 'Analysis of Variances' using GLM method to see the Effect of Bond Area on Bending Length of Sets – I, II, III samples of Staple Fiber Webs.

The GLM Procedure

Dependent Variable: bendlgth

Source	DF	Sum of Squares	Mean Square	F Value	Pr > F
Model	23	58.0241667	2.5227899	6.21	<0.0001
Error	168	68.2950000	0.4065179		
Corrected Total	191	126.3191667			

R-Square	Coeff Var	Root MSE	bendlgth Mean
0.459346	111.58811	0.637588	5.502083

Source	DF	Type I SS	Mean Square	F Value	Pr > F
Group	2	8.48666667	4.24333333	10.44	<.0001
Temp	7	41.95750000	5.99392857	14.74	<.0001
Group*Temp	14	7.58000000	0.54142857	1.33	0.1933

Source	DF	Type III SS	Mean Square	F Value	Pr > F
Group	2	8.48666667	4.24333333	10.44	<.0001
Temp	7	41.95750000	5.99392857	14.74	<.0001
Group*Temp	14	7.58000000	0.54142857	1.33	0.1933

APPENDIX VII

SAS Output for 'Analysis of Variances' using GLM method to see the Effect of Bond Size on Peak Load of Sets – III, IV, V samples of Staple Fiber Webs.

The GLM Procedure

Dependent Variable: pload

Source	DF	Sum of Squares	Mean Square	F Value	Pr > F
Model	22	0.20310489	0.00923204	7.68	<0.0001
Error	195	0.23448226	0.00120247		
Corrected Total	217	0.43758716			

R-Square	Coeff Var	Root MSE	pload Mean
0.464147	22.90763	0.034677	0.151376

Source	DF	Type I SS	Mean Square	F Value	Pr > F
Group	2	0.04156093	0.02078046	17.28	<.0001
Temp	7	0.08751956	0.01250279	10.40	<.0001
Group*Temp	13	0.07402440	0.00569418	4.74	<.0001

Source	DF	Type III SS	Mean Square	F Value	Pr > F
Group	2	0.042969634	0.02148467	17.87	<.0001
Temp	7	0.08678886	0.01239841	10.31	<.0001
Group*Temp	13	0.07402440	0.00569418	4.74	<.0001

APPENDIX VIII

SAS Output for 'Analysis of Variances' using GLM method to see the Effect of Bond Size on Tear Strength of Sets – III, IV, V samples of Staple Fiber Webs.

The GLM Procedure

Dependent Variable: tstrength

Source	DF	Sum of Squares	Mean Square	F Value	Pr > F
Model	23	6226.66667	270.72464	3.11	<0.0001
Error	96	8360.00000	87.08333		
Corrected Total	119	14586.66667			

R-Square	Coeff Var	Root MSE	tstrength Mean
0.426874	8.457866	9.331845	110.3333

Source	DF	Type I SS	Mean Square	F Value	Pr > F
Group	2	511.666667	255.833333	2.94	0.0578
Temp	7	1240.000000	177.142857	2.03	0.0584
Group*Temp	14	4475.000000	319.642857	3.67	<.0001

Source	DF	Type III SS	Mean Square	F Value	Pr > F
Group	2	511.666667	255.833333	2.94	0.0578
Temp	7	1240.000000	177.142857	2.03	0.0584
Group*Temp	14	4475.000000	319.642857	3.67	<.0001

APPENDIX IX

SAS Output for 'Analysis of Variances' using GLM method to see the Effect of Bond Size on Bending Length of Sets – III, IV, V samples of Staple Fiber Webs.

The GLM Procedure

Dependent Variable: bendlgth

Source	DF	Sum of Squares	Mean Square	F Value	Pr > F
Model	23	66.31750000	2.88336957	14.50	<.0001
Error	168	33.41500000	0.19889881		
Corrected Total	191	99.73250000			

R-Square	Coeff Var	Root MSE	bendlgth Mean
0.664954	8.268472	0.445981	5.393750

Source	DF	Type I SS	Mean Square	F Value	Pr > F
Group	2	0.46625000	0.23312500	1.17	0.3122
Temp	7	60.88583333	8.697976719	43.73	<.0001
Group*Temp	14	4.96541667	0.35467262	1.78	0.0447

Source	DF	Type III SS	Mean Square	F Value	Pr > F
Group	2	0.46625000	0.23312500	1.17	0.3122
Temp	7	60.88583333	8.697976719	43.73	<.0001
Group*Temp	14	4.96541667	0.35467262	1.78	0.0447

APPENDIX X

SAS Output for 'Analysis of Variances' using GLM method to see the Effect of Bond Area on Peak Load of Sets – 2,3,1 samples of Spunbond Webs.

The GLM Procedure

Dependent Variable: pload

Source	DF	Sum of Squares	Mean Square	F Value	Pr > F
Model	12	0.18114987	0.01509582	18.91	<.0001
Error	239	0.19082156	0.00079842		
Corrected Total	251	0.37197143			

R-Square	Coeff Var	Root MSE	pload Mean
0.486999	41.78744	0.028256	0.067619

Source	DF	Type I SS	Mean Square	F Value	Pr > F
Group	2	0.06375761	0.03187880	39.93	<.0001
Temp	4	0.10524596	0.02631149	32.95	<.0001
Group*Temp	6	0.01214630	0.00202438	2.54	0.0213

Source	DF	Type III SS	Mean Square	F Value	Pr > F
Group	2	0.04358676	0.02179338	27.30	<.0001
Temp	4	0.10665932	0.02666483	33.40	<.0001
Group*Temp	6	0.01214630	0.00202438	2.54	0.0213

APPENDIX XI

SAS Output for 'Analysis of Variances' using GLM method to see the Effect of Bond Area on Tear Strength of Sets – 2,3,1 samples of Spunbond Webs.

The GLM Procedure

Dependent Variable: tstrength

Source	DF	Sum of Squares	Mean Square	F Value	Pr > F
Model	12	888183.846	74015.321	9.57	<.0001
Error	52	40210.000	7730.962		
Corrected Total	64	1290193.846			

R-Square	Coeff Var	Root MSE	tstrength Mean
0.688411	32.52807	87.92589	270.3077

Source	DF	Type I SS	Mean Square	F Value	Pr > F
Group	2	151049.8462	75524.9231	9.77	0.0003
Temp	4	330514.8333	82628.7083	10.69	<.0001
Group*Temp	6	406619.1667	67769.8611	8.77	<.0001

Source	DF	Type III SS	Mean Square	F Value	Pr > F
Group	2	133100.8333	66550.4167	8.61	0.0006
Temp	4	330514.8333	82628.7083	10.69	<.0001
Group*Temp	6	406619.1667	67769.8611	8.77	<.0001

APPENDIX XII

SAS Output for 'Analysis of Variances' using GLM method to see the Effect of Bond Area on Bending Length of Sets – 2,3,1 samples of Spunbond Webs.

The GLM Procedure

Dependent Variable: bendlgth

Source	DF	Sum of Squares	Mean Square	F Value	Pr > F
Model	12	29.57788462	2.46482372	7.68	<.0001
Error	91	29.21250000	0.32101648		
Corrected Total	103	58.79038462			

R-Square	Coeff Var	Root MSE	bendlgth Mean
0.503108	11.58566	0.566583	4.890385

Source	DF	Type I SS	Mean Square	F Value	Pr > F
Group	2	6.55188462	3.27594231	10.20	0.0001
Temp	4	16.16100000	4.04025000	12.59	<.0001
Group*Temp	6	6.86500000	1.14416667	3.56	0.0032

Source	DF	Type III SS	Mean Square	F Value	Pr > F
Group	2	3.90333333	1.95166667	6.08	0.0033
Temp	4	16.16100000	4.04025000	12.59	<.0001
Group*Temp	6	6.86500000	1.14416667	3.56	0.0032

APPENDIX XIII

SAS Output for 'Analysis of Variances' using GLM method to see the Effect of Bond Size on Peak Load of Sets – 3,4,6 samples of Spunbond Webs.

The GLM Procedure

Dependent Variable: pload

Source	DF	Sum of Squares	Mean Square	F Value	Pr > F
Model	10	0.25345637	0.02534564	24.65	<.0001
Error	206	0.21183211	0.00102831		
Corrected Total	216	0.46528848			

R-Square	Coeff Var	Root MSE	pload Mean
0.544730	35.53934	0.032067	0.090230

Source	DF	Type I SS	Mean Square	F Value	Pr > F
Group	2	0.08451008	0.04225504	41.09	<.0001
Temp	3	0.14013694	0.04671231	45.43	<.0001
Group*Temp	5	0.02880935	0.00576187	5.60	<.0001

Source	DF	Type III SS	Mean Square	F Value	Pr > F
Group	2	0.04713877	0.02356938	22.92	<.0001
Temp	3	0.14065609	0.04688536	45.59	<.0001
Group*Temp	5	0.02880935	0.00576187	5.60	<.0001

APPENDIX XIV

SAS Output for 'Analysis of Variances' using GLM method to see the Effect of Bond Size on Tear Strength of Sets – 3,4,6 samples of Spunbond Webs.

The GLM Procedure

Dependent Variable: tstrength

Source	DF	Sum of Squares	Mean Square	F Value	Pr > F
Model	10	447482.7273	44748.2727	8.35	<.0001
Error	44	235910.0000	5361.5909		
Corrected Total	54	683392.7273			

R-Square	Coeff Var	Root MSE	tstrength Mean
0.654796	33.64460	73.22289	217.6364

Source	DF	Type I SS	Mean Square	F Value	Pr > F
Group	2	190885.6439	95442.8220	17.80	<.0001
Temp	3	167064.6528	55688.2176	10.39	<.0001
Group*Temp	5	89532.4306	17906.4861	3.34	0.0121

Source	DF	Type III SS	Mean Square	F Value	Pr > F
Group	2	145830.0694	72915.0347	13.60	<.0001
Temp	3	167064.6528	55688.2176	10.39	<.0001
Group*Temp	5	89532.4306	17906.4861	3.34	0.0121

APPENDIX XV

SAS Output for 'Analysis of Variances' using GLM method to see the Effect of Bond Size on Bending Length of Sets – 3,4,6 samples of Spunbond Webs.

The GLM Procedure

Dependent Variable: bendlgth

Source	DF	Sum of Squares	Mean Square	F Value	Pr > F
Model	10	19.66204545	1.96620455	5.57	<.0001
Error	77	27.17750000	0.35295455		
Corrected Total	87	46.83954545			

R-Square	Coeff Var	Root MSE	bendlgth Mean
0.419774	11.54101	0.594100	5.147727

Source	DF	Type I SS	Mean Square	F Value	Pr > F
Group	2	1.95902462	0.97951231	2.78	0.0686
Temp	3	13.30074653	4.43358218	12.56	<.0001
Group*Temp	5	4.40227431	0.88045486	2.49	0.0379

Source	DF	Type III SS	Mean Square	F Value	Pr > F
Group	2	0.90418403	0.45209201	1.28	0.2836
Temp	3	13.30074653	4.43358218	12.56	<.0001
Group*Temp	5	4.40227431	0.88045486	2.49	0.0379

VITA

Praveen Kumar Jangala was born in Vijayawada, India, on March 09, 1975. He did his schooling in Hyderabad. He joined Karnataka University, Raichur (India) in August 1993 and received his Bachelor of Technology Degree in Textile Technology in May 1997. He worked in Shri Textiles Ltd., Sholapur (India), as Process Engineer from 1997 to 1999. In Fall 1999, he joined the Master's program in Textile Science at the University of Tennessee, Knoxville, where he received his degree in August 2001. He was employed as Graduate Research Assistant in the department of Textile Science during his stay at the University of Tennessee.